Assessment of the Sustainability of Geothermal Development within the Truth or Consequences Hot-Springs District, New Mexico

Open-file Report 551
October, 2013

Principal Investigators:

Mark Person, Fred Phillips, NM Tech Hydrology Program
Shari Kelley, Stacy Timmons, NM Bureau of Geology & Mineral Resources

Students: Jeff Pepin, Luke Blom, Kim Haar

Co-Investigator: Mark Murphy

New Mexico Tech
SCIENCE · ENGINEERING · RESEARCH · UNIVERSITY

New Mexico Bureau of Geology and Mineral Resources
New Mexico Tech
Earth Science for the 21st Century

The views and conclusions are those of the authors,
and should not be interpreted as necessarily
representing the official policies, either expressed or implied,
of the State of New Mexico.

New Mexico Tech Hydrology Program

New Mexico Bureau of Geology and Mineral Resources

A division of New Mexico Institute of Mining and Technology

Socorro, NM 87801
(575) 835-5490
Fax (575) 835-6333
www.geoinfo.nmt.edu

Assessment of the Sustainability of Geothermal Development within the Truth or Consequences Hot-Springs District, New Mexico

Open-file Report 551
October, 2013

Principal Investigators: Mark Person, Fred Phillips, Shari Kelley, Stacy Timmons,
Students: Jeff Pepin, Luke Blom, Kim Haar
Co-Investigator: Mark Murphy

NM Tech Hydrology Program
New Mexico Bureau of Geology and Mineral Resources

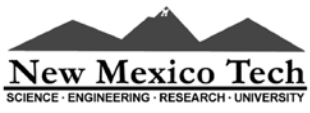

PROJECT FUNDING

City of Truth or Consequences
New Mexico Bureau of Geology and Mineral Resources, Aquifer Mapping Program
Department of Energy award DE-EE0002850 (funded part of the temperature logging effort)
Partial support from the
National Science Foundation (EPSCoR) under Grant No. IIA-1301346

TABLE OF CONTENTS

APPENDICES

EXECUTIVE SUMMARY

Between October 1, 2012 and Sept 30, 2013 NM Tech hydrology faculty and students, and personnel from the NM Bureau of Geology and Mineral Resources conducted a 1-year study to assess the subsurface flow patterns and the sustainability of the Truth or Consequences geothermal system. This report presents a summary of our findings.

Changes in appropriation

There has been significant increase in the water appropriated for geothermal use within the hot-springs district. Based on water-rights appropriations filed with the NM Office of the State Engineer, appropriations have grown substantially from about 130,000 gallons per day to 1.5 million gallons per day since the Theis et al. (1941) study was published. However, the extent to which the actual geothermal water use has increased is unclear as comprehensive hot-springs district pumping data are not available.

Changes in the hydrologic system

We analyzed the change in water-table elevation from the spring season of 1939 (included in the report by Theis et al., 1941) to the spring of 2013 as part of this study. Analysis of the hydrologic data suggests that water-table elevations have dropped by one to two feet (or by up to 10%) since the study of Theis et al. (1941). However, it is not possible to unequivocally link the observed drop in water levels to increased geothermal production. Other factors that may explain this drop include but are not limited to:

1) Different well locations were used in constructing the two water-table maps.
2) A larger magnitude of pumping may have occurred during the spring of 2013 when water level measurements were collected.
3) The river stage during 1939 water level measurements was not reported. Discharge upstream of town at USGS gauge 08361000 below Elephant Butte dam reports an average discharge value of 18 cfs on the day Theis made his head measurements compared to 0.26 cfs during the 2013 measurements.
4) The ongoing drought in New Mexico could have affected spring 2013 water levels.
5) Potential changes to stream geometry may affect the observed head gradient as well.

In order to compare water-level measurements from these two periods, separated by 74 years, a common topographic datum must be found to tie the two surveys together. There is some uncertainty whether the two datums are actually the same. Taking this into account in addition to the uncertainty inherent in the differential GPS survey (±1 inch) probably adds about six inches of uncertainty to our water table measurements.

There is evidence that upward groundwater flow has declined locally within the confined "artesian" aquifer beneath the hot-springs district. This aquifer was artesian in 1939 but according to the limited data available, deep artesian wells since that time have ceased to flow at the surface. However, there are very few deep wells in the hot-springs district today; limiting our ability to reach firm conclusions regarding pressure changes within the deep artesian reservoir. We found that total geothermal discharge to the Rio Grande in the summer of 2013 was 2.1 million gallons per day (3.3 ft^3/s). This is very similar to the geothermal discharge estimated by Theis et al. (1941): 3.5 ft^3/s. For comparison, the current geothermal-water appropriations in the hot-springs district total about 70% of the estimated natural discharge.

A comparison of the temperatures of hot-spring district waters between spring 1939 and spring 2013 was undertaken as part of this study. We found that the overall temperature

patterns have shifted in the hot-springs district since 1939. Some areas within the hot-springs district appear to have dropped several degrees Fahrenheit since the study of Theis et al. (1941). However, the present-day well depths are significantly shallower than the wells reported by Theis et al. (1941). Pumping from shallower depths would be expected to produce cooler waters. We also compared the salinity and water quality from 1939 with current values. Again, direct comparison is generally not possible because the wells are not the same, but within this limitation, we did not observe any systematic changes.

Geothermal water recharge

Using a technique known as the "Maxey-Eakin method", which relates the amount of groundwater recharge to the amount of precipitation, we have estimated that the net recharge to the watershed supplying the hot-springs district totals about 20 million gallons per day (about 10 times the hot-springs district discharge). Applying the same method but only accounting for zones where geologic relationships promote infiltration of recharge, yields estimates that are closer to two million gallons per day. This is approximately equal to the measured discharge of the hot-springs district. Virtually all groundwater is recharged at high elevations (>6500 feet) in the Sierra Cuchillo and the San Mateo Mountains to the west of Truth or Consequences. Although estimation of groundwater recharge has substantial uncertainty, these results make it clear that a substantial proportion of the total recharge in the groundwater source area is discharging, either naturally or by pumping, in the hot-springs district.

Groundwater flow model

We developed a 58 km long by 6 km deep (36 mi by 3.7 mi) two-dimensional hydrothermal model to understand groundwater flow patterns beneath Truth or Consequences and the source of heat to the hot-springs district. Dissolved silica concentrations of hot-springs district waters suggest that they were heated to over 100°C (212°F). Owing to the permeable nature of the crystalline basement rocks, and the consequent rapid rise of the groundwater, the groundwater retains much of its heat as it ascends into the hot-springs district. We were able to estimate the permeability of the crystalline basement by matching computed and observed hot-springs district temperatures and ^{14}C groundwater age. Based on the model results, we conclude that as groundwater circulates to depths of up to 4 km (2.5 mi), it is heated by the Earth's natural geothermal gradient (about 40°C/km, equivalent to about 115°F/mile, in the Rio Grande valley) and ascends relatively rapidly to form the hot-springs district in Truth or Consequences. Erosion of the fine-grained sedimentary confining units (especially the Percha Shale) off the permeable granite and carbonate aquifers underlying the hot-springs district also plays an important role in explaining why hot waters rise to shallow depths within Truth or Consequences. Our findings are supported by geochemistry data from the groundwater samples collected within the hot-springs district. The hot-springs district sodium-chloride dominated geothermal water likely results from equilibration with minerals associated with crystalline basement rocks such as granites at temperatures around 100°C. Geothermal groundwater that has equilibrated only with carbonate aquifers has a distinctively different composition.

We also developed a relatively simple, 6-layer three-dimensional groundwater flow model of the hot-springs district that used hydraulic properties for the deep aquifers consistent with our regional cross-sectional model. We assigned hydraulic conductivity values for shallow alluvial sediments consistent with hydraulic analysis of the shallow aquifer (3.3 to 13 feet/day, equivalent to 1 to 4 m/day). We represented geothermal exploitation from the hot-springs district by using 17 wells that were pumped at equal rates. We varied the pumping rates for these wells between 115,000 gal/day/well and 760,000 gal/day/well. To put these pumping rates into perspective, the natural geothermal discharge of 2.2 million gallons per day divided among the 17 wells would represent a pumping rate of 130,000 gal/day/well. Using the higher hydraulic conductivity limit and pumping at or below 380,000 gal/day/well did not result in a cone of depression or drawing water from the Rio Grande into the hot-springs district wells. However, pumping at 760,000 gal/day/well did draw Rio Grande water into the hot-springs district. Alternatively, using the lower-limit hydraulic conductivity for the alluvium produced flow lines that began to approach the Rio Grande at ~13,000 gal/day/well.

Recommendations

1) Rational management of the geothermal resource requires comprehensive data on the system. The most critical missing information is the stress put on the system by the collective pumping and artesian discharges. We strongly recommend that the City set up a program to collect data on well discharges. This could be accomplished by meters, records of electrical consumption, voluntary reporting or other means.

2) In spite of the excellent baseline information provided by the report of Theis et al. (1941), we have had difficulty defining the extent to which water levels in the alluvial aquifer have actually declined, due to lack of continuous records and lack of continuity in the locations of wells. We recommend that the City set up a monitoring program to collect continuous, or at least periodic, data on water levels and temperatures in selected wells at carefully selected locations.

3) The formerly-artesian carbonate aquifer is the immediate source of supply for all of the geothermal water uses in Truth or Consequences, but at present access to that aquifer has been reduced to one well. We are unable to ascertain whether differences in temperature between 1939 and 2013 are due to shallower well depths or an actual temperature decline. Locating or drilling at least one well near the source of geothermal upflow that can be used to monitor hydraulic head and temperature could provide unambiguous data, early warning of declines in the system, and enable analysis of its sensitivity to pumping of the alluvial aquifer.

4) With regard to the sustainability of the geothermal discharge, our analysis indicates grounds for concern. Artesian flow has declined to the vanishing point in the remaining artesian well and water-table elevations have pervasively declined by one to two feet. Temperatures are now lower than those measured by Theis in 1939, but whether this is due to a change in the system temperature, or just well depths, cannot be definitively established. These changes are still fairly mild, but they dictate caution regarding overexploiting the system. There is little doubt that unlimited pumping will result in lowered water levels and cooling of the system as Rio Grande water flows in to replace over-pumped geothermal water. As an absolute upper limit for pumping, the estimated system discharge of about two million gallons per day could be used. We would recommend a more conservative limit, ranging from 25% to 50% of the natural discharge (i.e., 0.5 to 1.0 million gallons per day). The degree to which the City wishes to be conservative or expansive in setting limits is one that has to be made by entities with appropriate political accountability, and should obviously be made in consultation with potentially affected businesses, landowners, and other stakeholders.

5) We feel that a well-drilling moratorium is of limited value in managing the geothermal resource. The critical issue is the amount of geothermal water pumped, not the number of wells. As described above, this is at present poorly quantified, preventing any meaningful management of the resource. Only after the present level of total pumping is quantified can prudent future expansion of exploitation (if any) be estimated. The most reasonable procedure would be to first establish a legal basis for regulation of the resource, taking into account, of course, existing water rights. Then, once data has been obtained on current pumping by each well, the optimal next step would be to establish an equitable and agreed-upon allocation among existing users and a procedure for approving additional future uses, if these were deemed prudent. Future wells will need to be allowed, if for no other reason, due to the short lifetime of wells as a result of the corrosive water. In summary, although the drilling moratorium may be useful in the short run in preventing overdrilling due to a ‘hot-water rush’, it should be replaced as soon as possible by a true management system.

6) Lack of knowledge regarding the nature of the geothermal system, its current state, and the possible effects of future changes in exploitation have hindered discussion that might have been helpful to its management. We feel that it would be beneficial for the City to set up a venue, such as a web page, where this information could be readily available and kept up to date. The City might also wish to explore the option of setting up a public forum in which issues related to the management of the geothermal resource could be discussed and that could provide input to the City Council regarding the management. We would be glad to assist in these efforts.

I. INTRODUCTION

From its establishment in 1913, the utilization of hot springs and bathhouses have been an important source of revenue for the town of Truth or Consequences (Lund and Witcher, 2002). During the 1930s, the NM State Engineer declared a 97 km^2 (37.5 mi^2) region around Truth or Consequences as "the Hot Springs underground water basin" (Lund and Witcher, 2002). The amount of natural geothermal discharge within the hot-springs district of Truth or Consequences was first estimated to be about 3.5 cubic feet per second (cfs) or about 2.2 million gallons per day in a seminal study lead by the renowned U.S. Geological Survey hydrogeologist C.V. Theis (Theis et al. 1941). The total number of wells at that time was about 32 with a mean depth of 129 feet (Fig. 1A). Minton (1941) reported that some of the wells were not properly constructed and used vertical velocity profile data to argue that deep, saline geothermal water from depth was leaking into the shallow alluvial formations along improperly constructed bores. At the time of Theis et al. (1941), the hot-springs district utilized about 6% of the natural discharge (about 130,000 gallons per day). At that time the town population was less than 3000 residents. Today, there are about 6475 year-round residents and eight commercial spas. The combined net permitted well discharge of the estimated 150 wells located within the hot-springs district today now totals about 1.5 million gallons per day or about 70% of the natural geothermal waters (Office of State Engineer WATERS database; Table 1). The number of permitted wells in the hot-springs district has increased today to an estimated 150 in the hot-springs district, with a mean depth of less than 80 feet. However, it is important to note that we have depth measurements for only 29 of these 150 wells due primarily to the presence of pumps restricting access (Fig. 1A). Domestic users hold an estimated 14% of the net permitted water rights (Table 1).

Theis et al. (1941) reported numerous artesian wells completed in a confined aquifer within a limestone (likely a Lower-Paleozoic limestone) with a maximum head rising about 4 feet above land surface. Today, we are aware of only two deep wells completed within the Paleozoic limestone. During the past decade, only one of these hot-springs wells has produced water using natural artesian heads. Discharge from this artesian well (TC-13, Fig. 1E) has declined during the past decade, possibly suggesting over-production of geothermal waters within the hot-springs district. During the past few years, dozens of new domestic well applications were awarded by the Office of the State Engineer (OSE). The dramatic rise in the number of new well permits prompted the City of Truth or Consequences to institute a moratorium on drilling until a safe total aquifer yield could be determined.

The City of Truth or Consequences contracted with the Hydrology Program at NM Tech and the New Mexico Bureau of Geology and Mineral Resources to conduct a 1-year study to address the following questions:

1) Have thermal and hydrologic conditions changed since the time of the Theis et al. (1941) study?
2) What is the location and amount of recharge that supplies natural geothermal discharge within the hot-springs district?
3) What are the flowpaths responsible for the relatively hot (up to 46 °C) geothermal discharge within the hot-springs district?
4) What pumping rate will adversely affect the shallow geothermal reservoirs of the hot-springs district?

The project ran from October 1, 2012 to September 30, 2013. In order to address the above questions, the following activities were performed:

1) We measured water-table elevations in a campaign-style sampling (measuring many wells in one day) in addition to long-term monitoring using pressure transducer/data loggers. In order to accurately compare water table maps produced by Theis et al. (1941), we also had to accurately measure the elevations of many wells in and around the hot-springs district. We accomplished this by means of a differential-GPS survey directed by Dr. Mark Murray.
2) We collected high-resolution (meter-scale) temperature profiles in wells.

3) We collected geochemical samples to measure total salinity, major ions and trace elements, and groundwater age of the hot-springs district wells.
4) We conducted stream gauging, collecting both flow and salinity data within the Rio Grande above and below Truth or Consequences to establish net discharge from the hot-springs district.
5) We completed an electrical resistivity survey on the southeast side of the Rio Grande across from the hot-springs district to establish the depth of saline groundwater below and adjacent to the Rio Grande.
6) We constructed a regional-scale, cross-sectional hydrothermal model along a northwest-south transect following Alamosa Creek. This 58 km (36 mi) long cross-sectional model was relatively detailed, including 14 geologic units and several faults. The purpose of the cross-sectional model was to determine the regional flow patterns responsible for hydrothermal fluid discharge within the hot-springs district.
7) We developed a more local-scale (12 km by 7 km; 7.5 mi by 4.3 mi) three-dimensional, 6-layer hydrogeologic simulation using the USGS groundwater flow model MODFLOW. The purpose of the three-dimensional model was to determine an upper limit on pumping rates for sustainable geothermal development within the hot-springs district of Truth or Consequences, NM.

In this report, we summarize the results of our study. Special emphasis is placed on comparing modern field measurements of water-table elevations, salinity, and subsurface temperatures to those collected by Theis et al. (1941).

Table 1–Estimated 2013 Permitted Well Discharge in Truth or Consequences hot-springs district.

Use	afpy	gpd	% of Total
Commercial	1495	1334807	84.6%
Domestic	242	216044	13.7%
Municipal	30	26782	1.7%

Abbreviations
Q, pumping rate; gpd, gallons per day; afpy, acre-feet per year.

HS-#	afpy	gpd	HS-#	afpy	gpd	HS-#	afpy	gpd
1	16.5	14730	826	3	2678	955	3	2678
2	50.4	45003	827	3	2678	956	3	2678
4	112	100000	836	3	2678	958	3	2678
24	30	26782	846	3	2678	960	3	2678
55	11	9820	847	3	2678	962	3	2678
56	11	9820	851	3	2678	964	3	2678
62	9.2	8213	857	3	2678	965	3	2678
68	6	5356	873	3	2678	968	3	2678
76	10.5	9374	874	3	2678	971	3	2678
203	3	2678	903	3	2678	975	1	893
209	6.7	5999	905	3	2678	976	1	893
214	214	191047	907	3	2678	977	1	893
215	3	2678	912	3	2678	978	1	893
216	303.2	270680	913	3	2678	981	1	893
217	241.9	215955	915	3	2678	982	1	893
220	101.5	90613	918	3	2678	983	1	893
221	155	138375	919	3	2678	986	1	893
221A	5	4464	921	3	2678	987	1	893
285	16	14284	924	3	2678	988	1	893
379	13.5	12052	926	3	2678	989	1	893
449	3	2678	927	3	2678	991	1	893
450	3	2678	928	3	2678	992	1	893
459	3.1	2794	929	3	2678	993	1	893
475	3	2678	930	3	2678	994	1	893
483	3	2678	931	3	2678	1008	1	893
490	3	2678	933	3	2678	1013	1	893
505	9	8035	934	3	2678	1014	1	893
519	3	2678	935	3	2678	1017	3	2678
571	3	2678	936	3	2678	1026	1	893
594	3	2678	937	3	2678	1030	1	893
599	3	2678	938	3	2678	1034	1	893
633	3	2678	939	3	2678	1035	1	893
659	15	13391	940	3	2678	1036	1	893
668	70	62492	941	3	2678	1037	1	893
679	80.6	71955	942	3	2678	1039	1	893
698	10	8927	943	3	2678	1053	1	893
712	3	2678	944	3	2678	1057	1	893
725	3	2678	945	3	2678	1060	1	893
739	3	2678	946	6	5356	1061	1	893
762	3	2678	948	1	893	1064	1	893
764	3	2678	950	3	2678	1065	1	893
798	3	2678	951	3	2678	1067	1	893
812	3	2678	952	3	2678	1071	1	893
815	3	2678	953	3	2678	1076	1	893
820	3	2678	954	3	2678	1090	3	2678
Total Acre-Feet Per Year						**1767**		
Total Gallons Per Day						**1,577,633**		

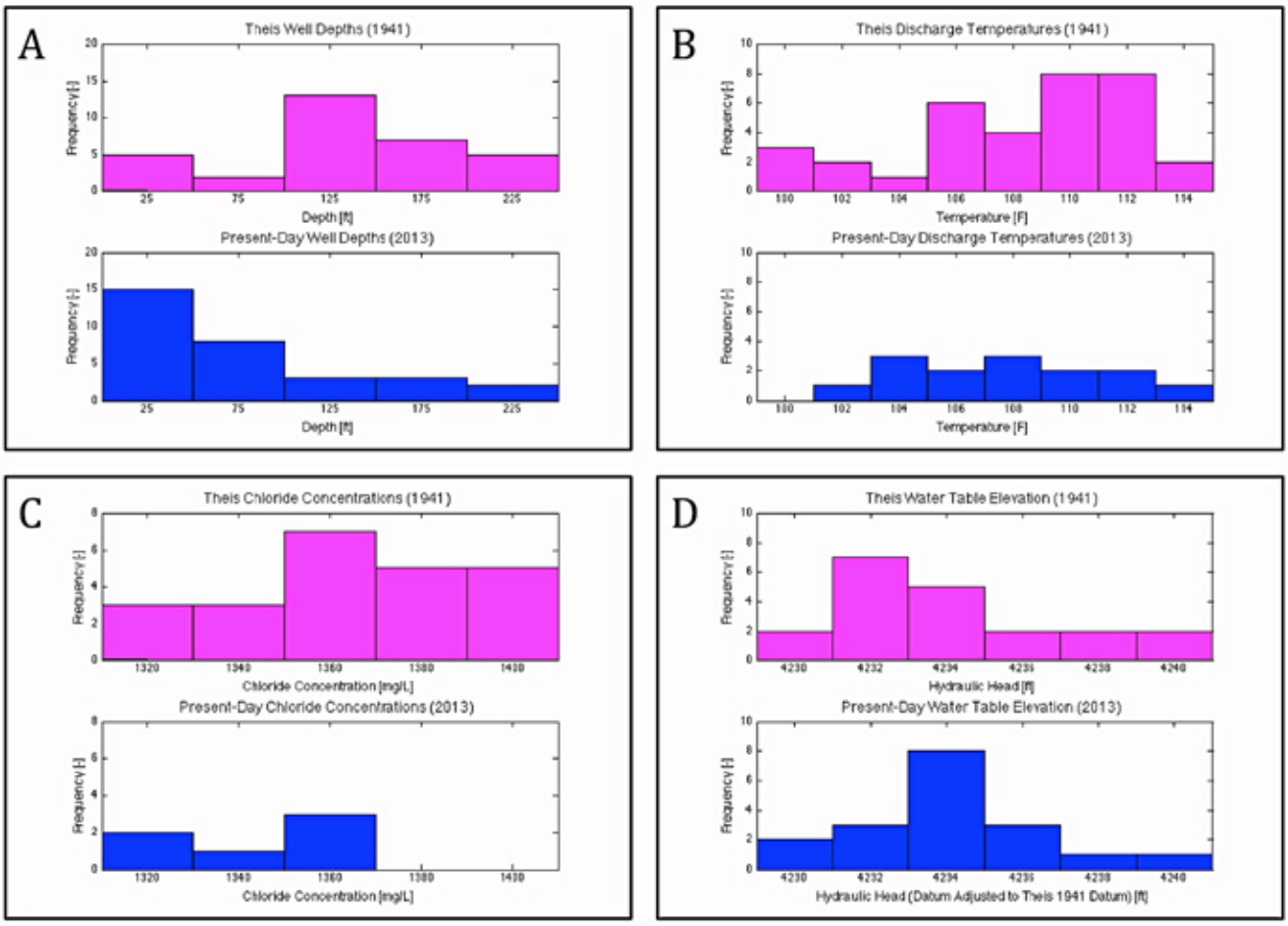

Figure 1–Histograms comparing (A) well depths, (B) well discharge temperature, (C) chloride concentrations, and (D) water table elevation for the hot-springs district wells between 1939 and 2013. Data source: Theis et al. (1941). The mean well depth in 1939 was about 125 feet. In 2013, the mean well depth was about 50 feet. Very few wells from the time of Theis' report are accessible today.

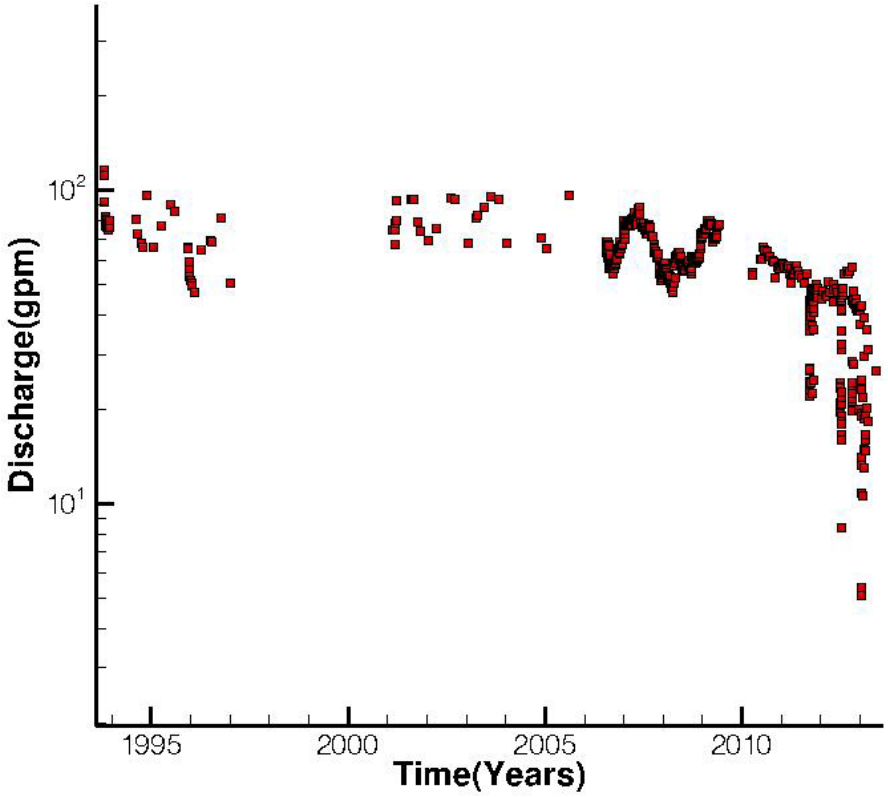

Figure 1E–Combined discharge of well TC-13 and TC-14 (Data provided by William Martin).

II. CLIMATE, ELEVATION, AND RECHARGE

Mean annual air temperature and annual precipitation of Truth or Consequences is 60°F (15.4°C) and nine inches/year (about 2 cm/month), respectively. The altitude of Truth or Consequences is about 4265 feet (about 1300 m). At this temperature and level of precipitation, potential evapotranspiration (about 7 cm/month estimated using the temperature-based Thornthwaite equation; Dingman, 2002) exceeds precipitation by more than a factor of two, and there is likely very little local recharge through the soil. Any recharge the hot-springs district may receive likely comes from the Rio Grande, and then only if the water table is lower than the elevation of the river due to pumping. The principal source of recharge for the geothermal water is from the mountains to the west of Truth or Consequences. The elevation of the Sierra Cuchillo Mountains to the west of Truth or Consequences, NM is about 2400 m (7874 feet). The highest elevations of the San Mateo Mountains is 3090 m (about 10,000 feet). At these elevations, annual average precipitation is about 20 inches per year. This, combined with lower average annual temperature, is conducive to recharge.

We estimated recharge for the watershed that includes Truth or Consequences and Alamosa Creek using the Maxey-Eakin approach (Fig. 2). The Maxey-Eakin methodology assumes that the fraction of precipitation that is available for subsurface recharge increases with increasing precipitation. This makes physical sense since higher precipitation is associated with higher elevations and lower temperatures (and hence, less evapotranspiration). It is important to note that the coefficients reported in Table 2 are empirical. They vary from region to region in the southwestern USA, and they represent only approximations of local circumstances. The fractional values reported in Table 2 were used by Anderholm (2001) to estimate mountain-front recharge from the Sandia Mountains to the east of Albuquerque, NM. Using this approach, we estimate that the total amount of available recharge to Truth or Consequences is about 20 million gallons/day (2.8 x 107 m^3/year; Figure 2A). If one assumes that hot-springs district recharge only comes from regions where the metamorphic and plutonic crystalline basement rocks as well as the Paleozoic limestone crop out at the land surface (Fig. 2B), then the amount of available recharge to the hot-springs district decreases to 2.5 million gallons per day. This latter number is very close to the natural discharge estimated by Theis et al. (1941; 2.2 million gallons/day).

It is important to note that these numbers are estimates and are uncertain. Anderholm (2001) found for the Sandia Mountains, NM, which recharge estimates based on the Maxey-Eakin approach were about eight times higher than those based on the alternative chloride-mass-balance method. Furthermore, some groundwater may discharge along the Rio Grande and other drainages outside of the hot-springs district. The chloride-mass-balance method could not be implemented for this project, as the chloride-bromide ratios are too high to provide accurate results.

Wells and Granzow (1981) argued that the aquifer is also recharged near the Mud Spring Mountains about ten kilometers to the northwest of the hot-springs district. Carbonate aquifers crop out in the ephemeral course of Cuchillo Creek and these authors proposed that during times of high discharge and during cooler wetter climatic periods during the Pleistocene, significant amounts of recharge occurred along Cuchillo Creek.

Table 2–Precipitation amount and fraction of precipitation available for recharge using the Maxey-Eakin Approach.

Precipitation (in/year)	Recharge (%)
0-8	0
8-12	3
12-15	7
15-20	15
>20	25

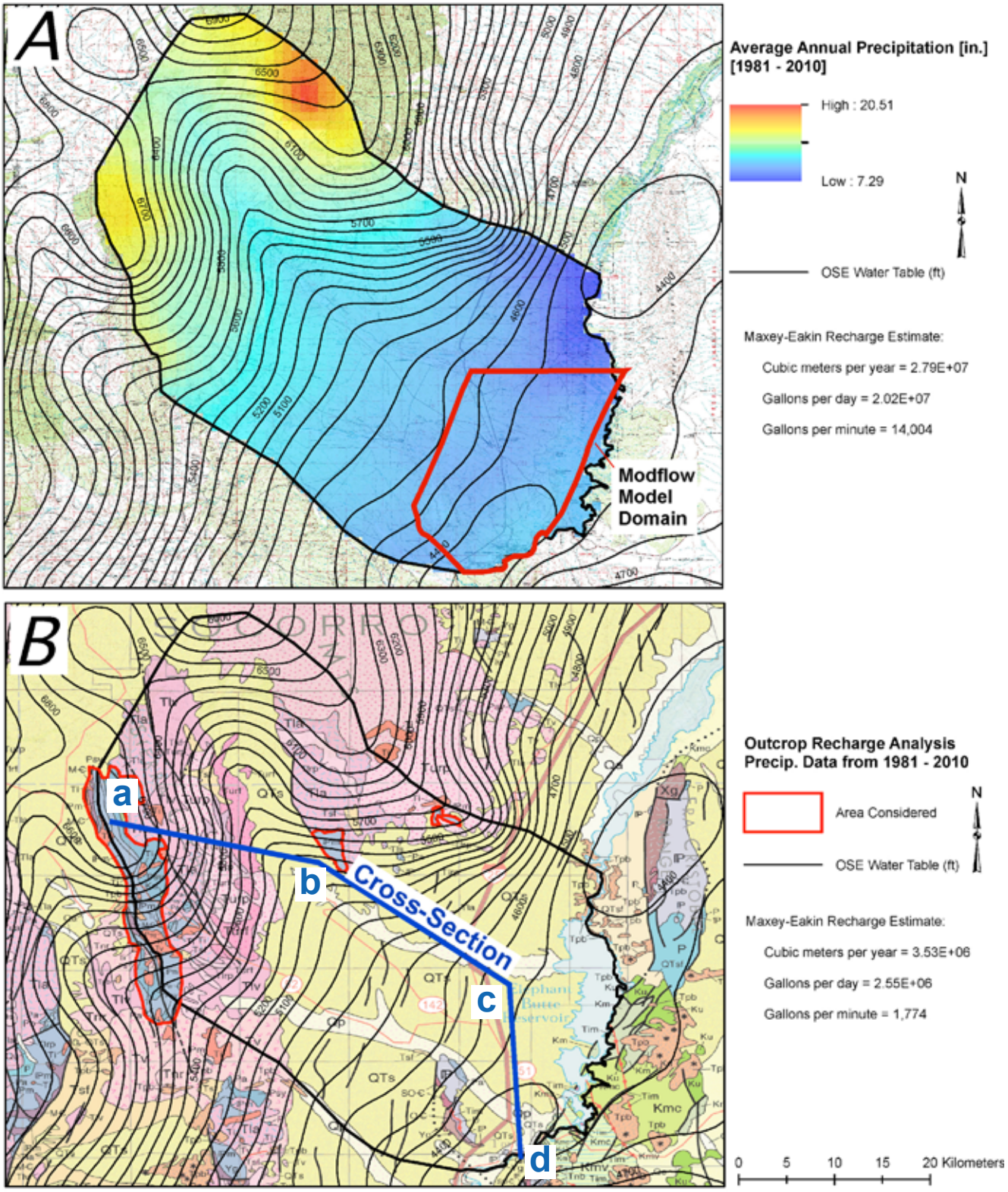

Figure 2–Basemap delineating the estimated groundwater contributing area of the Truth or Consequences, NM hot-springs district. The color contours in Figure 2A denotes the spatial distribution of precipitation. Warm colors denote high levels of precipitation. Net annual recharge is listed to the right of Figure 2A. The approximate lateral extent of the three-dimensional Modflow model is indicated by the red line in Figure 2A. The black contour lines in Figure 2 B denote the estimated water table contours. The blue line shows the location of the cross-section in Figure 3A. (Precipitation data from PRISM Climate Group at Oregon State University, 2012; Geology from NMBGMR; 2003)

III. HYDROTHERMAL FLOW SYSTEM

Both Theis et al. (1941) and Wells and Granzow (1981) proposed that Truth or Consequences hot-springs-district geothermal water are the result of magmatic heating. Magmatic heat related to recent (<200,000 years) rift volcanism can also affect temperature gradients, but the youngest magmatism in the Mud Springs Mountains dates to about 5 million years ago (McLemore, 2012). Heat associated with this volcanic activity dissipated within less than 1 million years after the eruption of the 5 million-year-old basalts (Carslaw and Jeager, 1959), suggesting that there is no current magmatic heating. In addition, swarms of microearthquakes, characteristic of magmatic injection, have not been detected beneath Truth or Consequences.

We propose two alternative hypotheses for the source of hot waters in Truth or Consequences. One involves a deep circulation and heating of groundwater in a high heat flow setting (92 to 117 mW/m^2; Reiter et al., 1975) within the crystalline basement (Hypothesis #1, black arrows; Fig. 3A). Focused upflow occurs in the hot-springs district because of the absence of a Paleozoic confining unit (i.e. the Percha Shale), which was removed by erosion on the upthrown side of the reverse fault. This hypothesis is consistent with the hydrologic-window hypothesis first proposed by Witcher (1998). A "hydrologic window" is a contact in the subsurface, such as a fault or erosional contact, which juxtaposes aquifers that ordinarily are separated by low-permeability units. Hypothesis #1 relies on vertical flow beneath the Truth or Consequences hot-springs district, which is an efficient mechanism for heat transfer (Bredehoeft and Papdopolus, 1965). An alternative hypothesis is that groundwater enters the Magdalena Group aquifer to the north of Truth or Consequences along a fault that places the Palomas Formation against Magdelena Group limestone at a depth of about 2.5 km (1.2 mi; Hypothesis #2 white arrows, Fig. 3A) and travels horizontally to the hot-springs district, advecting heat from depth. In this hypothesis, lateral heat transfer is necessary to supply the required heat (Lu and Ge, 1996).

In order to evaluate these hypotheses, we constructed a geologic cross-section from the Sierra Cuchillo to Truth or Consequences as part of this project. This cross-section follows Alamosa Creek out of the Sierra Cuchillo, crossing the Willow Draw fault before turning south through the center of the Engle basin. The cross section is oriented perpendicular to the regional water-table contours (Fig. 2) and includes Quaternary through Paleozoic strata as well as a several kilometers of Proterozoic rocks (Fig. 3A). The lower Paleozoic strata include numerous limestone, sandstone, and shale units. Permeable strata that could potentially serve as geothermal aquifers at depth include the Magdalena Group limestones, lower Paleozoic limestone units, and fractured crystalline basement. The Percha Shale is an important lower Paleozoic confining unit (Fig. 3) that is present in the Mud Springs and southern Caballo mountains, but is absent in the northern Caballo Mountains (Seager and Mack, 2003). The Paleozoic strata are strongly folded upward at the southern terminus of the Engle basin where Truth or Consequences is located. Fracturing caused by faulting and folding has likely created a higher permeability zone beneath the hot-springs district, in comparison to adjacent rocks. The absence of the Percha shale between the crystalline basement rocks and the Magdalena Group limestones beneath the hot-springs district may allow heated groundwater to flow into the Magdalena Group. The hot-springs district is located in an area of near vertically dipping Magdalena Group limestone beds that are partially overlain by Palomas Formation and Quaternary fluvial deposits composed of sand, gravel and clay layers about 200 feet thick. Reconnaissance geologic mapping carried out as part of this study indicates that the Percha Shale is absent in the hot-springs district outcrops and may provide a "hydrologic window" allowing deep groundwater to discharge along the path of least resistance. Alternatively, the carbonate rocks underlying the hot-springs district may be Lower Paleozoic units that underlie the Percha Shale. In this case, geothermal water can simply discharge upward toward the alluvium overlying the Lower Paleozoic Limestones.

The difference between the "vertical flow" and the "horizontal flow" hypotheses comes down to the assumed permeability assigned to the crystalline basement rocks. If the fractured crystalline bedrock has permeability comparable to that of the Paleozoic

limestone (about 1 m/day; 3.3 ft/day), then hypothesis #1 is more likely. If the Paleozoic limestone is much more permeable than the underlying crystalline basement and flow rates are high enough to permit lateral heat transfer through the Magdalena Group limestone without significant conductive cooling, then hypothesis #2 is a more likely explanation for hot-springs district temperatures.

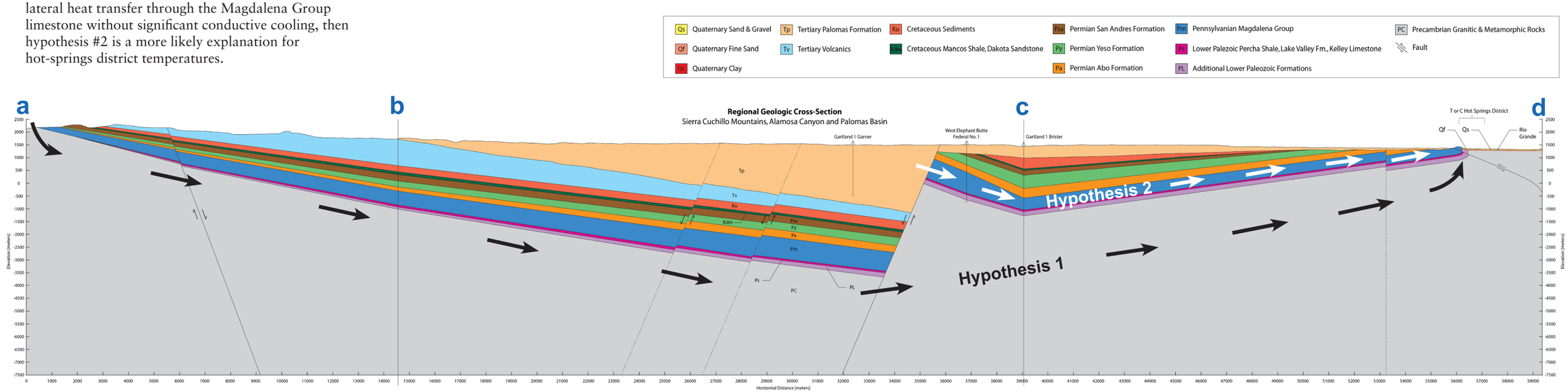

Figure 3A–Geologic cross section from the Sierra Cuchillo along Alamosa Creek drainage, turning south near Interstate 25 and terminating at the southern limit of the Engle Basin in Truth or Consequences, NM. The cross section was constructed perpendicular to the regional water table map presented in Fig. 2. The black arrows depict a deep flow path in the Proterozoic basement (hypothesis 1) and the white arrows highlight a shallow flow path within the carbonates of the Magdalena Group (hypothesis 2).

Figure 3B–Geologic cross section through the Truth or Consequences hot-springs district. The location of the cross section is shown on the aerial photograph at the right.

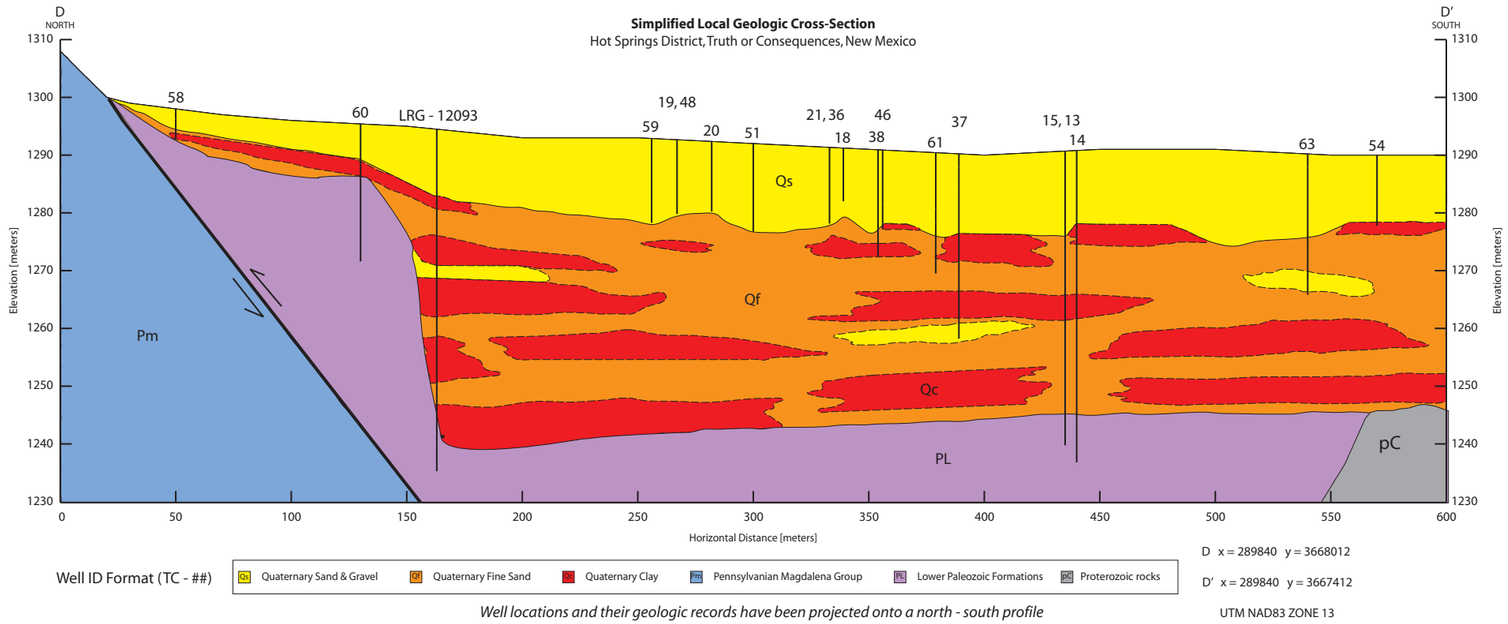

Well locations and their geologic records have been projected onto a north - south profile

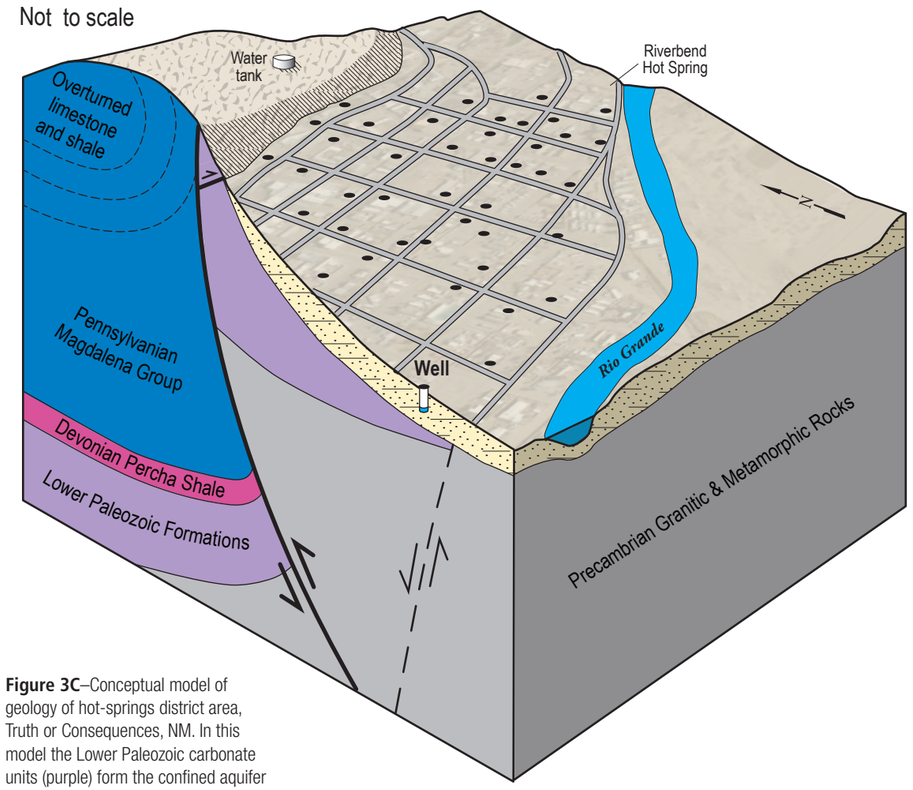

Figure 3C–Conceptual model of geology of hot-springs district area, Truth or Consequences, NM. In this model the Lower Paleozoic carbonate units (purple) form the confined aquifer beneath the hot-springs district, but note discussion in the text regarding the identity of the formation(s) comprising this aquifer.

IV. GEOLOGIC SETTING

A. STRUCTURE

The location of the geothermal system at Truth or Consequences is controlled, in part, by geologic structures that formed during three major tectonic events that affected New Mexico and the southwestern United States. First, folds and thrust faults with a NW-striking trend and strike-slip faults with a NNE-striking trend were created in the vicinity of Truth or Consequences during NE-SW directed compressional Laramide deformation between 75 to 45 million years ago (Seager and Mack, 2003; Harrison and Cather, 2004). Some of the folds created by this deformation are visible from Truth or Consequences in the western escarpment of the Caballo Mountains to the east of town and in the Mud Springs Mountains to the west of town. One of these folds, a NW-trending overturned syncline, and at least one low-angle fault, are preserved in the limestone hill topped with the water storage tank just north of downtown (Kelley and Silver, 1952). This faulted, overturned syncline is an important structure in forcing water travelling southward out of the Engle Basin toward the surface.

Laramide compression was followed by voluminous eruptions in the Mogollon-Datil volcanic field starting about 37 million years ago (Harrison et al., 1993). Fracture permeability was enhanced by the collapse structures associated with seven calderas that have been identified in the recharge area in the San Mateo Mountains (Ferguson et al., 2012). Volcanic units from eruptions in the San Mateo Mountains also cover the highest elevations of the Sierra Cuchillo and are buried in the Engle Basin.

The third major tectonic event that shaped the landscape in the region around Truth or Consequences is Rio Grande rift extension that began about 36 million years ago and peaked at 16 to 5 million years ago (Kelley and Chapin, 1997; Seager and Mack, 2003). This event caused the uplift of the Caballo Mountains to the east of town and the Mud Springs Mountains, the Sierra Cuchillo, and the San Mateo Mountains to the west and northwest of Truth or Consequences. Material eroded from the rising rift flank uplifts filled the Engle Basin with as much as 2700 m (8860 ft) of sediment. North to northeast-striking normal faults associated with rift formation variably served as conduits and barriers to groundwater flow in the Engle Basin.

B. LITHOLOGY

The stratigraphic rock types that have been mapped in the vicinity of Truth or Consequences (Kelley and Silver, 1953; Lozinsky, 1985; Maxwell and Oakman, 1990) are here divided into fourteen rock units that share similar water-storage and water-movement properties. The following descriptions were taken from Seager and Mack (2003). On a regional scale the units, from youngest to oldest, are:

Tertiary Palomas Formation—Weakly to moderately cemented sandstones, conglomerates, and siltstones deposited in the Engle Basin to the north of Truth or Consequences during Rio Grande rift extension. These porous and permeable units were deposited by streams and debris flows derived from the rising mountains.

Tertiary volcanics—Lava flows, ash flow tuffs, debris and stream deposits that formed during voluminous eruptions in the Mogollon-Datil volcanic field. Fracturing has increased the originally low porosity and permeability of these units.

Undivided Upper Cretaceous Sedimentary Rocks—Sandstone, shale, and conglomerate of the marginal marine Gallup Sandstone and fluvial Crevasse Canyon Formation. The Gallup Sandstone is a good aquifer while the Crevasse Canyon Formation is a poor aquifer.

Cretaceous Mancos Shale and Dakota Sandstone—Fluvial sandstone, shale, and conglomerate of the Dakota grades up into shale and siltstone of two tongues of Mancos Shale intercalated with sandstone. The sandstones are aquifers and the Mancos Shale tongues act as confining units.

Permian San Andres Formation—Fossiliferous marine limestone that is an aquifer where fractured.

Permian Yeso Formation—Sandstone overlain by a succession of dolomite, limestone, red siltstone, and gypsum interpreted to have been deposited in a hypersaline lagoon. This unit is a poor aquifer.

Permian Abo Formation—River floodplain mudstone and siltstone, sinuous channel sandstones, and rare carbonate lake deposits. This formation is generally a confining unit because of its fine-grained nature.

Pennsylvanian Magdalena Group—Fossiliferous limestone, cherty limestone, shale, dolomite, and conglomerate deposited in shallow ocean water that grade up into Abo Formation that is an aquifer where fractured.

Mississippian and Devonian Sedimentary Rocks—The Devonian Percha Shale includes shale intercalated with thin siltstone and limestone beds. The Percha Shale grades up into the carbonates of the Mississippian Lake Valley Formation. The Percha Shale is a confining unit and the Lake Valley Formation is an aquifer where fractured.

Lower Paleozoic Sedimentary Rocks—Cambrian to Silurian shallow marine limestone, dolomite, shale and sandstone; includes, from oldest to youngest, Bliss Sandstone, El Paso Formation, Montoya Formation, and Fusselman Dolomite. These formations are aquifers where fractured.

Proterozoic Granitic and Metamorphic Rocks—Metamorphosed volcanic rocks, sandstone, and shale deposited in an extensional basin about 1.60 to 1.65 billion years ago later intruded by 1.4 billion year age granite. These rocks are aquifers where fractured.

Within the downtown area of Truth or Consequences, we have developed a conceptual model of geologic structures and rock units important in describing the geothermal system (Fig. 3B). In this model, a north-directed thrust fault has folded the Pennsylvanian Magdalena Group, forming an overturned syncline. A splay of that thrust fault has brought Ordovician Montoya Formation cherty dolomite against the Pennsylvanian rocks just north of Main Street; the overlying Percha Shale confining unit that should be above the Montoya Formation has been stripped away by erosion. Much of the downtown area consists of deformed Lower Paleozoic carbonates that are overlain by Quaternary to Tertiary coarse sand and gravel, fine sand, and clay (Fig. 3C). The clay-rich confining unit is discontinuous, as would be expected in a fluvial system. Proterozoic metasedimentary rocks are exposed south of downtown. Several minor NE-striking faults that contain manganese and calcite fills cut the Proterozoic basement and some of the manganese-enriched fluid leaked up into the Quaternary terrace gravels sitting on the basement rock along the river south of the VA Hospital.

This conceptual hydrogeologic model is not the only one possible for the hot-springs district. The immediate geothermal "reservoir" for the heated waters is the limestone underlying the district. Unfortunately, it is covered by 50 to 200 feet of Rio Grande alluvium, preventing field inspection. It is possible that, rather than Lower Paleozoic carbonate rocks, this unit is actually the Pennsylvanian Magdalena Group limestone. Theis et al. (1941) always referred to the carbonate rock encountered in drill holes as "Magdalena limestone." Unfortunately, no cores or cuttings from wells drilled into this unit have been preserved for inspection or geochemical analyses, which might answer the question. We feel that the interpretation that the "geothermal reservoir rock" is Lower Paleozoic limestone makes more sense from the perspective of the geological structure (Kelley and Silver, 1952; Witcher, 1986; Lozinsky, 1987; Maxwell and Oakman, 1990), but the issue cannot be resolved without additional data. We will therefore refer to the "reservoir rock" as "Paleozoic limestone" without attempting to further specify the stratigraphy.

V. RESULTS

A. WATER LEVEL DATA

In the spring of 1939, Theis et al. (1941) measured water levels across the hot-springs district (black contour lines, Fig. 4). Theis et al. (1941) installed a series of shallow piezometers around the hot-springs district in order to construct their water-table map. Water-table elevations were found to be higher than the Rio Grande with a southward-directed gradient. Because it seems likely that geothermal water production has increased substantially in recent decades, one might expect that the water table within the hot-springs district may have declined. In the Theis et al. (1941) study, elevations were surveyed in based on local sea-level elevation. Almost all of the wells used by Theis et al. (1941) to construct their water-table map no longer exist.

In this study, we used a network of existing monitoring wells and production wells. We conducted a differential GPS survey to obtain centimeter-scale accuracy for well elevations (Table 3, Appendix 1 and 2). Fortunately, one well (TC-13) surveyed by Theis et al. (1941) still exists today that allowed us to determine a common datum for our 2013 water table map. We computed a water-table map using 21 wells. All of the water levels were measured on the same day (March 22, 2013). This is very close to the day of the year that Theis measured his water levels (March 29, 1939). While measurements were made on non-pumping wells, it was not known if wells at nearby

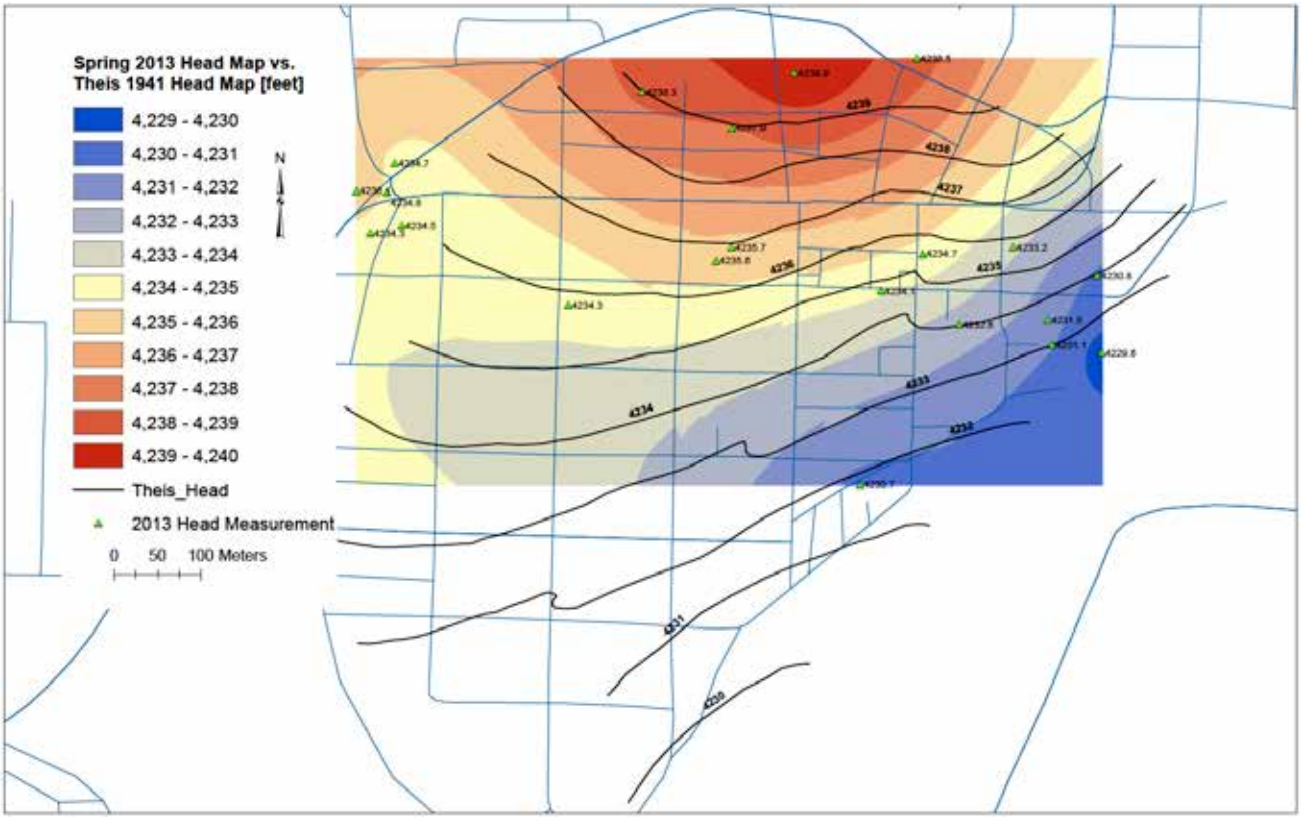

Figure 4–Comparison of measured water table configuration within the Truth or Consequences hot-springs district presented by Theis et al. (1941) (black lines with head contours in feet) and those measured in spring, 2013(colored contours). The green triangles are wells used to construct the 2013 map.

Table 3–Elevation of wells used to construct water table contour map.

ID	Elevation (m)	Elevation (ft)	Notes
TC-2	1291.19	4236.17	TOC
TC-12	1294.48	4246.97	TOC
TC-13	1292.40	4240.17	Land surface elevation
TC-19	1293.88	4245.00	TOC
TC-20	1293.72	4244.50	TOC
TC-21	1293.38	4243.36	TOC
TC-22	1293.12	4242.51	TOC
TC-25	1295.33	4249.78	TOC
TC-26	1294.24	4246.18	TOC
TC-28	1294.85	4248.18	TOC
TC-30	1295.52	4250.38	TOC
TC-31	1294.64	4247.49	TOC
TC-37	1293.47	4243.66	TOC
TC-38	1293.45	4243.60	TOC
TC-46	1292.82	4241.53	TOC
TC-48	1293.14	4242.59	TOC
TC-51	1293.04	4242.26	TOC
TC-52	1294.67	4247.59	TOC
TC-58	1294.50	4247.05	TOC
TC-60	1293.73	4244.53	TOC
TC-61	1293.57	4244.00	TOC
TC-62	1470.24	4823.63	TOC
TC-63	1292.75	4241.29	TOC
TC-66	1375.57	4510.56	TOC
TC-67	1293.23	4242.89	TOC
TC-74	1317.95	4323.98	TOC
TC-77	1324.05	4344.01	TOC

TOC = Top of casing

spas or residences were pumping when we collected water level measurements. The green triangles denote the wells used in producing the 2013 water table contour map. The 2013 water table contour map (color contours, Fig. 4) is nearly identical to the Theis et al. (1941) map (black lines) in terms of water-table patterns. However, the 2013 water levels shown in Figure 4 are generally about one foot less than those in 1939, and on the east side of the mapped area, about two feet less. Whether this difference is significant is unclear. It constitutes about 10% of the total head difference between the western water-table mound and the elevation of the Rio Grande. As described above, today's wells are on average about 50 feet shallower than those of Theis' time. This will produce shallower heads. Modern heads vary seasonally by between four feet (near the Rio Grande) and one foot (distant from the Rio Grande). Thus the differences we observe in Figure 4 could represent natural variability in an essentially stable system, or a small but significant long-term decline due to pumping. In any case, we do not observe a major or catastrophic water-table decline.

We also installed a series of pressure transducer-data loggers in several wells within the hot-springs district. These wells were located at different lateral distances from the Rio Grande (Fig. 5). One transducer was placed within the Rio Grande (TC-504; Fig. 5). Water levels were recorded every two hours for the duration of the project (Fig. 6). Gaps in data reflect equipment malfunctions. We saw no consistent trends of declining water levels during the one-year project period in any of the wells. Water levels are well-correlated with the stage height of the Rio Grande. The amplitude of water-level fluctuations decreases with increasing distance from the river (Rorabaugh, 1964). The pressure transducers also measured temporal changes in groundwater temperature (Fig. 7). Temporal changes in groundwater temperature are complex, with some wells showing a seasonal pattern of increasing temperature during summer months, while others are inversely correlated to season. One well close to the Rio Grande appears to show temperature changes that reflect variations in river stage.

B. TEMPERATURE DISTRIBUTION

Theis et al. (1941) presented a contour map of Truth or Consequences hot-springs-district temperatures reported at discharging wells and springs (black contour lines, Fig. 8). We developed contour maps of temperature for monitoring wells (i.e., wells with no pumps in them; temperature measured just below water table; color contour patterns, Fig. 8A) and producing wells (wells that were pumped; colored contour patterns, Fig. 8B) within the hot-springs district. Geothermal waters were produced from the Paleozoic limestone reservoir as well as in the shallower alluvial sediments. Theis et al. (1941) reported that in March 1939, temperatures ranged between 99 and 114°F (36.6–45.6°C) within the hot-springs district. In 2013, the shallow alluvial wells have maximum temperatures of 46.1°C. Thermal waters were restricted to a relatively small region of about 750 m by 750 m (2460 by 2460 ft). Current measured temperatures are cooler than those that Theis et al. (1941) measured by about 3 to more than 10°F. (Figs. 1B, 8B).

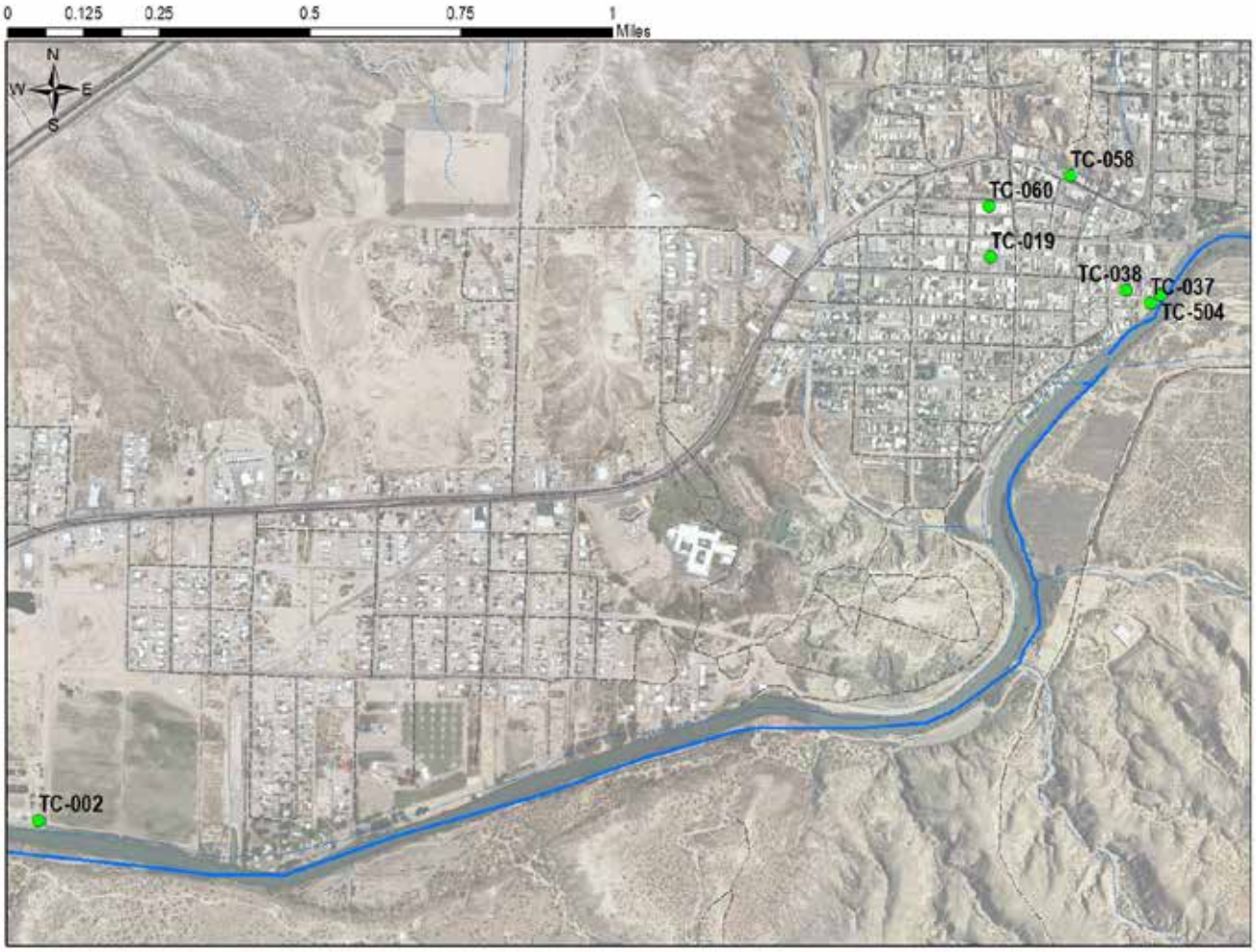

Figure 5–Location of wells in hot-springs district where continuous water level measurements were collected using data logger/pressure transducers.

However, it is important to note that the wells were deeper in the 1930s, on average, than modern wells (Fig. 1A). Most wells were typically completed in the lower Paleozoic limestone in the 1930s whereas most modern wells are completed in the unconsolidated alluvium of the Palomas Formation (Santa Fe Group). This biases modern well temperatures toward cooler values. It is also important to note that the two contour maps created decades apart were based on different wells. In 2013, we did not have access to any wells located in the center of the high-temperature "bull's eye" from the Theis et al. (1941) contour map. Whether this is a matter for concern is difficult to ascertain. Without more modern wells in the deep aquifer it is not possible to determine the extent to which differences in the two maps can be attributed to differences in well construction as compared to changes in the hydrological system.

We were able to collect data from at least five wells that were originally drilled to depths of more than 150 ft, including TC-13, TC-17, TC-35, TC-56, and TC-72 (See Appendix 1 and 2). Three of these wells were originally drilled to depths of 205 to 219 feet, but these wells now have obstructions at depths of 20 to 144 ft. It is unknown what the cause of this change in well depth is, but it may be related to the corrosive nature and mineralization of the geothermal water in this region.

C. TEMPERATURE PROFILES

Temperatures measured as a function of depth in wells can be affected by regional heat flow, changes in surface temperature, and vertical movement of groundwater (Bredehoeft and Papadopoulos, 1965). Surface temperature decreases at higher elevation; thus wells in a conductive setting at lower elevation will have a higher surface temperature compared to those at higher elevations in a similar setting. Temperatures in boreholes can also be disturbed by fluid flow. Temperature-depth profiles that are concave

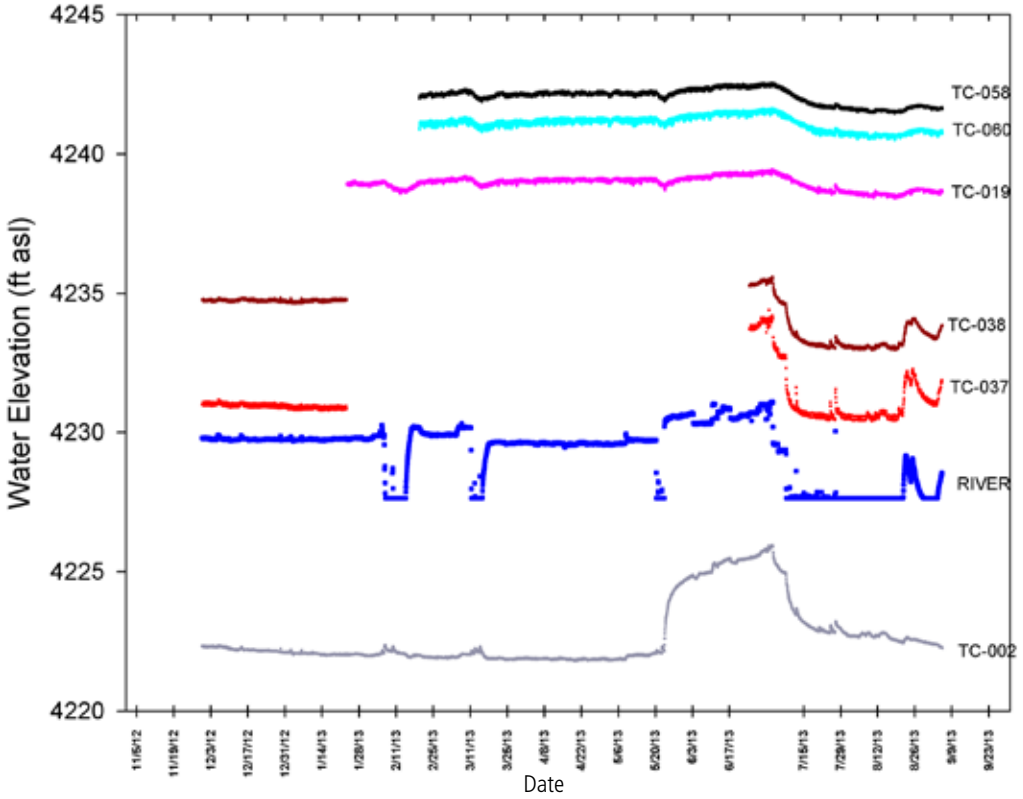

Figure 6–Water level fluctuations in wells and the Rio Grande near Truth or Consequences during project study period. River levels were monitored by TC-504 (Figure 5). TC-002, TC-037, and TC-038 are within 0.06 mile of the river and TC-019, TC-058, and TC-060 are about 0.3 miles from the river (Figure 5). Groundwater table elevation appears to mimic stream fluctuations. Amplitude changes decrease with distance away from the river.

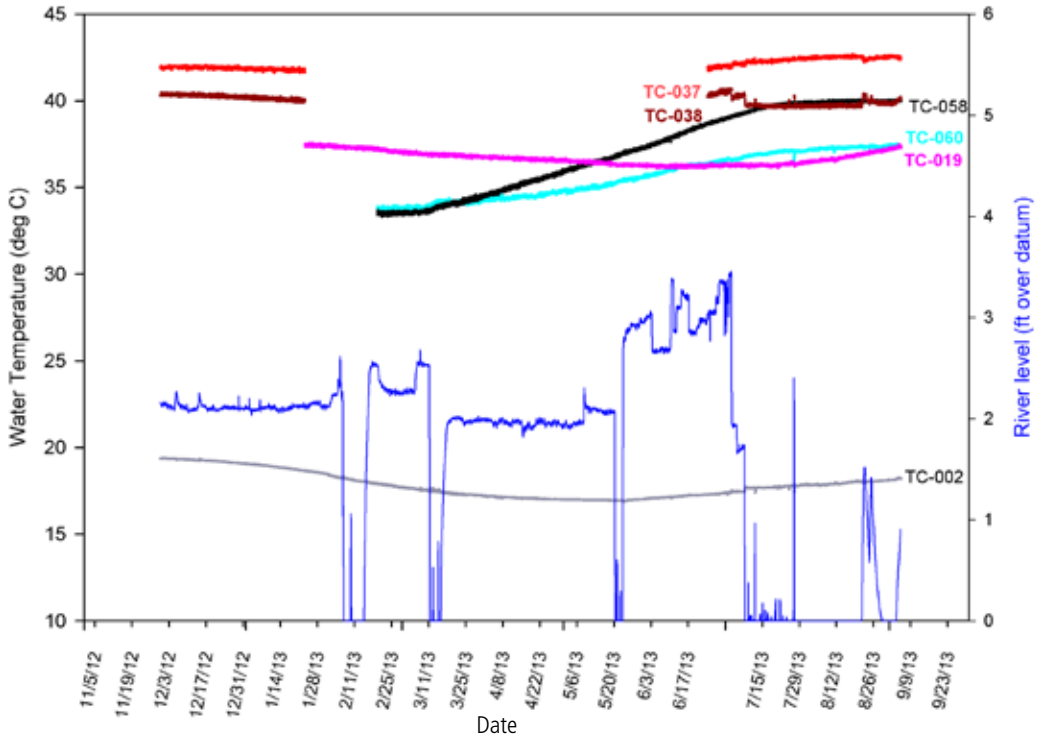

Figure 7–Water temperature fluctuations in wells and the Rio Grande near Truth or Consequences during project study period. Five of the six wells show a temperature increase during the spring and summer months. Only one well, TC-038, shows strong correlation to river stage. TC-037 located close to the river shows cooling during the 8/26/12 river level spike, while nearby TC-038 warms. The overall cooling of TC-019 was also observed in the repeat measurement of the thermal profile (Figure 12; Appendix 4).

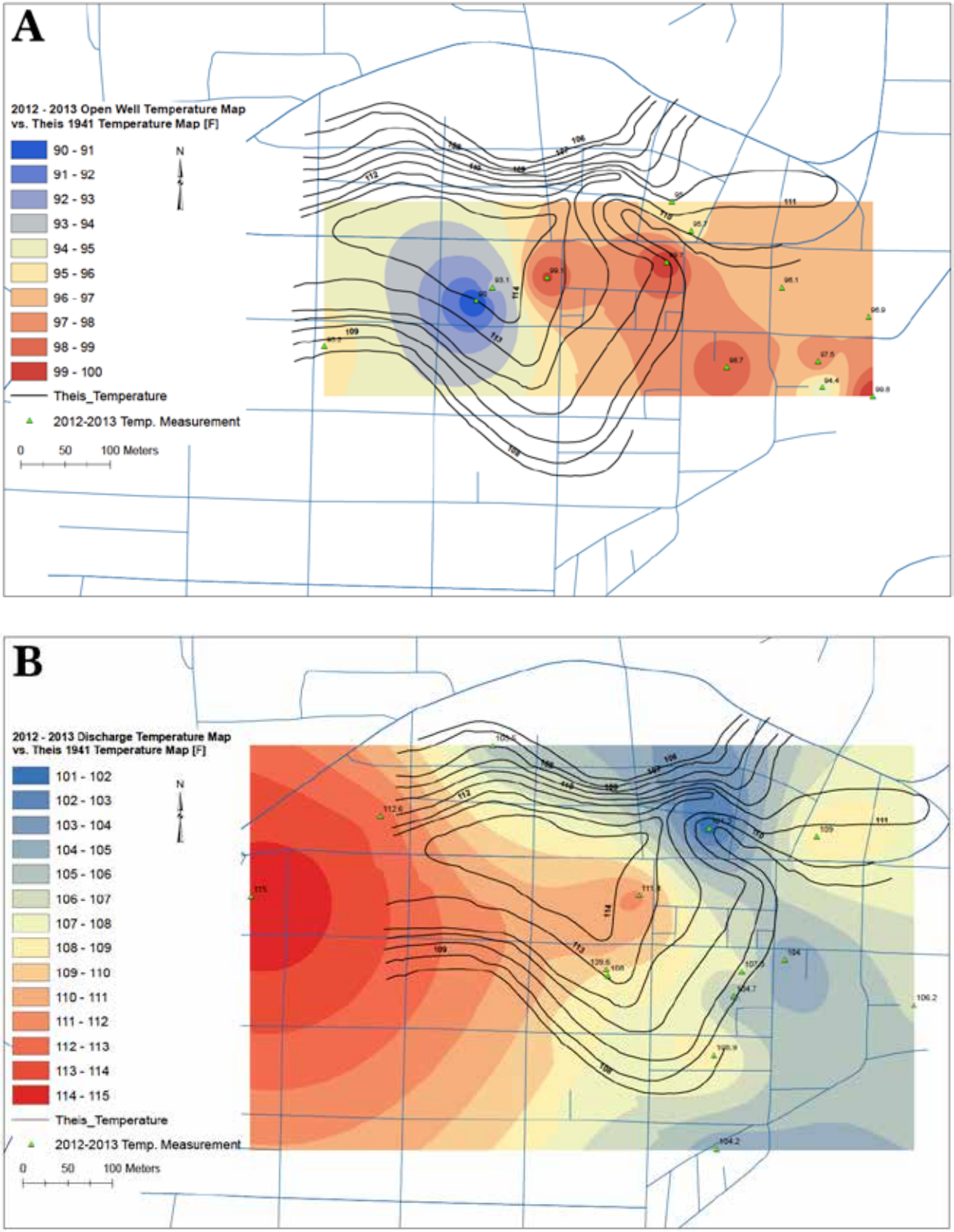

Figure 8–(A) Comparison of temperatures measured just below water table in monitoring wells (not pumped) during the fall of 2012 and the spring of 2013 (colored contours) within the Truth or Consequences hot-springs district with those presented by Theis et al. (1941; black lines with temperatures in °F) . (B) Comparison of measured temperatures from producing wells measured in 2012 and 2013 within the Truth or Consequences hot-springs district (colored contours) with those presented by Theis et al. (1941) (black lines with temperatures in°F).

upwards may indicate downward groundwater seepage; in other words, as water moves downward, the upper section intersected by the well is cooled (Wade and Reiter, 1994). In contrast, convex-up logs are associated with upward groundwater flow, where warm water from depth heats up the shallower part of the well (Wade and Reiter, 1994). Very high temperature gradients (>100°C/km) can result from upwelling related to deep-seated hydrothermal systems beneath the borehole. Water that enters the borehole from a discrete fracture or local aquifer commonly is manifested as an abrupt increase (warm water) or decrease (cool water) in temperature. Depending on the construction of the well and relative hydraulic head among aquifers, water that enters a borehole can travel up or down the hole and then leave the borehole at a fracture or local aquifer that has a lower hydraulic head, resulting in another abrupt change in temperature. In another case, warm water traveling laterally in an aquifer through or around a borehole can cause a high gradient above the aquifer, an isothermal zone within the aquifer, and a reversal of gradient and gradual adjustment to background gradient below the aquifer. A relatively straight log implies a conductive thermal regime. Conductive logs commonly have an abrupt kink in geothermal gradient caused by changes in rock type and associated thermal conductivity. Also, a gradual increase in thermal conductivity with depth may cause a convex-up log, and a gradual decrease in conductivity with depth can result in a concave-up temperature profile (Wade and Reiter, 1994).

Seventeen wells were logged as a function of depth using a truck mounted logging system built by Reiter et al. (1980) using a thermistor with an accuracy of 0.1°C at one meter intervals. Five wells located in buildings or inaccessible by road were logged using a handheld system with temperatures read directly using a rugged reader. Here the data were gathered on two to three meter intervals and the precision of the measurements was 0.1°C.

The locations of the wells logged within the hot-springs district as part of this study are shown in Figure 9 and are tabulated in Table 4. Three types of wells were logged:

1) Capped, cased wells that have not been pumped since drilling for one to five years. This type of well was best for documenting the "equilibrium" temperature of the system, although in this case the system is so dynamic, the term "equilibrium" is a bit of a misnomer.

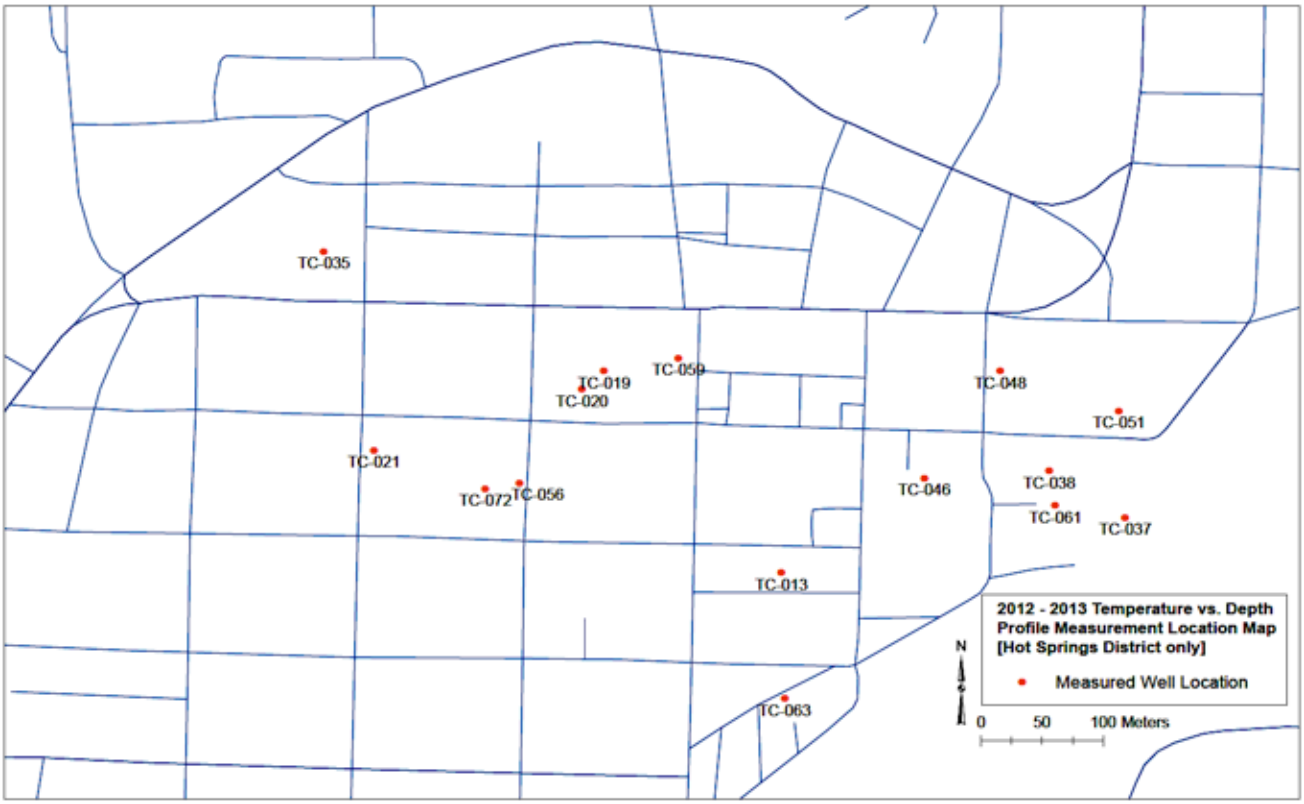

Figure 9–Location of wells in the Truth or Consequences hot-springs district where temperature-depth profiles were measured. Data provided in Appendix 4.

Table 4–Summary information for wells with thermal profiles. UTM NAD83 location data provided in Appendix 1.

Point ID	Elevation (ft.)	Elevation (m)	Original Well Depth (ft)	Original Well Depth (m)	Logged well depth (m)	Drill date	Date measured	Maximum temperature (°C)	Top casing slots (ft.)	Top casing slots (m.)	Rock unit top (ft.)	Rock unit top (m.)	Rock type
TC-013	4239	1292	177.0	53.9	53.0	3/24/1962*	12/5/2012	42.69	no slots		1	0.30	fill
											42	12.80	clay
											100	30.48	conglomerate
											154	46.94	sandstone
											176	53.64	sand
TC-019	4249	1295	42.0	12.8	12.0	8/11/12	11/16/2012	40.68	22	6.71	0	0.00	fill
							9/5/2013	39.60			9	2.74	sand, gravel, boulders
TC-020	4249	1295	40.0	12.2	12.0	8/4/06	11/16/2012	37.99	30	9.14	0	0.00	sand
							9/5/2013	37.87					
TC-021	4251	1296	40.0	12.2	11.5	6/30/06	12/5/2012	42.42	30	9.14	0	0.00	sand
							9/5/2013	42.70					
TC-035	4255	1297	208.0	63.4	6.7	1930s	1/4/2013	22.12	n.d.	n.d	n.d.		n.d.
TC-037	4235	1291	60.0	18.3	17.0	8/12/10	11/16/2012	42.86	40	12.19	0	0.00	coarse sand and gravel
							9/5/2013	43.30			17	5.18	rocks
											21	6.40	sand, gravel, rocks
											45	13.72	clay
											50	15.24	silty sand
TC-038	4536	1383	69.0	21.0	18.0	5/28/07	11/16/2012	42.08	40	12.19	0	0.00	sand and gravel
							9/5/2013	42.42			53	16.15	brown clay
TC-046	4239	1292	47.0	14.3	13.5	4/10/06	12/5/2012	43.80	25	7.62	0	0.00	fill
							9/5/2013	43.93			7	2.13	sand
											23	7.01	coarse sand and gravel
											31	9.45	coarse gravel
											42	12.80	red-brown clay
TC-048	4239	1292	42.0	12.8	12.0	7/9/12	12/5/2012	42.78	22	6.71	0	0.00	fill
											9	2.74	sand, gravel, boulders
TC-051	4236	1291	50.0	15.2	14.5	8/20/00	12/5/2012	42.81	40	12.19	0	0.00	sand
											10	3.05	gravel
TC-056	4249	1295	205.0	62.5	44.0	1/1/38	12/18/2012	42.60	n.d.		n.d.		
TC-059	4247	1294	48.0	14.6	9.7	8/22/06	1/4/2013	44.10	38	11.58	0	0.00	sand
TC-061	4236	1291	69.0	21.0	21.0	2/4/09	12/5/2012	41.91	49	14.94	0	0.00	coarse sand and gravel
							9/5/2013				32	9.75	gravel and sand
											40	12.19	gravel, sand and clay
TC-063	4236	1291	100	30.5	30.0	1/18/10	1/8/2013	40.57	20	6.10	0	0.00	conglomerate
											6	1.83	rocks, sand, gravel
TC-066	4543	1385	n.d.	n.d.	26.0	n.d.	1/8/13	20.45	n.d.	n.d.	n.d.	n.d.	n.d.
TC-072	4249	1295	219	66.8	24.1	10/18/49	2/19/13	41.39			0	0.00	Sand
											54	16.46	Clay
											94	28.65	clay and gravel
											149	45.42	red rock
TC-073	4232	1290	90	27.4	26.6	n.d.	2/19/13	20.04	n.d.	n.d.	n.d.	n.d.	n.d.
TC-074	4321	1317	>7	>2.1	2.1	n.d.	2/19/13	24.37	n.d.	n.d.	n.d.	n.d.	n.d.
TC-078	4721	1439	720	219.5	12.0	2004?	3/22/13	19.89	n.d.	n.d.	n.d.	n.d.	n.d.
TC-079	4257	1298	73	22.3	22.0	n.d.	3/23/13	20.19	n.d.	n.d.	n.d.	n.d.	n.d.
TC-080	4271	1302	35	10.7	10.6	n.d.	3/23/13	20.75	n.d.	n.d.	n.d.	n.d.	n.d.

* Owner states this well was originally drilled in 1930's.

2) Wells with surface jet pumps that are in use. These wells produced water the day before measurement (e.g., TC-056, TC-063, TC-072)

3) One flowing artesian well (well that flows above the land surface without a pump)

Produced-water temperatures were measured during water sampling of pumped wells that could not be logged using the thermistor. Producing wells have higher temperatures and near isothermal profiles. In general, for wells that are not producing, there is an increase of temperature with depth with steepest gradients near the water table (Fig. 10). Curvature in the temperature profiles near the water table suggests vertical flow.

We separated the analysis of temperatures in wells located along Austin Street into two clusters based on spatial proximity to one another (Fig. 11). The wells in each cluster are within tens of meters of each other and the two clusters are about 400 m (~1300 ft) apart. Three of the four wells in the eastern cluster near the Rio Grande show a slight decline in temperature as a function depth near the bottom of each well. This slight roll-over is interpreted to be caused by lateral flow through a thin-to-thick (2-12 m; 6-39 ft) interval of sand and gravel in the shallow aquifer above a finer-grained, less-permeable, interval composed of clay or silt. The top of the zone of lateral flow does not necessarily coincide with the perforated interval, so the water may be slowly flowing around both the cased and perforated parts of the wells. The slight decline in temperatures near the bottom of the well does coincide with reports of clay or silty sand near the bottom of the two of the wells (TC-037 and TC-038). The driller's log for TC-061 mentions clay below about 12.2 m (40 ft), but the exact depth to the top of the clay is not described. Based on the temperature log, the top of the finer-grained material may be at about 19 m (62 ft). The high projected surface temperatures of 32-36°C indicate that upflow is also an important process in controlling the shape of the thermal profiles in these wells (Table 4, 2-3 m/yr; 6-10 ft/yr). Alternatively, the slight roll-over could be related to an incursion of slightly cooler Rio Grande water just above the fine-grained interval superimposed on an overall upwelling thermal regime. Drilling to depths greater than 70 m (230 ft) through and below the roll-over is needed to distinguish between the hypotheses.

In contrast, the western cluster profiles show pronounced lateral flow of warm water along a narrow zone into the bottom of these wells (TC-019, TC-020, TC-021). The lateral flow does not coincide with the perforations, so the warm water is entering the wells

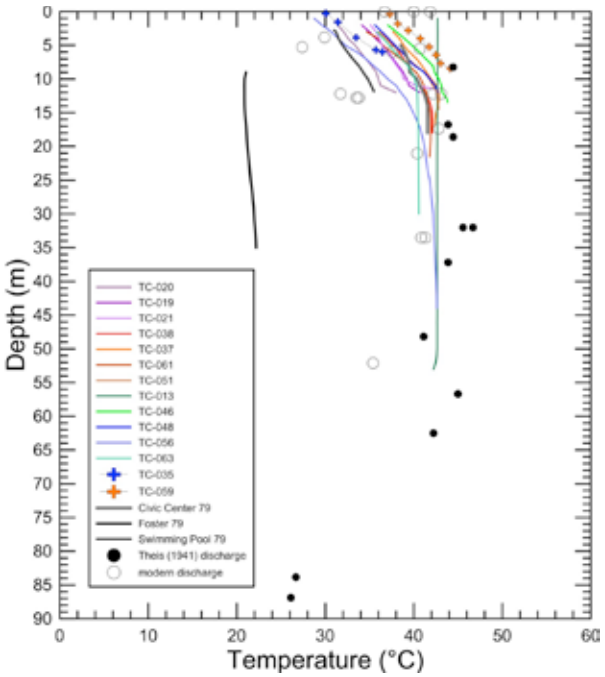

Figure 10–Plot of representative thermal data from the downtown area. The colored lines are data collected during this study by the truck-mounted system; the colored points were collected during this study by the hand-portable system, the gray lines are temperature data from Wells and Granzow (1981) measured in 1979; the black dots are discharge temperatures from Theis et al. (1941) and open circles are discharge temperatures measured during this study. One of the Wells and Granzow logs (Foster) was collected to the northeast of the downtown area, and two of the cool, deep Theis et al. 1941 points are from city wells measured near Williamsburg. The hottest temperatures are in TC-059 near the north edge of downtown and the temperatures are generally cooler toward the south (Swimming pool 79).

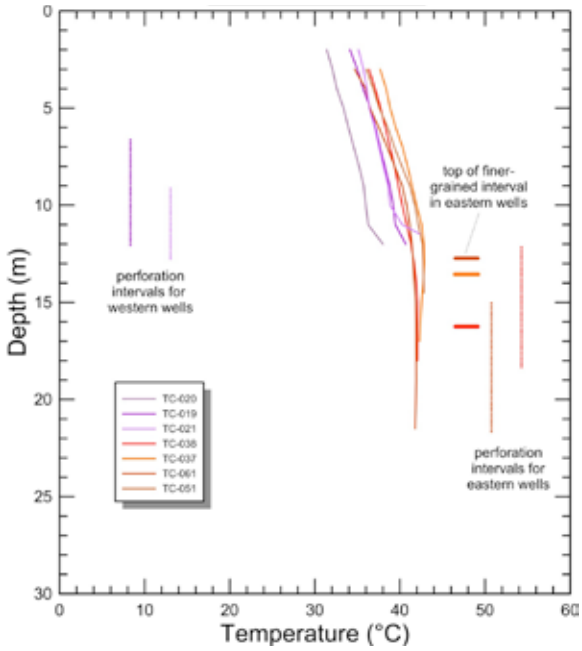

Figure 11–Temperature-depth profiles from two clusters of wells located on Austin Street that are open, capped boreholes with no pumps.

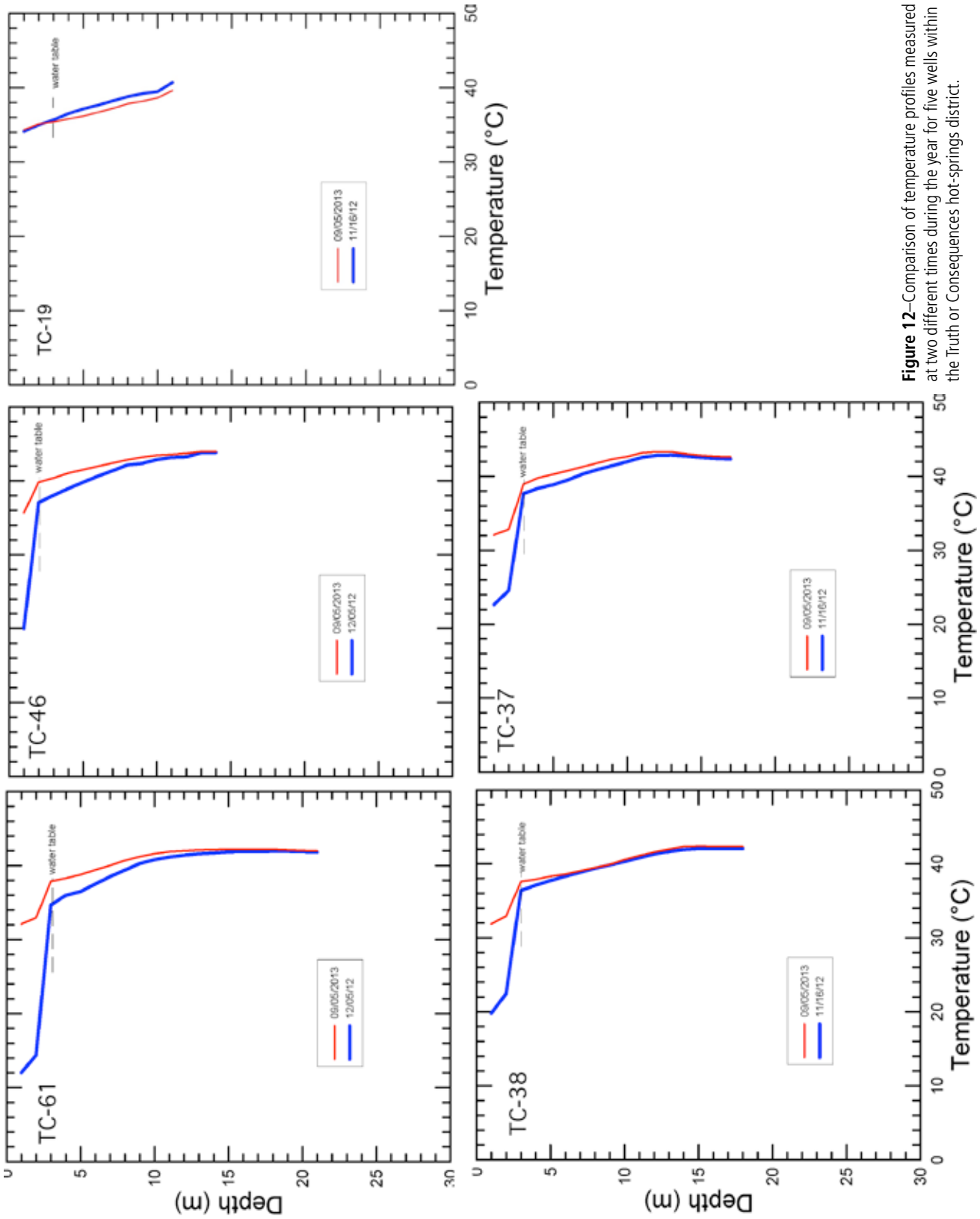

Figure 12–Comparison of temperature profiles measured at two different times during the year for five wells within the Truth or Consequences hot-springs district.

through a permeable interval within the rocks below the top of the perforated interval, either through a sandy or conglomeratic unit or along a fracture. Clay is not mentioned in the driller's logs. The difference in flow regime between the eastern and western clusters could be caused by a fault or by a facies change (change in the type of sediment) in the rocks forming the shallow aquifer between the two clusters.

Comparison of temperature profiles collected within the late fall of 2012 and late summer of 2013, suggest the groundwater flow conditions are not changing in the deeper part of the flow system beneath the eastern cluster of wells (Fig. 12). The difference in the shallow part of the profiles is primarily caused by seasonal changes. We did measure a temperature decrease of 1°C at the bottom of TC-019 and a 0.1°C decline in nearby TC-20 in the western cluster between 2012 and 2013, which corresponds to the temperature decrease recorded by the data logger over the same time period (Fig. 7).

D. PECLET-NUMBER ANALYSIS

Curvature in well temperature profiles can be used to estimate vertical flow rates. We conducted a curve-matching exercise using the analytical solution of Bredehoeft and Papadopoulos (1965) to estimate the vertical flow rates. This solution is formulated in terms of a dimensionless number known as the 'Peclet Number'. These authors solved the following steady-state conductive/convective heat-transfer equation:

$$\lambda \frac{\partial^2 T}{\partial z^2} = \rho_f c_f q_z \frac{\partial T}{\partial z} \qquad (1)$$

where T is temperature, z is elevation, λ is thermal conductivity, ρ_f is fluid density, c_f is fluid heat capacity, and q_z is the vertical groundwater flux. The solution to this differential equation subject to two specified temperature boundary conditions ($T(z/L=0) = T_1$, $T(z/L=1) = T_2$)is given by:

$$T(Pe, z/L) = \frac{\exp(\frac{P_e z}{L}) - 1}{\exp(P_e) - 1} \qquad (2)$$

where Pe is the Peclet number, L is the distance over which flow occurs, z is height above a datum, and T_1 and T_2 are the specified temperatures at the top and bottom of the system. The Peclet number is a dimensionless number that defines the ratio of convective to conductive heat transfer ($Pe = L\rho_f c_f q_z/\lambda$) where ρ_f is the fluid density (1000 kg/m^3), c_f is the fluid heat capacity (4180 J/kg), q_z is the vertical groundwater flow rate (m/yr), and λ is the bulk thermal conductivity of the sediments (2 W/m-°C). Note that L and the maximum temperature (T_2) must be assumed. Here we used the maximum temperature in the well bore for T_2 and 50 m for L. T_1 was taken as the water-table temperature. The Pe equation can be rearranged to solve for the groundwater flux (q_z). Figure 13 shows examples of the best-fit Peclet number (Pe) analysis.

Table 5–Peclet number analysis of select wells.

Well ID	Pe (-)	L (m)	Vertical velocity (m/yr)
TC-046	-2	11.5	2.6
	-11	50	3.3
TC-048	-0.5	10	0.7
	-12	50	3.6
TC-051	-2	11.5	2.6
	-13	50	3.9
TC-056	-6	50	1.8
TC-059	-0.5	8.1	0.9
	-10	50	3
TC-063	-9	27	5
	-13	50	3.9
TC-072	-3	22.6	2
	-8	50	2.4
TC-037	-2	14	2.2
	-10	50	3
TC-038	-2	15	2
	-10	50	3
TC-061	-4	18.5	3.2
	-10	50	3

We found that the best-fit Pe ranged between 5.5-13 providing calculated velocities of two to four meters per year (6-13 ft/yr; Table 5).

E. GEOTHERMAL DISCHARGE ESTIMATE

Theis et al. (1941) measured changes in Rio Grande discharge and salinity above and below the hot-springs district to estimate the total flux of geothermal discharge. They were able to do this because the geothermal waters within the hot-springs district are much more saline than shallow groundwater. The average total dissolved solids concentration measured by Theis et al. (1941) was about 2475 mg/L. Today, based on our measurements, the total dissolved solids concentration is about 2573 mg/L. Theis et al. (1941) used the following mass balance model to estimate the geothermal discharge:

$$Q_T c_T = Q_{hs} c_{hs} + Q_{RG} c_{RC} \qquad (3)$$

where Q_T and c_T are the downstream discharge and concentration of the Rio Grande, respectively; Q_{hs} and

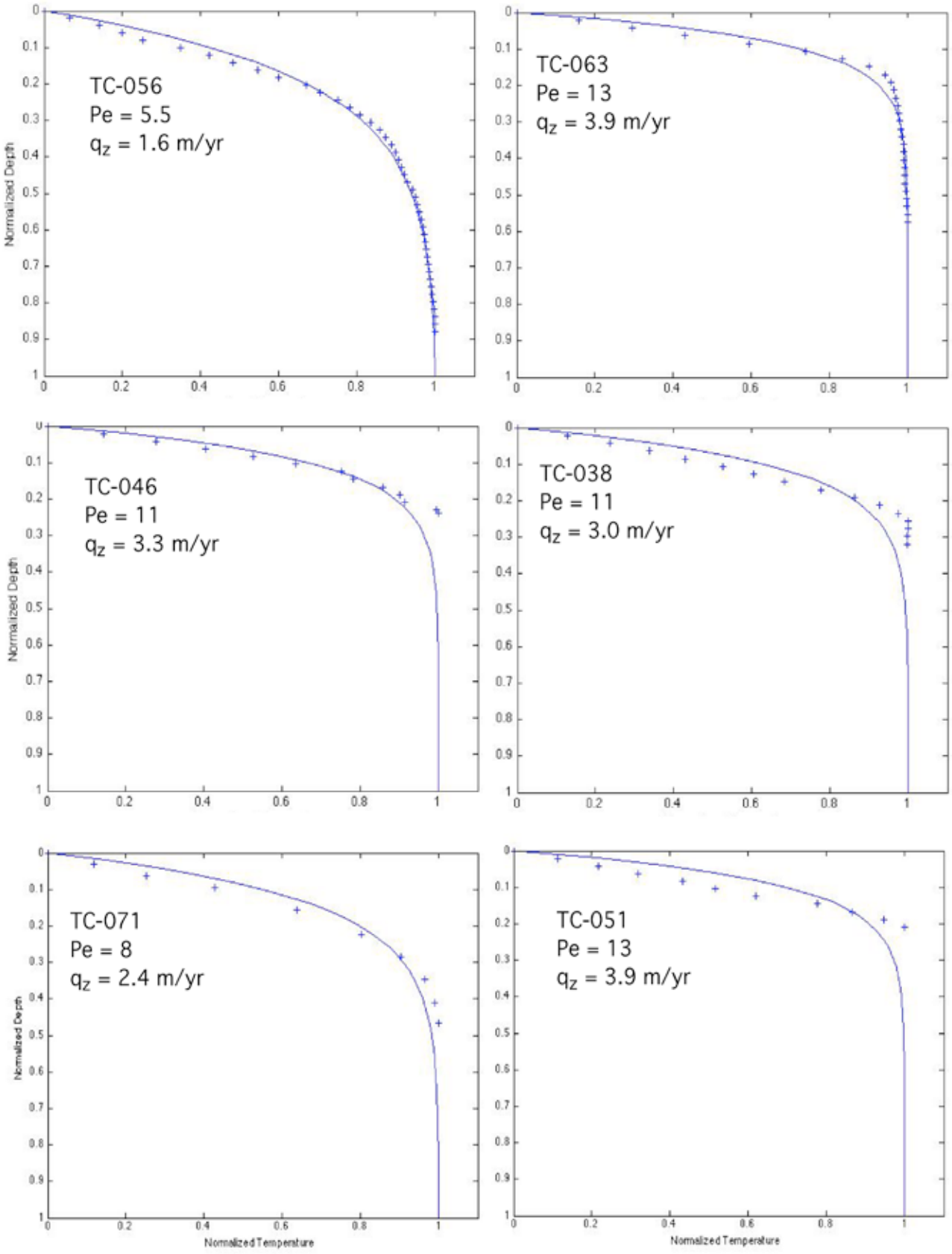

Figure 13–One-dimensional Peclet (Pe) number analysis of select wells from Truth or Consequences hot-springs district (Table 5). See text for explanation.

c_{hs} are the discharge and concentration of geothermal water from the hot-springs district, respectively; and Q_{RG} and c_{RG} are the discharge and concentration of the Rio Grande upstream of Truth or Consequences, respectively. The only unknown in equation (3) is Q_{hs}. Theis et al. (1941) rearranged equation (3) to solve for for Q_{hs} and found geothermal discharge to range from 2.9 to 3.5 cubic feet per second or 1.8 to 2.2 million gallons per day (about 7100 to 8500 m^3/day) after adding contributions they measured from the hot water drain in town. Theis et al. (1941) assumed that the geothermal water was discharging into an area of about one quarter mile radius (about 500,000 m^2). This yielded a vertical discharge velocity of about 20 ft/yr (6 m/yr). This exceeds our median estimate of 8 ft/yr (2.5 m/yr), based on the Peclet number analysis of the temperature profiles, by a factor of over two. However, neither of these estimates are highly precise. The area estimate by Theis et al. (1941) appears to be rather

Table 6–Estimates of hot spring's district discharge using Rio Grande salinity and stream gauging. In these measurements, chloride concentration and specific conductance are used as a proxy for total salinity.

Study	Discharge (cfs)	Cl Conc./ Conductance	Date	Comments
DOWNTOWN ABOVE HOT WATER DRAIN				
Theis 1941	1.46	1300 ppm	11/29/1939	Measured upstream of hot water drain and slightly upstream hot-springs district
This Study	2.15	4997.4 µS	08/05/2013	Measured upstream of hot water drain and slightly upstream hot-springs district
HOT WATER DRAIN				
Theis 1941	1.45	Not Applicable	11/29/1939	
Theis 1941	2.10	Not Applicable	04/09/1940	6:20 pm, maximum daily stage at this time and date was near annual maximum flow
This Study	0.24	Not Applicable	07/23/2013	
HOT WATER DRAIN PLUS DOWNTOWN				
Theis 1941	2.91	1300 ppm	11/29/1939	Using 1.45 drain measurement
Theis 1941	3.56	1300 ppm	04/09/1940	Using 2.10 drain measurement
This Study	2.39	4997.4 µS	08/05/2013	
BELOW WASTEWATER TREATMENT PLANT				
This Study	3.33	4997.4 µS	07/23/2013	Measured downstream of WWTP and well upstream of city

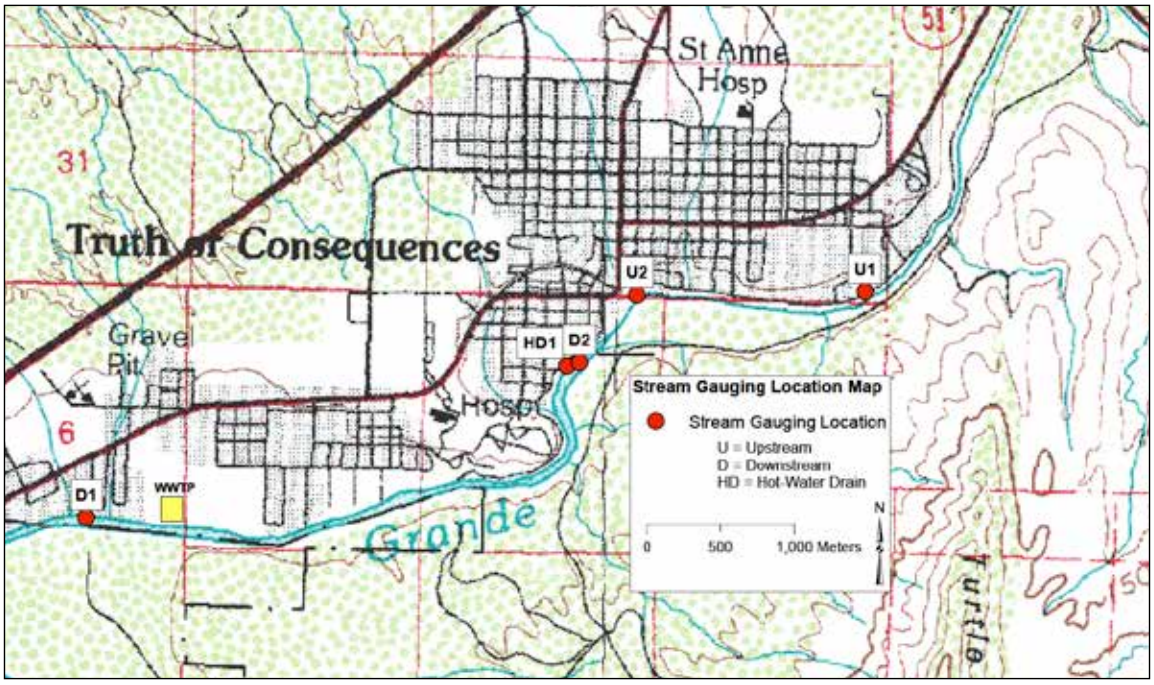

Figure 14–Stream gauging locations used to determine volume of geothermal discharge from the Truth or Consequences hot-springs district (Table 6).

minimal; increasing the area by a factor of two would bring the two estimates into fairly good agreement.

On August 5, 2013, we estimated the natural geothermal discharge to the Rio Grande following the approach of Theis et al. (1941; Table 6) and measured a similar flow rate of 2.4 cfs. Doing the same procedure on July 23, 2013 with our upstream station above the hot-springs district and our downstream station below the wastewater treatment plant yielded a flow rate of 3.3 cfs, providing a discharge range of 2.4 to 3.3 cfs for this study. The locations of our stream discharge and salinity measurements are shown in Figure 14. Since the measurement error of stream velocity measurements is at least 10%, there is no statistically significant difference between our measurements of hot-springs-district discharge and that of Theis et al. (1941). It is worth noting that discharge contributions from the hot water drain measured on August 5, 2013 were much less than those measured by Theis et al. (1941), possibly suggesting discharge is reaching the stream by other means (Table 6). The apparently lower flow velocity derived from the temperature-profile analysis may be consistent with the total discharge estimates from both Theis et al. (1941) and our similar estimate derived using the same method if a significant fraction of the total geothermal discharge is now through wells rather than natural seepage into the river.

F. GROUNDWATER RESIDENCE TIMES

The ^{14}C samples were collected within and adjacent to the hot-springs district to assess groundwater residence times. Shallow circulation within alluvial deposits will generate ages of less than 100 years. We hypothesize the groundwater ages must be relatively old (greater than 1000 years) in order to accommodate deep (greater than 1.25 miles, or 2 km) geothermal circulation. In contrast, slow-flowing groundwater will result in very old groundwater ages and conductive cooling as groundwater rises towards the discharge area. Within the Truth or Consequences hot-springs district, uncorrected carbon-14 groundwater ages range between 4,040 to 11,480 years old (Fig. 15). To the north, groundwater ages are younger within the alluvial deposits.

G. GROUNDWATER GEOCHEMISTRY

Data on the geochemistry of the waters in the hot-springs district goes back at least to Theis et al. (1941). This is fortunate, as shifts in the geochemistry have potential to be one indication of

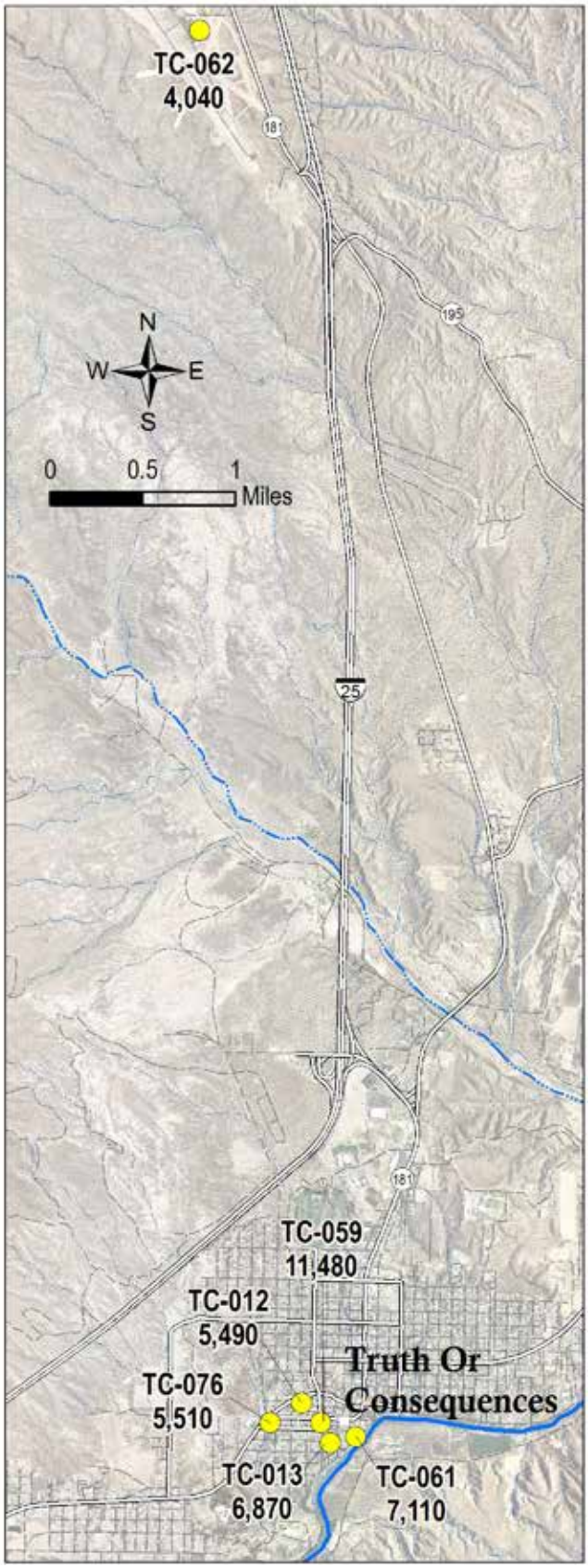

Figure 15–Groundwater residence time based on uncorrected ^{14}C ages in years.

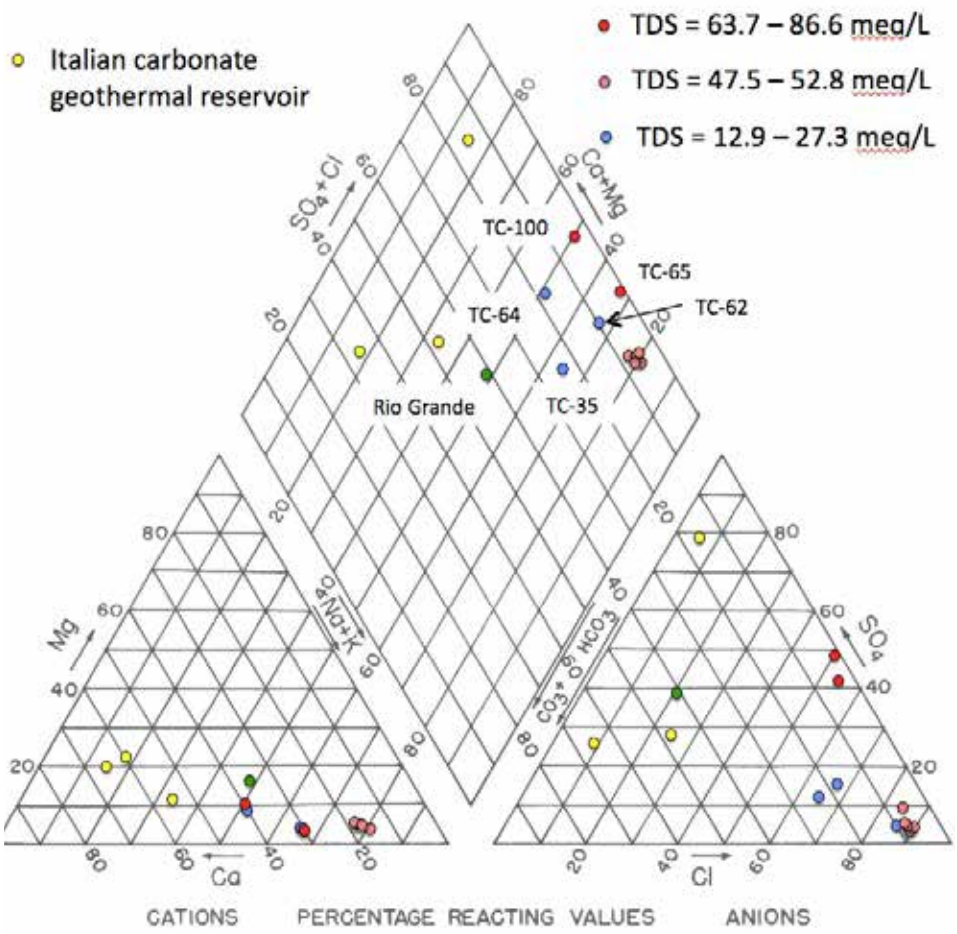

Figure 16–Piper plot of geochemical analyses of waters from in and near the hot-springs district in Truth or Consequences, the Rio Grande just upstream from Truth or Consequences (green dot) and comparative data from a geothermal reservoir in carbonate rocks in Italy, from Chiodini et al. (1995) (yellow dots).

exploitation-induced changes in the system. Geochemical data, both from this study and from previous ones, are given in Appendix 3 of this report. The data are summarized on a 'Piper plot' in Figure 16. This standard type of graph relies on the fact that all waters must be in a state of electrical neutrality: that the sum of electrical charges from anions must balance the sum of the charges from cations. The concentrations of the ions are reduced to the percentage they contribute to the total anion or cation charge per unit volume.

The great majority of the geothermal waters have total dissolved solids (TDS) contents of about 50 milliequivalents per liter (meq/L) and are shown with brown dots in Figure 16. (A milliequivalent is the electrical charge possessed by 1/1,000 of a mole of an ion having a unit charge, such as Cl^- or K^+.) This is equivalent to about 2,600 ppm, which is fairly high salinity. For comparison, the United States Environmental Protection Agency secondary (i.e., recommended, not enforced) limit for total dissolved solids concentration for drinking water is 500 ppm.

The analyses of the great majority of geothermal waters are very similar, such that most of them plot on top of each other in Figure 16. They are classified as sodium-chloride (Na^+–Cl^-) waters. We have also plotted an analysis of Rio Grande waters using a green dot in Figure 16, for comparison. The sample was collected from the Rio Grande below Elephant Butte Dam. In contrast, the Rio Grande has a mixed Na^+–Ca^{2+} cation composition, anions dominated by HCO_3^- and SO_4^{2-}, and is relatively dilute. There are several water samples that have salinities intermediate between the geothermal waters and the Rio Grande; they are shown by blue circles on Figure 16. They tend to lie between the geothermal and Rio Grande data points, which may indicate that they are a result of mixing of the geothermal and Rio Grande end members.

In addition to the classical Truth or Consequences geothermal waters (brown dots), two samples of differing composition are shown using red dots. These are mildly geothermal waters (~20°C) with significantly higher concentrations of Ca^{2+} and SO_4^{2-} than the classic geothermal waters, but otherwise similar composition.

They are both from the part of Truth or Consequences in the Cuchillo Negro drainage that is north of the hot-springs district.

The Na^+–Cl^- composition of the classic Truth or Consequences geothermal waters is characteristic of high-to-moderate temperature geothermal fluids in igneous rocks (Kühn, 2004). The Na^+ is known to be derived from rock alteration reactions at relatively high temperatures and the Cl- is released from fluid inclusions as the rock is altered (Ellis and Mahon, 1964; Ellis and Mahon, 1967). Above we have hypothesized that the distribution of sample compositions in Figure 16 may be influenced by mixing of dilute surficial water (most likely derived from the Rio Grande) with a more concentrated geothermally-derived water. We further explore this below by plotting a number of parameters that are closely associated with typical geothermal waters against the concentration of Cl^-. If the constituents show covariation with the Cl^- concentration, this would support a pattern of dilution of water from the geothermal source.

All three geothermally associated parameters tend to co-vary in a linear fashion with Cl^- (Fig. 17). The anomalously saline wells north of the hot-springs district in some cases do not follow the general trend. The temperatures are lower than the trend and the boron content is higher. The lower temperature suggests that these waters have undergone additional cooling during a slower ascent from depth than the geothermal waters, and that at least one of them has had boron added due to contact with a lithology not present under the hot-springs district, most likely shale. However the covariation of the remaining samples with Cl^- strongly supports the hypothesis that the hot-springs district is supplied by a geothermal aquifer of quite homogeneous composition that is in places diluted by cool surficial water with a composition similar to that of the Rio Grande.

In Figure 18, we plot against Cl^- the concentrations of two constituents that are not commonly associated with moderate-to-high temperature geothermal waters in igneous rocks: HCO_3^- and SO_4^{2-}. Unlike the constituents plotted in Figure 17, HCO_3^- and SO_4^{2-} do not co-vary with Cl^-. Instead, they maintain approximately constant concentrations as Cl^- decreases. This pattern also holds for Ca^{2+} and Mg^{2+} (graphs for these are not shown). This suggests that even as the waters undergo mixing, they achieve a constant concentration of these reactive ions by means of maintaining chemical equilibrium with rock types that react relatively rapidly.

The anomalous (relative to the geothermal waters) compositions of the wells from the northern part of Truth or Consequences are also evident in

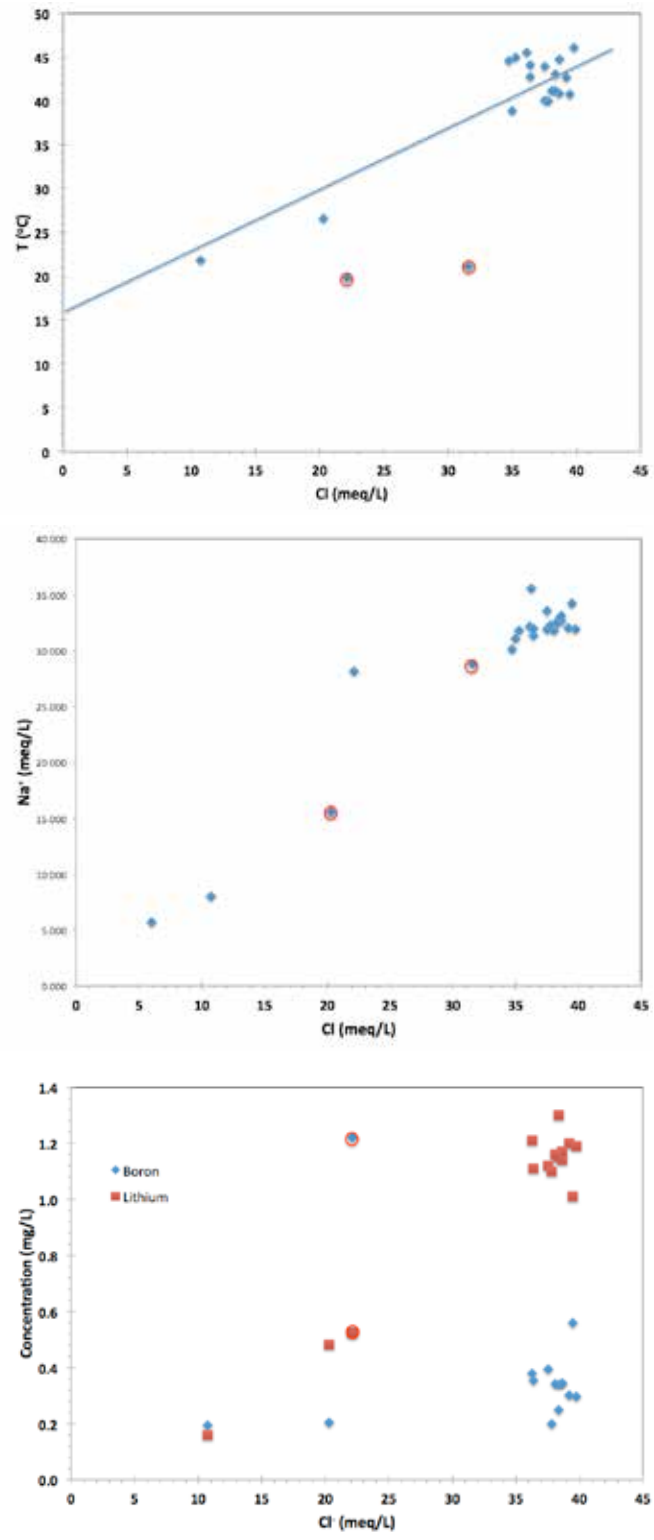

Figure 17–Plots of temperature (top), Na^+ (middle), and B and Li^+ (bottom) against Cl^-. The two samples having anomalously high TDS and SO_4^{2-} concentrations from the Cuchillo Negro drainage are circled in red. The blue line in the top figure is between the mean annual temperature of Truth or Consequences (16.5°C) and the temperature of the geothermal waters.

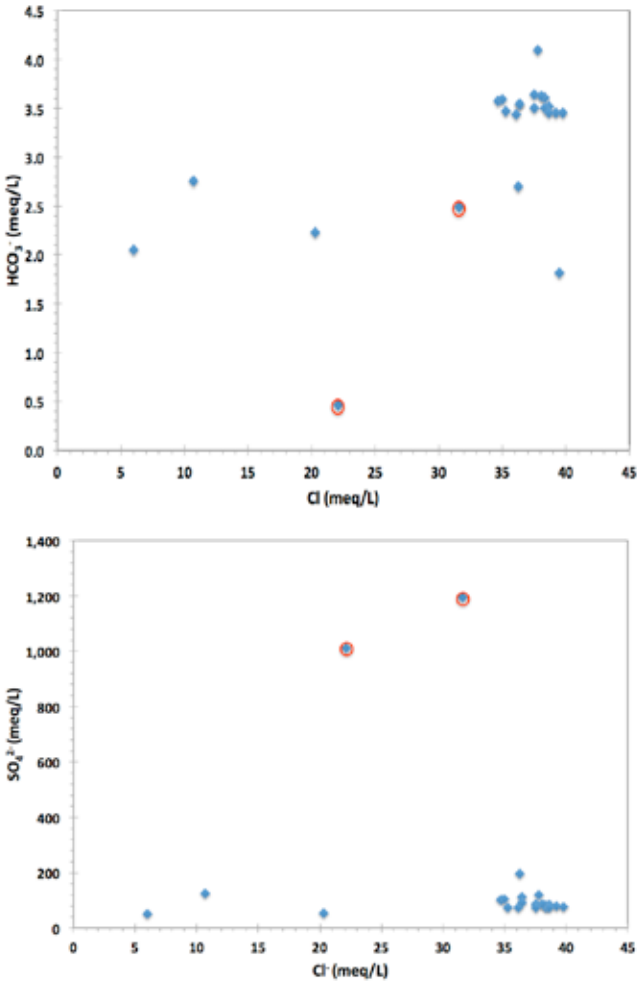

Figure 18–Plots of HCO_3^- (top) and SO_4^{2-} (bottom) against Cl^-. The two samples having anomalously high TDS and SO_4^{2-} concentrations in the Cuchillo Negro drainage are circled in red.

Figure 18. Both wells have SO_4^{2-} concentrations that are about 10 times that of the geothermal waters and one of them also has anomalously low HCO_3^-.

The most obvious candidate for maintaining the geochemistry of Ca^{2+}, Mg^{2+}, HCO_3^- and SO_4^{2-} at constant levels is the Paleozoic limestone that forms the confined aquifer supplying the geothermal waters. The rocks in this formation are mostly limestone (composed mainly of calcite: $CaCO_3$) and dolomite ($CaMg(CO_3)_2$) , with minor gypsum ($CaSO_4 \bullet 2H_2O$). To test the hypothesis that Ca^{2+} and HCO_3^- are controlled by equilibrium with calcite, we computed the saturation index (SI) for all of the chemical analyses shown in the graphs. A saturation index of 1 indicates that the water is in equilibrium with the specified mineral, one of less than 1 indicates that it is undersaturated with respect to the mineral (concentrations are too low to be in equilibrium) and one greater than 1 indicates it is supersaturated.

Most of the samples in Figure 19 show saturation indices that are in the range of 0.5 to 2.0. Given the typical accuracy of saturation index calculations, these SI values would normally be taken to indicate that the samples are at, or very close to, equilibrium with calcite. These results therefore strongly support the hypothesis that the relatively constant concentrations of Ca^{2+}, Mg^{2+}, HCO_3^- and SO_4^{2-} are due to local equilibrium with minerals in the confined aquifer supplying the geothermal water.

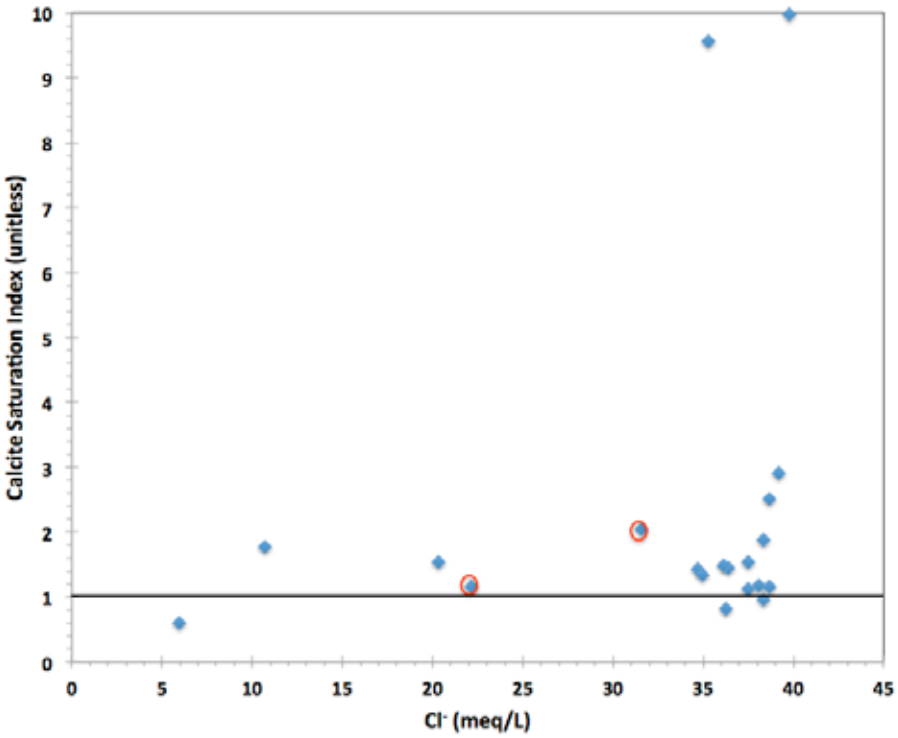

Figure 19–Calcite saturation index plotted against Cl^- concentration. The horizontal line at saturation index equals one indicates that the sample is in chemical equilibrium with calcite.

The patterns in the aqueous geochemistry of the water samples can be related to the hydrogeological setting of the Truth or Consequences geothermal system. Evidence presented above indicates that the waters are recharged over a large area, predominantly in the Sierra Cuchillo and the San Mateo Mountains. This water flows downward until it contacts the low-permeability crystalline basement rocks. The geological structure provided by the Mud Springs Fault funnels the water, flowing steadily deeper as it travels, toward Truth or Consequences. Some distance north of Truth or Consequences the crystalline basement rocks begin to curve upward due to the action of the fault. This flexure causes fracturing of the basement rocks, enabling the deep groundwaters to move into it and to react with the granitic rocks at high temperatures (probably greater than 100°C) for an extended period. The rock/water chemical reactions in this environment produce a characteristic geothermal Na^+/Cl^- composition. Groundwater residing in carbonate rocks at high temperature would be expected to exhibit a $Ca^{2+}/HCO_3^-/SO_4^{2+}$ composition. This is illustrated in Figure 16, where three samples from the 'Etruscan Swell' area of Italy, from a study by Chiodini et al. (1995), are plotted for comparison. Their compositions are quite distinct from the Truth or Consequences geothermal waters.

The heated waters then flow toward the lowest point in the system, which is the Rio Grande adjacent to Truth or Consequences. The granitic basement rocks are more resistant to erosion than the limestones stratigraphically above them and today form the terrace next to the Rio Grande on which the Veteran's Hospital sits. The lowest point is therefore the low area underlain (beneath Rio Grande alluvium) by the Paleozoic limestones. The geothermal waters therefore leave the fractured granitic basement and flow nearly vertically upward through the limestone. As they do so, they react with the calcite and dolomite and achieve concentrations of Ca^{2+}, Mg^{2+}, HCO_3^- and SO_4^{2-} that are controlled by equilibrium with these minerals.

As the geothermal waters approach the surface, they may mix with cool, dilute groundwater in the alluvium, producing the linear mixing lines observed in Figure 17. If a large amount of alluvial

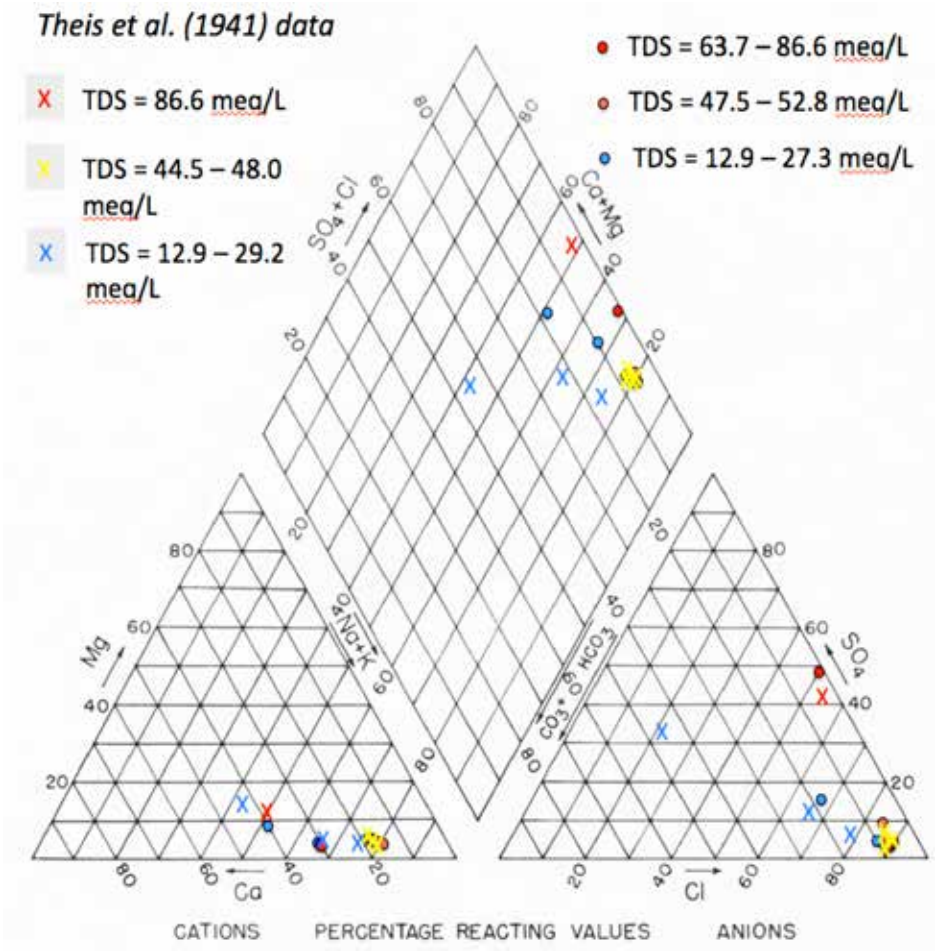

Figure 20–Piper plot comparing analyses from Theis et al. (1941) with more modern analyses of groundwater from the Truth or Consequences area.

groundwater invades the aquifer beneath Truth or Consequences, it could significantly cool the geothermal water, lowering its value for the commercial spas and domestic residents there. To examine whether there has been any shift in the chemical composition of the waters since Theis' study in 1940, we have in Figure 20 distinguished his analyses from more recent ones.

The samples of interest to address this question are those with total dissolved solids between 44 and 53 meq/L, which are the geothermal waters. The figure shows that the analyses from Theis et al. (1941) plot on top of the younger analyses, indicating that there has been no large-scale shift in the composition of the geothermal waters. This, in turn, probably indicates that exploitation has not caused widespread mixing of the geothermal discharge with cool near-surface waters.

H. GEOTHERMOMETRY

Concentrations of certain elements or molecules that have been dissolved from common rock-forming minerals such as quartz, feldspar, or calcite during interactions with hot water at depth are regularly used to estimate the temperature of the source of geothermal fluids (Fournier et al., 1974; Powell and Cummings, 2010). Several assumptions are associated with these estimates. First and foremost, the dissolution of rocks by hot water at depth (100s to 1000s of feet below the earth's surface) is assumed to be controlled by temperature-dependent chemical reactions. Water-rock equilibrium is presumed to occur within the geothermal reservoir. Second, as the water moves from the reservoir toward the surface and cools slightly, the composition of the fluid is assumed to change little. Third, as water from depth moves toward the surface, mixing with water in shallow, cool aquifers is presumed to be minimal.

Several of the geothermometers that are based on interactions of hot water with feldspar, a mineral common in volcanic and Proterozoic basement rocks, were calibrated in high temperature settings (>180°C) near active volcanoes. In general, these cation geothermometers (Na-K-Ca-Mg) assume equilibration with Na- and Ca-plagioclase at temperatures greater than 180°C and tend to overestimate the reservoir temperature in low temperature systems (Fournier and Potter, 1979). However, the K-Mg geothermometer, which is based on interaction of hot water with K-feldspar, approaches equilibrium at a lower temperature compared to plagioclase and thus is more appropriate for assessing reservoir temperatures in a lower temperature system like that of Truth or Consequences.

Similarly, the silica geothermometer that is based on equilibration of quartz with water in geothermal systems with temperatures greater than 180°C can overestimate the reservoir temperature in low temperature systems. Chalcedony is the dominant silica phase in geothermal systems with temperatures less than 150°C; the chalcedony geothermometer should be used to evaluate low temperature systems like that of Truth or Consequences (Fournier, 1981).

Geothermal reservoir estimates for Truth or Consequences were calculated using the Excel spreadsheet of Powell and Cummings (2010) and water-chemistry data collected during this study and the study of Theis et al. (1941). The chalcedony temperatures range from 51 to 77°C, the quartz estimates are 83 to 107°C, and the K/Mg

Table 7–Summary of geothermometer calculations.

Sample Name	Chalcedony	Quartz	K/Mg
TC-012	64.5	95.4	n.d.
TC-012	64.9	95.8	104.1
TC-013	66.7	97.4	105.8
TC-017	65.9	96.7	106.1
TC-018	65.0	95.9	103.6
TC-035a	33.3	65.6	73.0
TC-035	65.8	96.6	104.8
TC-059	61.8	92.8	100.8
TC-061	66.2	97.0	102.9
TC-062	88.4	117.3	75.7
TC-063	77.1	107.0	110.8
TC-064	51.3	83.0	55.7
TC-065	14.1	45.8	67.7
TC-094	58.7	89.9	99.1
TC-098	50.9	82.6	98.7
TC-100	27.3	59.6	61.3
TC-101	59.9	91.1	n.d.
TC-101	62.2	93.3	n.d.
TC-101	62.2	93.3	103.7
TC-101	62.2	93.3	103.4
TC-101	66.6	97.3	109.8
TC-505	56.2	87.6	97.0
TC-505	67.8	98.4	107.4
TC-507	49.9	81.7	106.1
TC-508	57.4	88.8	93.1
TC-013B	69.3	99.9	104.5
TC-076	67.5	98.2	104.9

Temperatures in degrees C, n.d. = no data

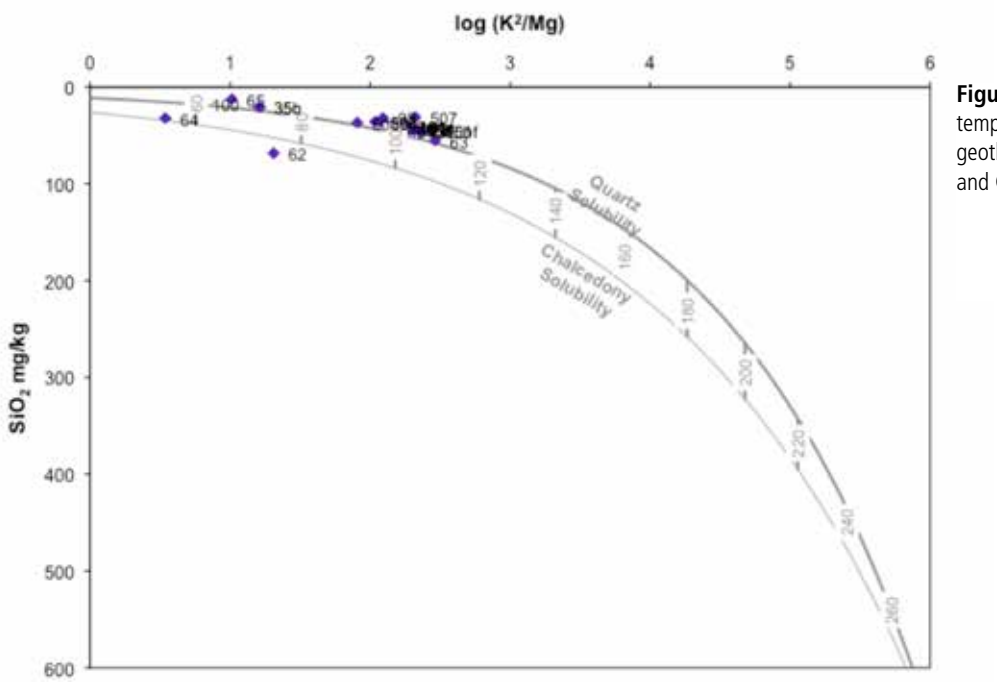

Figure 21–Estimate of geothermal temperatures based on K/Mg and silica geothermometry derived from Powell and Cummings (2010).

geothermometer ranges from 93 to 111°C within the Hot Spring district (Table 7). The airport well (TC-062) yields 88°C, 117°C, and 76°C for chalcedony, quartz, and K/Mg, respectively (Table 7). Figure 21 is a plot that combines the K/Mg and silica geothermometers; samples falling within the envelope on this diagram indicate excellent agreement between the estimates derived from these two techniques. The samples from this study lie just outside the envelope, suggesting good agreement between the two methods (Powell and Cummings, 2010). This plot indicates that waters in the hot-springs district were in equilibrium with quartz at temperatures of 90 to 110°C. The water collected from the airport well (TC-62) equilibrated at about 75°C and water from the two wells in the Cuchillo Negro drainage (TC-64 and 65) equilibrated at temperatures of 55 to 65°C.

I. ELECTRICAL RESISTIVITY SURVEY

In an effort to provide boundary conditions for the Truth or Consequences geothermal model, a Direct Current (DC) Resistivity survey was conducted on the south banks of the Rio Grande River adjacent to the Hot-springs district. DC resistivity is a near-surface geophysical technique that is ideal for investigating subsurface fluid properties and distributions, as a fluid with a dissolved ion component is a much more efficient electrical conductor than similar, but dry subsurface material (by up to four orders of magnitude increase in electrical conductivity). Three DC resistivity transects (Fig. 22) were completed in the spring of 2013, and pieced together into a three-dimensional model (Fig. 23).

The purpose of the surveys was to identify to what extent the saline, and possibly geothermal, waters were reaching the opposite side of the Rio Grande from the hot-springs district of Truth or Consequences. The surveys were completed on the unconsolidated alluvium of the southern banks of the Rio Grande. At the site of the surveys, the surface of the alluvial fill is approximately 16 to 26 feet (5-8 meters) above the bed of the Rio Grande. The alluvium is poorly sorted, with grain size ranging from silt-sized particles to clasts several centimeters in diameter. The dry alluvium of the surface was expected to be a relatively poor electrical conductor, projected to be in the range of high 100's to low 1000's Ohm/m, due to being unconsolidated and unsaturated. What was unknown was whether the alluvium of the survey site was sitting on a freshwater table, indicating no geothermal waters reaching the other side of the Rio Grande, or if the subsurface boundary of the geothermal system reached across the Rio Grande. This basic question could be easily answered by looking at the electrical properties of the subsurface water table interface; the ionic load of the geothermal water would be substantially more conductive (less electrically resistant) than fresh water. In water, electricity is transmitted through dissolved ions, or dissolved solids. Increased amounts of dissolved solids equates to increased ability to conduct electricity. The dissolved-solid content of the Truth

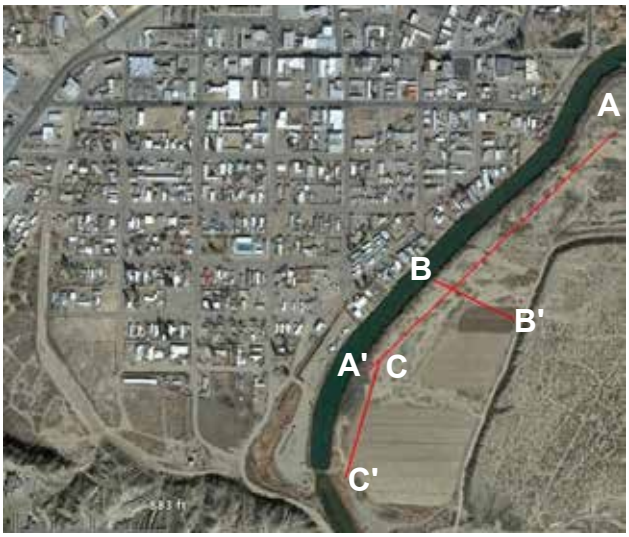

Figure 22–Map view of the three transects of the DC resistivity survey adjacent to the hot-springs district of Truth or Consequences, NM.

or Consequences geothermal system is about 3070 mg/L, which leads to a significantly decreased electrical resistivity (anticipated to be in the range of 1-10 Ohm/m) in comparison to fresh water. The survey geometry was designed to capture the subsurface architecture of fluid distribution in three dimensions. Three transects were identified; two along the banks of the Rio Grande, and one roughly perpendicular to the river. The surveys ranged from 160 meters to 620 meters in length, and were located by handheld GPS. Upon identifying the transects, 14 inch iron stakes were hammered into the ground along the transect with four meter intervals between each stake. The depth of investigation is predicated on the total initial array length. Utilizing a 220 meter (56 electrodes spaced at four meter intervals) initial array length, a ~50 meter depth of investigation was achieved. Electrodes, capable of both measuring voltage and emitting current, were connected to each stake. During the surveys, a two amp current was injected into the ground while several other electrodes measured the voltage drawdown over 1.2 second sample durations. Two different array types were employed

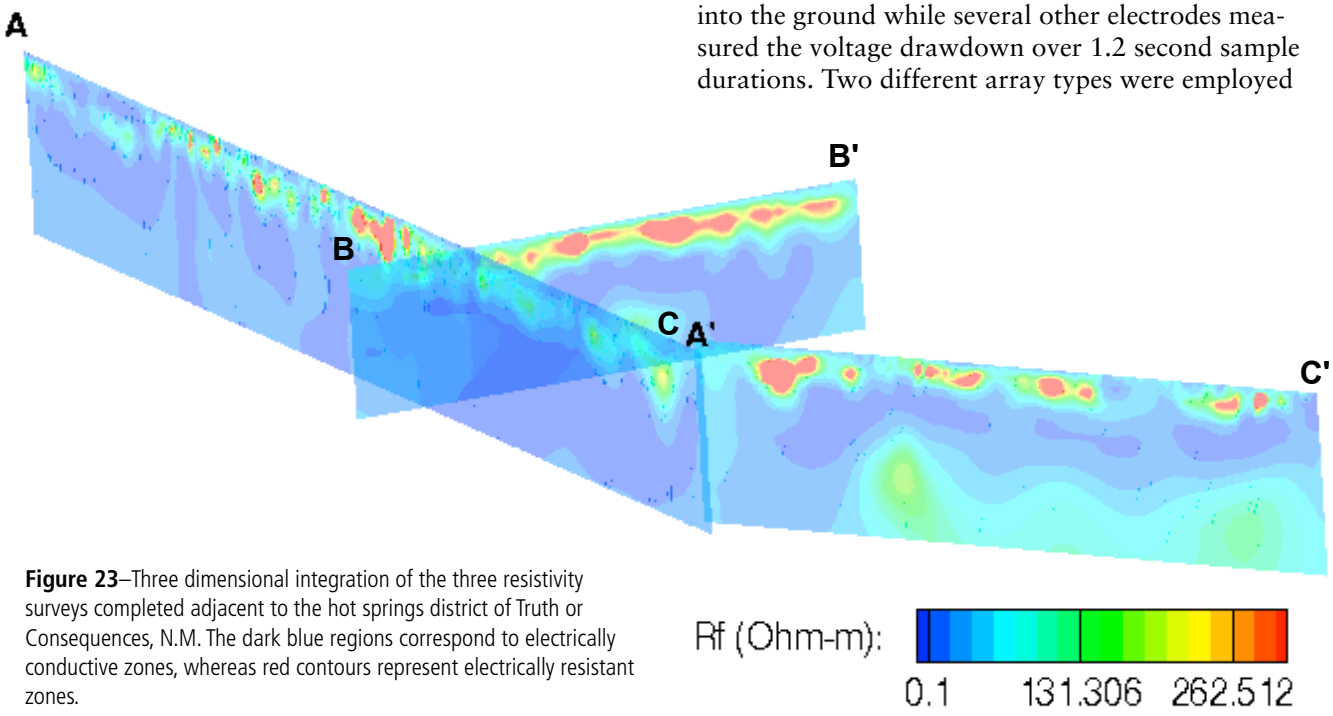

Figure 23–Three dimensional integration of the three resistivity surveys completed adjacent to the hot springs district of Truth or Consequences, N.M. The dark blue regions correspond to electrically conductive zones, whereas red contours represent electrically resistant zones.

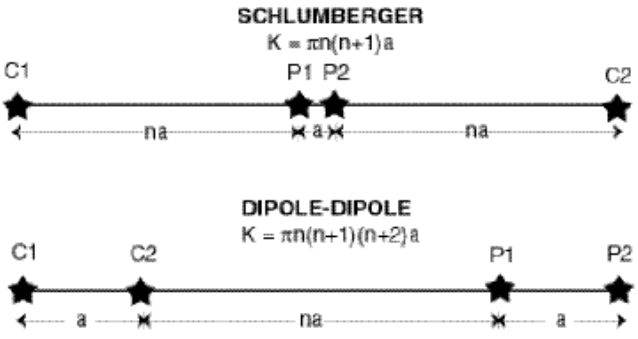

Figure 24–The array types employed for all three surveys. P1 represents the electrode that is injecting current into the subsurface, while P2 acts as a current sink. C1 and C2 are the electrodes measuring the voltage drawdown. While the Dipole-Dipole array was employed as seen in this diagram, the inverse of the Schlumberger array was also utilized for the survey. By using the two array types in tandem, both the vertical and horizontal resolution of the inverted cross section was improved.

for this survey to ensure both horizontal and vertical resolution. The geometry of the array types used, Dipole-Dipole and Inverse Schlumberger (Fig. 24), dictate which electrodes act as a current source, and which electrodes act as a current sink and measure voltage. By combining the data sets from both arrays at each transect, the final inverted electrical cross section was robust in both resolution and accuracy.

Based on the three-dimensional integration of the results of the completed resistivity survey, it appears that saline water is crossing the Rio Grande in the subsurface. In all three individual transects there is an abrupt transition from hundreds Ohm/m to less than 10 Ohm/m at approximately 10-12 meter depths. In line with the original hypothesis, the plume of saline water that was imaged appeared to grow in both thickness and concentration towards the hot-springs district. The resistivity measurements indicate that some saline waters are reaching the southeast side of the river via groundwater flow. This method cannot determine groundwater temperature. Well temperatures measured on the southeast side of the river are only 20 to 21°C at depths of 11 to 27 m (TC-73, TC-79, TC-80, Table 4; Appendix 4). Thus, the results of the combined geophysical studies suggest that cool, saline waters are present beneath the floodplain southeast of the Rio Grande.

J. RORABAUGH ANALYSIS OF ALLUVIAL AQUIFER

Rorabaugh (1964) demonstrated that water-table fluctuations in wells completed in shallow alluvial aquifers mimic river stage changes with two important differences: 1) the amplitude of the well fluctuations becomes damped, with less fluctuation further from the river and 2) the peaks in the groundwater fluctuations are out of phase (delayed) with the river stage as distance increases.

We employed a simple one-dimensional, transmissivity-based model to try to reproduce water-level fluctuations in the alluvial aquifer:

$$S_y \frac{\partial h}{\partial t} = \frac{T\partial^2 h}{\partial x^2} + R \qquad (4)$$

where h is head, t is time, x is distance from the Rio Grande, S_y is the specific yield of the aquifer, T is aquifer transmissivity and R is the average deep geothermal recharge into the upper aquifer (1.8 million gallons per day divided by the estimated area of the model domain, 775 m by 775 m (2540 by 2540 ft). We imposed a time-dependent specified head boundary condition equal to the water level of the Rio Grande (gray dashed line, Fig. 25). The goal was to back-calculate T and S for the shallow aquifer by matching the water-level fluctuations in the wells plotted in Figure 25. The best-fit aquifer parameters from our analysis were a transmissivity (T) of 15 m^2/hour (161 ft^2/hr) and a specific yield of 0.04. If we assume an alluvial aquifer thickness of 50 meters (estimated from the hot-springs district cross-section (Fig. 3C)), that provideahs a hydraulic conductivity value of approximately 7.2 m/day (24 ft/day).

K. REANALYSIS OF THEIS AQUIFER TEST DATA

Theis et al. (1941) conducted two, relatively short-duration (overnight) aquifer tests in the Paleozoic limestone. The first aquifer test was conducted in Well 18 at a pumping rate of 52 gallons per minute. Drawdown was observed in a number of adjacent wells (5, 7, 17, and 19). A second test was performed using the production well of the Carrie Tingley Hospital (now the Veteran's Hospital). During this test, 120 gallons per minute of water was produced. Water level fluctuations in Theis wells 4, 5, 10a, 12, 17, 18, 19, 25, 27, and 30 were monitored. During most of these tests, late-time drawdown flattened out, which is characteristic of vertical leakage across a confining unit. This was not accounted for in the aquifer-tests analyzed by Theis et al. (1941) as methods for this had not yet been derived. In Figure 26, we have reanalyzed select wells from both of these pumping tests using an analytical solution of Hantush and Jacob (1955). This solution accounts for vertical leakage and provides an estimate of not only transmissivity and storage, but also the vertical hydraulic conductivity of the confining unit that presumably separates the shallow alluvial aquifer and artesian limestone aquifer. The solution for drawdown in a leaky confined aquifer is given by Hantush and Jacob (1955):

$$s = \frac{Q}{4\pi T} L(u, v) \qquad (5)$$

$$v = \frac{r}{\sqrt{Tb'/K'}} \qquad (6)$$

$$u = \frac{r^2 S}{4Tt} \qquad (7)$$

$$K' = \frac{Tb'v^2}{r^2} \qquad (8)$$

where

L(u,v) = well function for a leaky, confined aquifer
b = thickness of aquifer

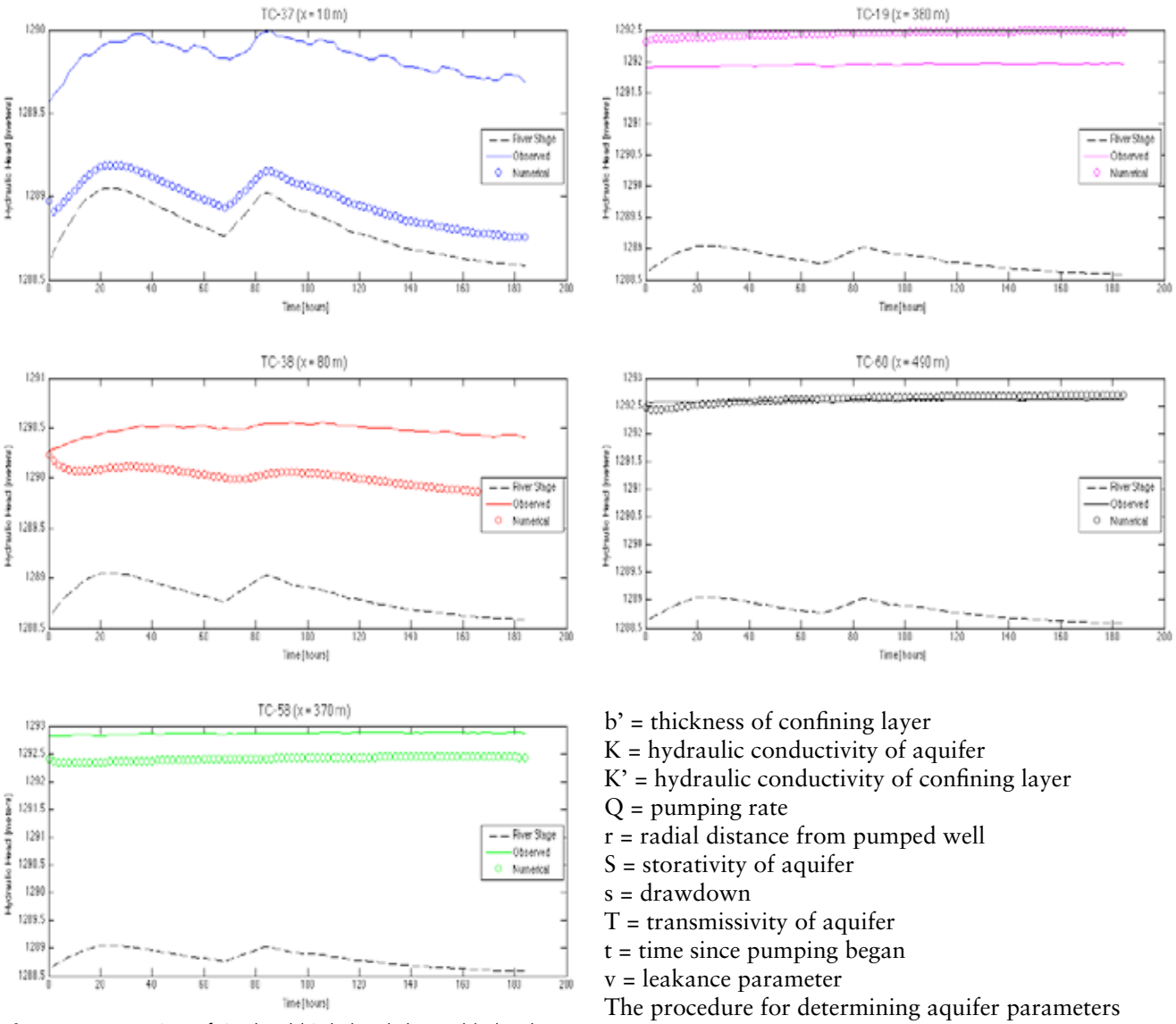

Figure 25–Comparison of simulated (circles) and observed (colored lines) alluvial aquifer water level fluctuations in wells in response to Rio Grande stage change (dashed line). The water level fluctuations decrease with increasing distance from the river. There is also a phase shift in the peaks. The distance from the river is noted as "X" in meters above each plot.

b' = thickness of confining layer
K = hydraulic conductivity of aquifer
K' = hydraulic conductivity of confining layer
Q = pumping rate
r = radial distance from pumped well
S = storativity of aquifer
s = drawdown
T = transmissivity of aquifer
t = time since pumping began
v = leakance parameter

The procedure for determining aquifer parameters from an aquifer pumping test in a leaky confined aquifer is to fit one of several analytical solution curves having different values of the leakage parameter (v) to the drawdown curve and to thus obtain match-point coordinates (Freeze and Cherry, 1979). Then the values of T, S, and K' can be determined, provided that the thickness of the confined aquifer (b) and the confining unit (b') are known.

We reanalyzed three wells from Theis et al. (1941) with relatively high-quality water-level measurements (Wells 10a, 5, and 12; Fig. 26). The results

Table 8–Aquifer parameters derived from re-analysis of Theis et al. (1941) pumping tests.

Well	Pump Test	Q (m^3/min)	r(m)	b(m)	b'(m)	T (m^2/min)	S (-)	K' (m/day)	v	K (m/day)
5	1	0.20	582	13	25	1.47	4.40E-05	0.014	0.3	161.5
10a	2	0.45	292.7	34	50	0.668	1.10E-04	0.202	0.6	28.3
12	1	0.20	538.1	29	25	0.77	3.30E-05	0.015	0.4	38.7

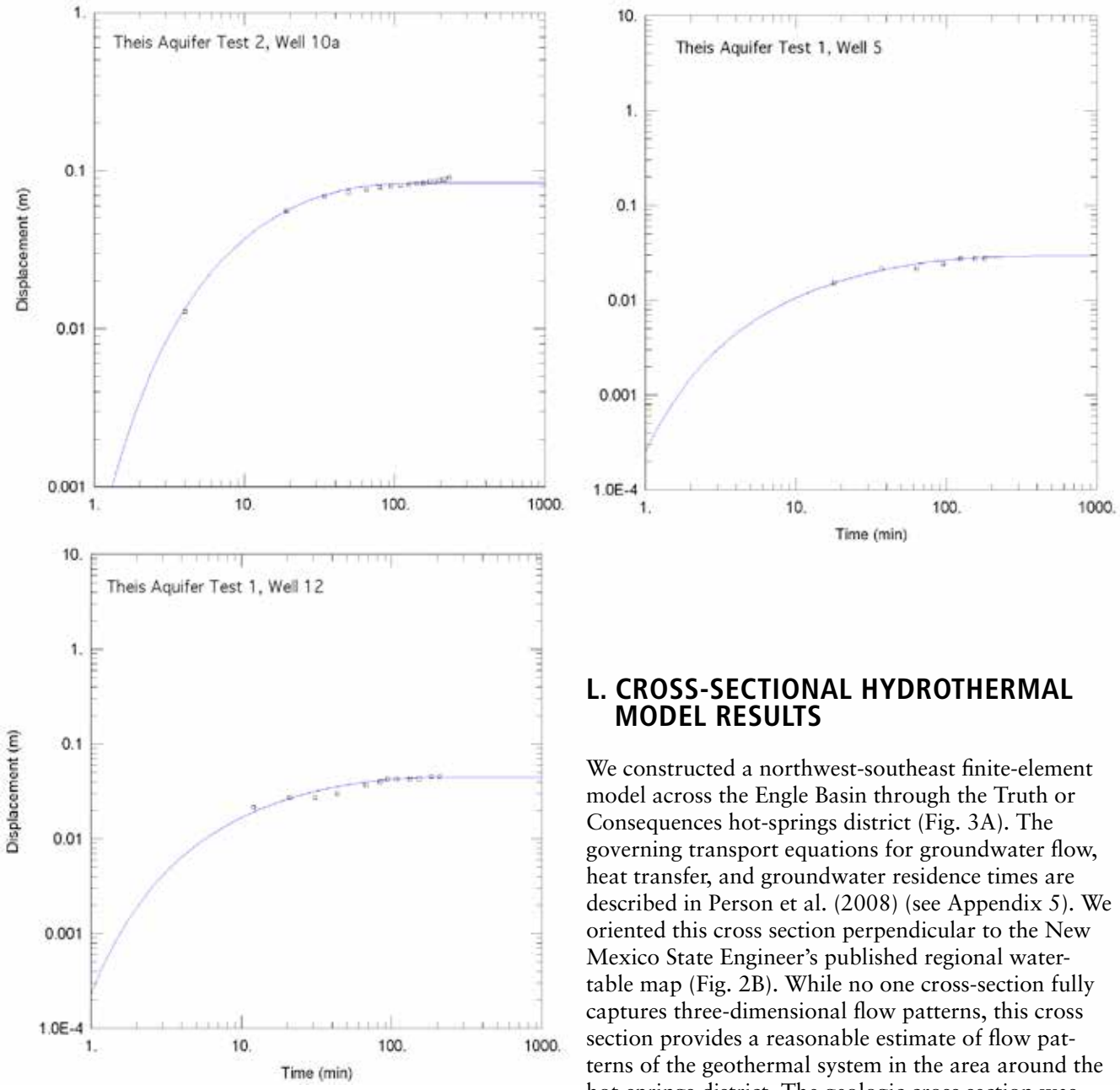

Figure 26–Reanalysis of aquifer test data from Theis et al. (1941) using Hantush-Jacob (1955) leaky aquifer test solution. The values used to generate these curves are in Table 8.

are presented in Table 8. The best-fit value for the horizontal hydraulic conductivity of the limestone aquifer in the hot-springs district ranged between 39-162 m/day (128 to 532 ft/day). The overlying confining unit yielded a value for vertical hydraulic conductivity that ranged between 0.01 to 0.2 m/day (0.03 to 0.06 ft/day). We assumed that about 50% of the well depth was comprised of the limestone aquifer (b) and 50% was comprised of the overlying alluvium confining unit (b').

L. CROSS-SECTIONAL HYDROTHERMAL MODEL RESULTS

We constructed a northwest-southeast finite-element model across the Engle Basin through the Truth or Consequences hot-springs district (Fig. 3A). The governing transport equations for groundwater flow, heat transfer, and groundwater residence times are described in Person et al. (2008) (see Appendix 5). We oriented this cross section perpendicular to the New Mexico State Engineer's published regional water-table map (Fig. 2B). While no one cross-section fully captures three-dimensional flow patterns, this cross section provides a reasonable estimate of flow patterns of the geothermal system in the area around the hot-springs district. The geologic cross section was constrained using oil-well data, an east-west regional cross section (Lozinsky, 1987), gravity data (Gilmer et al., 1986) and surface geologic maps (Harrison et al., 1993; Harrison et al., 2004). We used 14 hydrostratigraphic units to characterize groundwater flow patterns within the Engle Basin (Table 9, Fig. 27). The parameters (permeability, porosity) used in this model are representative of the rock types in the cross section (Freeze and Cherry, 1979). However, permeability can vary by about four orders of magnitude for a given lithology. We used temperature and groundwater residence time data to calibrate permeability of different formations. While we ran about 20 simulations, we present here only scenarios that best

fit the calibration data and that served to test the two forced-convection hypotheses.

The cross-sectional finite-element mesh included 3904 nodes and 7493 triangular elements (Fig. 28). The lateral dimensions of the grid varied from 1000 m (3280 ft) to the west to 50 m (164 ft) within the hot-springs district. We used 123 nodal columns to discretize the 14 hydrostratigraphic units. The mesh was vertically and laterally refined within the hot-springs district. Except for very thin units (about 20 m; 66 ft), there are generally two to three nodes per stratigraphic layer in the vertical directions. The transport parameters that were held constant between hydrostratigraphic units are listed in Table 10.

We imposed a specified hydraulic-head boundary condition assuming that the water table was

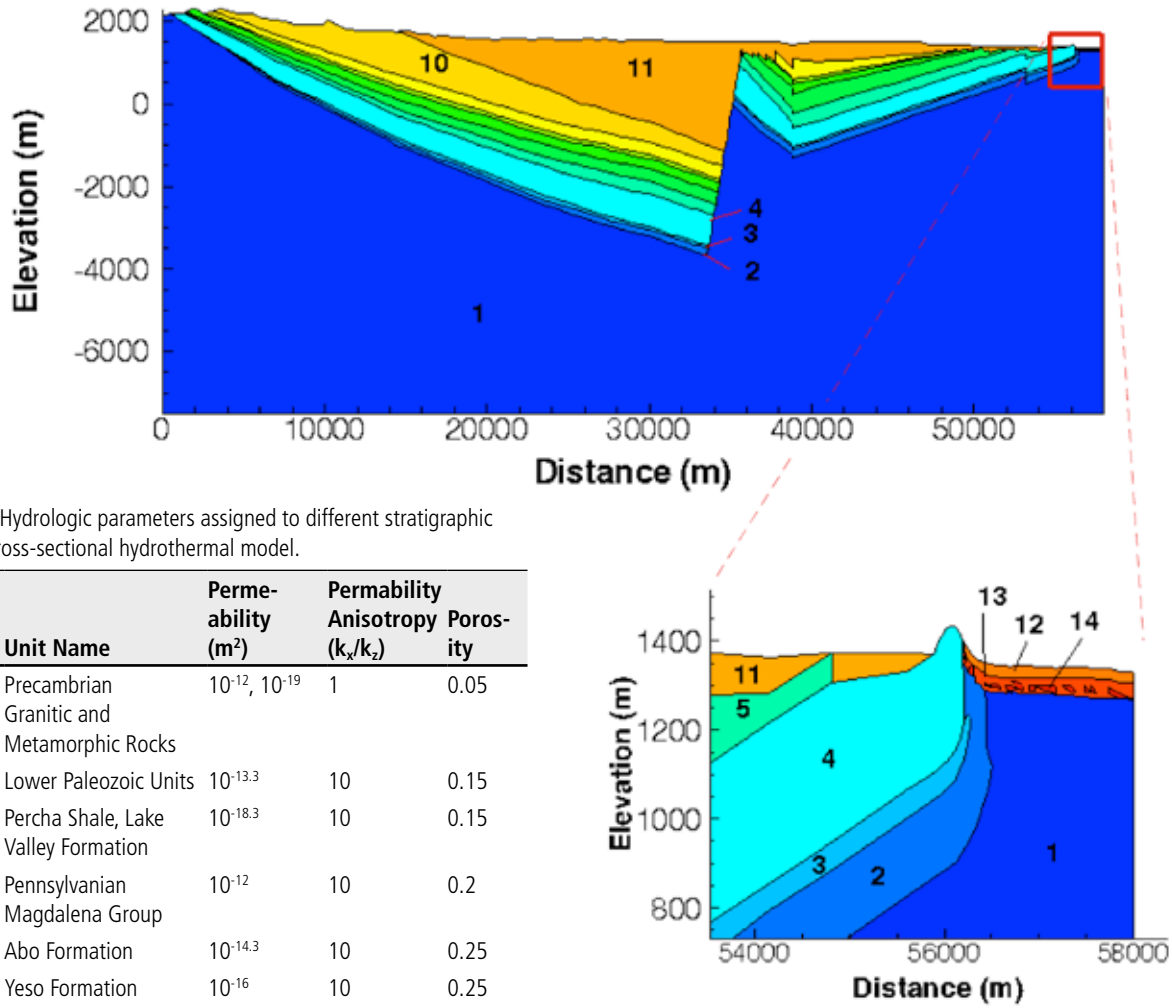

Figure 27–Stratigraphic units used in cross-sectional finite element models of hydrothermal fluid flow and groundwater residence times. The numbers refer to different stratigraphic units that are listed in Table 9. The inset depicts hydrostratigraphic units in the hot-springs district.

Table 9–Hydrologic parameters assigned to different stratigraphic units in cross-sectional hydrothermal model.

Unit Number	Unit Name	Permeability (m^2)	Permability Anisotropy (k_x/k_z)	Porosity
1	Precambrian Granitic and Metamorphic Rocks	10^{-12}, 10^{-19}	1	0.05
2	Lower Paleozoic Units	$10^{-13.3}$	10	0.15
3	Percha Shale, Lake Valley Formation	$10^{-18.3}$	10	0.15
4	Pennsylvanian Magdalena Group	10^{-12}	10	0.2
5	Abo Formation	$10^{-14.3}$	10	0.25
6	Yeso Formation	10^{-16}	10	0.25
7	San Andres Formation	10^{-16}	10	0.25
8	Mancos Shale, Dakota Sandstone	10^{-15}	100	0.25
9	Cretaceous Sediments	10^{-16}	10	0.3
10	Tertiary Volcanics	10^{-16}	1	0.3
11	Tertiary Palomas Formation	10^{-12}	100	0.3
12	Quaternary Fluvial Deposits	10^{-12}	100	0.3
13	Hot-springs District Alluvial Deposits	10^{-12}	100	0.3
14	Hot-springs District Fluvial Confining Unit	10^{-17}	10	0.3

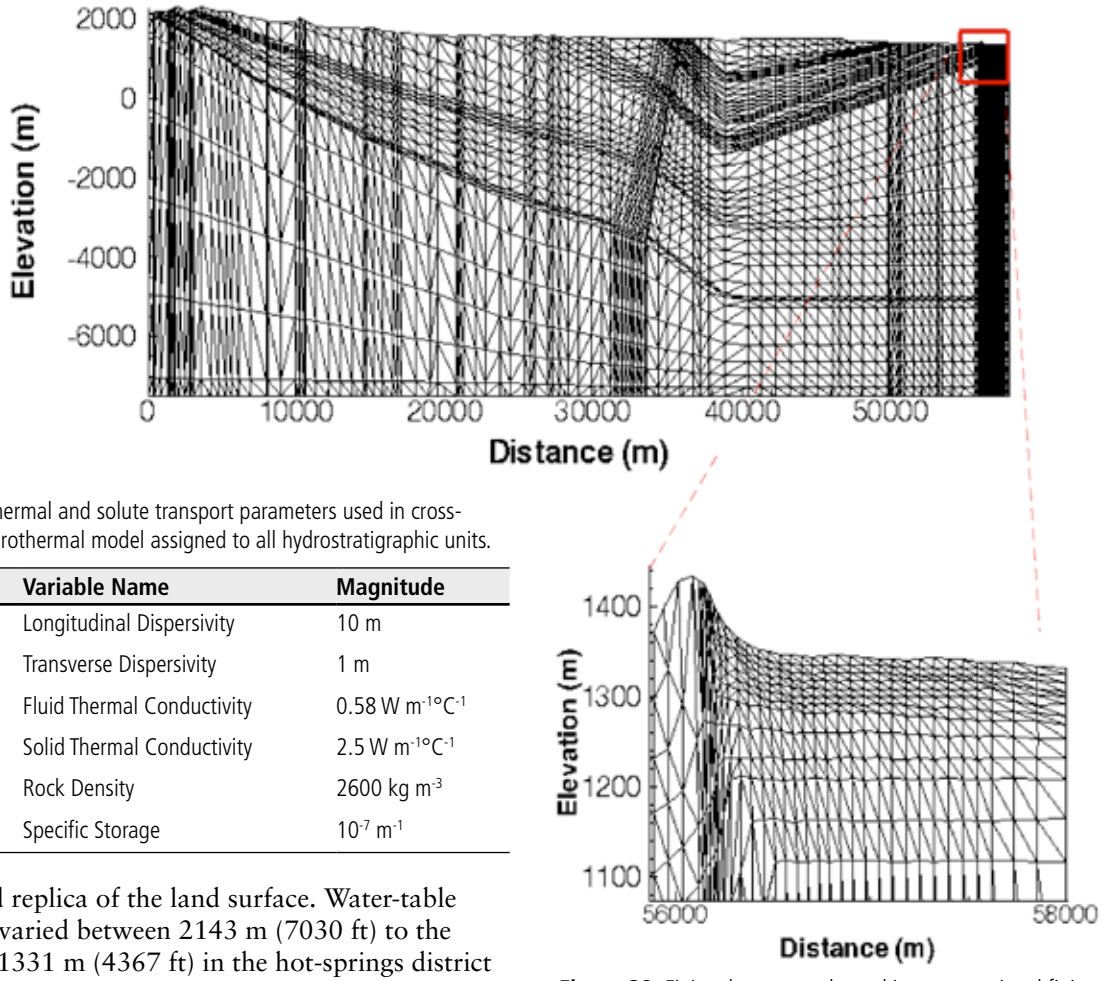

Figure 28–Finite element mesh used in cross-sectional finite element models of hydrothermal fluid flow and groundwater residence times. A total of 3897 nodes and 4057 triangular elements were used in this model.

Table 10–Thermal and solute transport parameters used in cross-sectional hydrothermal model assigned to all hydrostratigraphic units.

Symbol	Variable Name	Magnitude
α_L	Longitudinal Dispersivity	10 m
α_T	Transverse Dispersivity	1 m
λ_f	Fluid Thermal Conductivity	0.58 W $m^{-1}°C^{-1}$
λ_s	Solid Thermal Conductivity	2.5 W $m^{-1}°C^{-1}$
ρ_s	Rock Density	2600 kg m^{-3}
S_s	Specific Storage	10^{-7} m^{-1}

a subdued replica of the land surface. Water-table elevation varied between 2143 m (7030 ft) to the west and 1331 m (4367 ft) in the hot-springs district to the south. We used the lateral water-table gradient to assign a specified flux boundary condition for the steady-state

$$\frac{\partial \psi}{\partial z} = -K\frac{\partial h}{\partial x} \qquad (9)$$

where K is the hydraulic conductivity, h is hydraulic head, and ψ is the stream function. The sides and base of the solution domain were assigned a constant stream function of $\Psi = 0$ (i.e. a no-flow boundary condition). The no-flow boundary condition at the Rio Grande forces waters to rise and discharge. Because the Rio Grande is the regional topographic low point in the area, this seems like a valid assumption. Assigned water-table temperatures varied from 59°F (15°C) in the uplands to 75°F (24°C) in the hot-springs district. We assumed a temperature gradient of 115°F/mile (40°C/km). A basal heat flux typical of the continental crust (Sass, et al. 1981) of 0.08 W/m^2, which is in the range of measured heat flow values for the area (Table 11; Sanford et al., 1979), was imposed along the base of the solution domain. The sides of the model domain were assumed to be insulated ($\partial T/\partial x = 0$). For groundwater residence time, we assigned an age at the water table of zero in recharge areas. We allowed groundwater age to increase with depth using 4000 years/km as an initial condition. The base and sides of the model domain were assigned as no flux boundaries. Within the hot-springs district, a spring flux boundary condition was assigned along the water table ($\partial A/\partial z = 0$; A is groundwater age in years).

We present two simulations that quantitatively evaluate the two hypotheses discussed in the introduction. We set the crystalline basement permeability to be 10^{-12} m^2 to allow deep fluid circulation within the crust to depths of about four kilometers (2.5 mi) below the sedimentary units (Hypothesis #1; Fig. 29A). We present a second simulation (Hypothesis #2; Fig. 29B) in which the crystalline basement permeability was set to 10^{-19} m^2. This effectively restricts circulation to the Paleozoic strata and especially the Magdalena Group limestone (Unit 4, Fig. 27). In both models, the Magdalena Group limestone had a permeability of

Table 11–Summary of published heat flow values for the Truth or Consequences area.

Site ID	Elevation (m)	Interval top (m)	Interval bottom (m)	Interval length (m)	Gradient C/km	Therm Cond W/mK	Heat flow mW/m^2	Reference
W.ELEPHANT BUTTE [1]	1509	1000	2202	1202	40.6	2.87	117	1
W.ELEPHANT BUTTE [2]	1394	1091	2303	1212	32.4	2.93	95	1
T OR C NORTH	1650	20	160	140	42.99	2.14	92	1
16-76-1	1512	21	91	70	20.2	2.05	42	2
16-76-3	1497	30	104	74	36.6	2.05	75	2
16-76-6	1475	24	107	83	29.7	2.01	59	2
16-76-7	1494	21	152	131	41	2.18	88	2
16-76-15A	1329	67	146	79	17.7	2.26	42	2
16-76-17	1378	73	131	58	35	2.3	80	2
16-76-20	1387	76	152	76	40.8	2.55	105	2
16-76-23	1426	21	122	101	45.2	2.39	109	2
16-76-29	1497	61	152	91	41.7	1.76	75	2
16-76-31	1494	15	119	104	56.9	2.13	121	2
16-76-33	1513	30	137	107	51.4	2.05	105	2
16-76-34	1469	85	152	67	65.6	1.59	105	2
16-76-35	1384	91	152	61	60.9	1.76	109	2
16-76-37	1469	46	152	106	32.6	1.97	63	2
16-76-TT1	1650	20	160	140	43	2.18	92	2

[1] Reiter et al., 1975
[2] Sanford et al., 1979

10^{-12} m^2. Computed stream functions for these two end-member models are plotted in Figure 29. Groundwater circulates deeper when bedrock is permeable (Fig. 29A). Two stream tubes (two adjacent stream lines) discharge within the hot-springs district. The net discharge from these stream tubes is 1000 m^2/year (~11,000 ft^2/yr). If we multiply this discharge by the approximate width of the hot-springs district (~750 m; 2461 ft) we get a net discharge of 750,000 m^3/year (about 550,000 gallons per day). This underestimates the hot-springs district discharge of approximately two million gallons per day determined by Theis et al. (1941), and by this study, by a factor of about four. For the low-permeability bedrock scenario (Hypothesis 2; Fig. 29B), the flow is focused into the Paleozoic limestone but the discharge rates are at most one-third the magnitude of the deep-circulation hypothesis (averaging 250 m^2/year; 2691 ft^2/yr). When multiplied by the approximate width of the hot-springs district, the low-permeability scenario underestimates field-determined hot-springs-district discharge by a factor of about 13 and is approximately 187,500 m^3/year (about 140,000 gallons per day). Computed vertical velocities beneath the hot-springs district for the high-permeability bedrock case are around 10 ft/yr (3 m/yr) (Fig. 30A), which are very close to what was estimated in the Peclet number analysis (Fig. 13). In the simulation a region of high vertical velocities extends about five kilometers below the land surface in the hot-springs district. A region of high vertical flow occurs along the Engle fault, where a gap in the Paleozoic formations occurs. Here confining units are faulted out of continuity and fluids can ascend. For the low-permeability bedrock scenario (hypothesis #2), vertical flow rates of about 0.3 m/yr (1 ft/yr) are realized in the Paleozoic limestone (Fig. 30B). Upward flow rates of less than 0.1 m/yr (0.3 ft/yr), as well as downward flow, are lumped together and represented using the dark blue pattern.

High vertical flow rates associated with upward flow result in positive thermal anomalies along the Engle fault and in the Truth or Consequences hot-springs district area for the high permeability bedrock scenario (Fig. 31A). In contrast, lateral heat transfer rates within the Magdalena Group were not high enough to generate a thermal anomaly in the hot-springs district for the low permeability bedrock scenario (Fig. 31B). We conclude bedrock circulation to a depth of about four kilometers (2.5 miles) is required to account for elevated hot-springs district temperatures. A computed temperature profile with depth extracted from the finite-element model for the hot-springs district (Fig. 32) shows some curvature and the temperature range observed in Figures 10–12. However, the detailed structure including temperature overturns could not be reproduced by our regional hydrothermal model as the overturns are local phenomena.

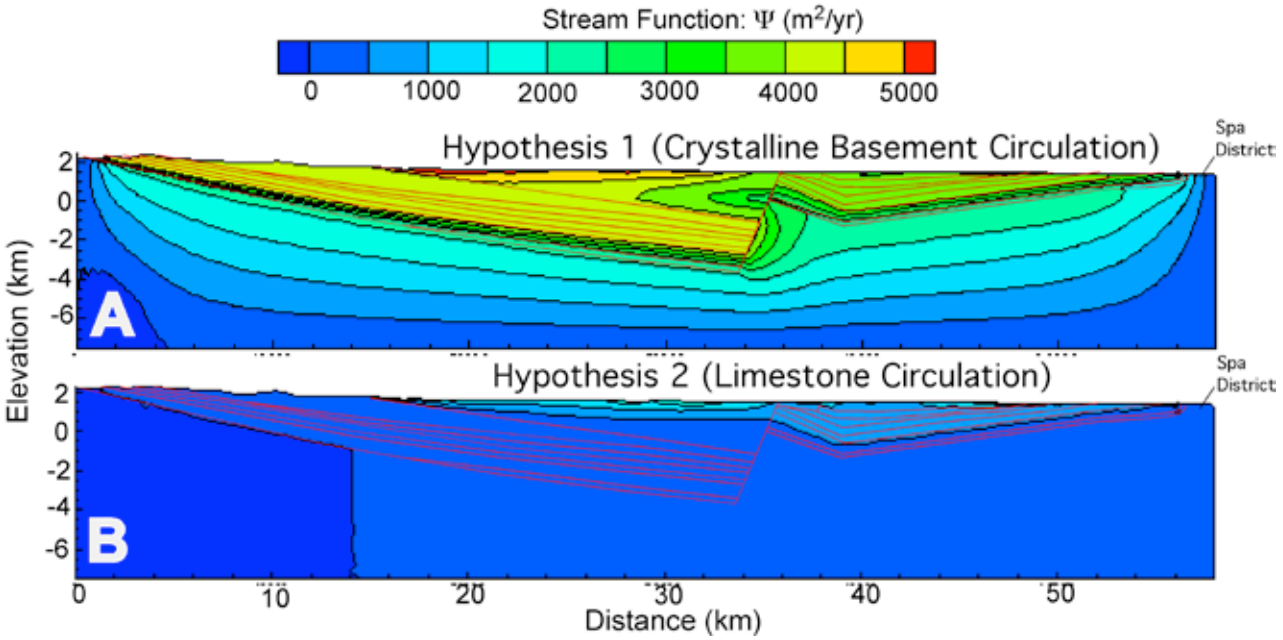

Figure 29–Comparison of computed stream functions for high (A, 10^{-12} m^2) and low permeability (B, 10^{-19} m^2) crystalline basement. Groundwater flow directions are everywhere parallel to stream lines. The stream functions represent the integrated discharge through the system. Areas where two adjacent stream functions converge are areas where groundwater velocity is increasing.

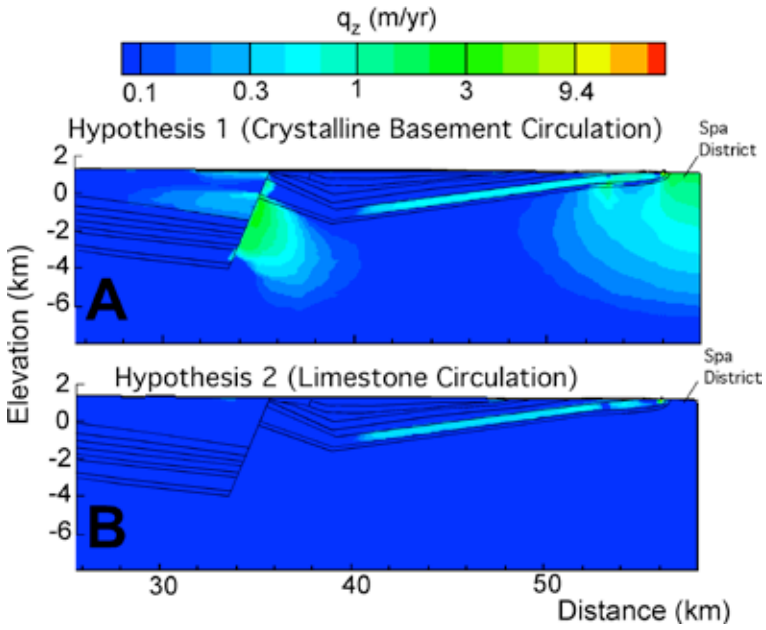

Figure 30–Comparison of computed vertical groundwater velocity (m/yr) for high (A, 10^{-12} m^2) and low permeability (B, 10^{-19} m^2) crystalline basement. Negative velocities are not plotted.

Computed groundwater residence time represents an independent means of testing the validity of the two hypotheses for hydrothermal circulation within the hot-springs district. Groundwater ages for the low-permeability crystalline basement case (Hypothesis #2) are consistently older than 50,000 years (Fig. 33B). The age of 50,000 years represents the limit of ^{14}C age dating. For the high-permeability crystalline basement case, the simulated ages are between 5,000-10,000 years, which is a reasonably good match with the observed uncorrected ^{14}C groundwater dates (Fig. 33A). The ages increase towards the Rio Grande, where the deepest groundwater circulation discharges beneath the river.

M. MODFLOW

Model Description and Results

The two-dimensional hydrothermal model discussed in section 5L is not able to represent the effects of pumping or radial flow to a well. To quantify these effects, we developed a three-dimensional model of groundwater flow for the region surrounding the hot-springs district (Fig. 34). We used the well-documented USGS groundwater flow model MODFLOW (McDonald and Harbaugh, 1991). The three-dimensional model had lateral dimensions of 7 km by 12 km (4.3 mi by 7.5 mi) and was discretized

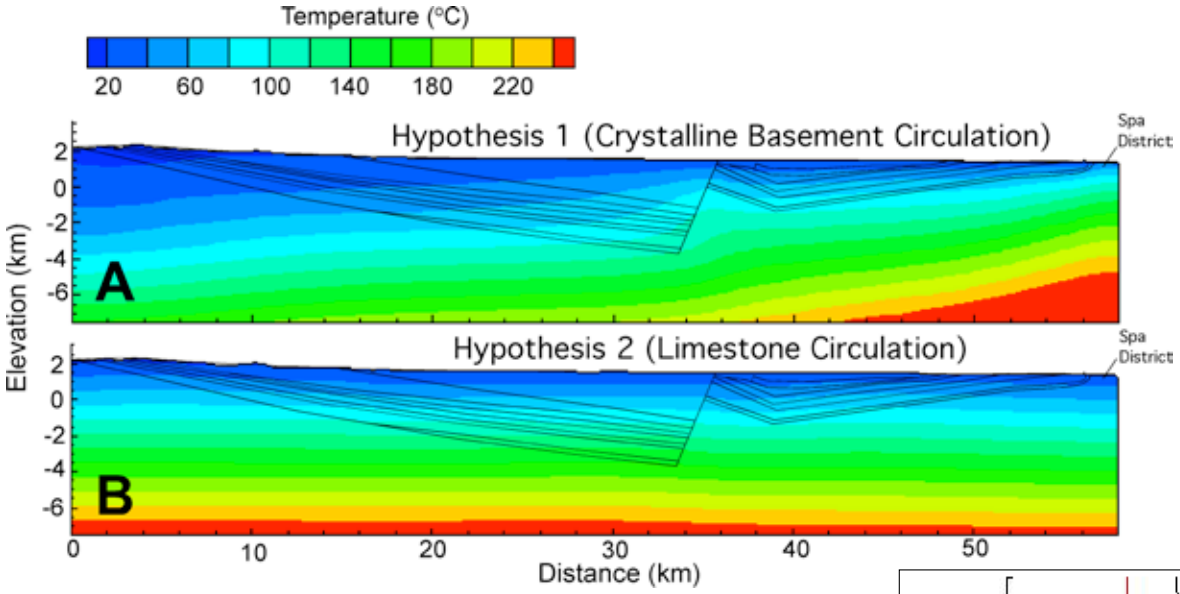

Figure 31–Comparison of computed temperatures for high (A, 10^{-12} m^2) and low permeability (B, 10^{-19} m^2) crystalline basement. In areas where groundwater flow is downward (left portion of figures), isotherms are cooler. In areas of groundwater discharge (right portion of figures), temperatures are elevated. These relationships are more evident in the upper diagram (Fig. 31A) due to the system's simulation parameters.

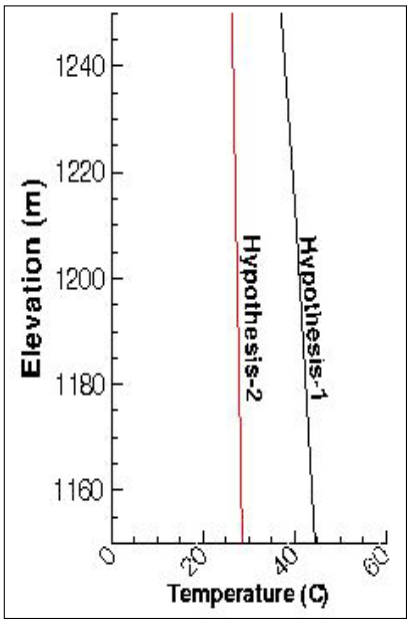

Figure 32–Comparison of computed temperature profiles from hot-springs district.

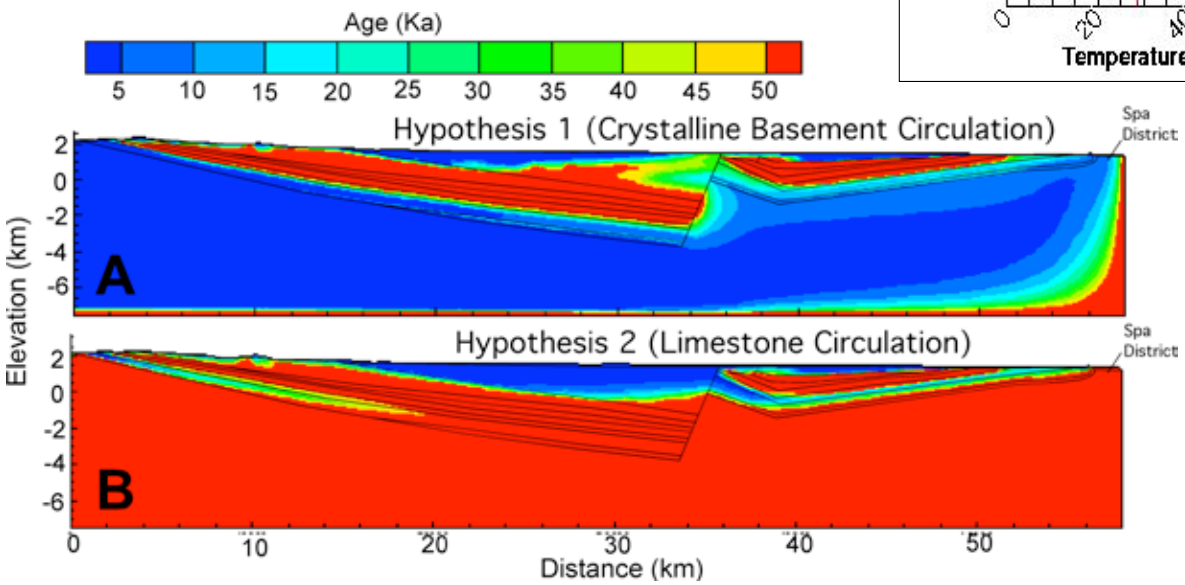

Figure 33–Comparison of computed groundwater residence times for high (A, 10^{-12} m^2) and low permeability (B, 10^{-19} m^2) crystalline basement. Age is depicted in thousands of years.

using a grid having 98 rows in the x-direction and 100 columns in the y-direction. We were not able to extend the model to the recharge area to the west due to lack of geologic well control and time constraints. The model had six layers in the vertical direction (Fig. 35). Several stratigraphic units were lumped together (Table 12) because of the lack of field data against which to calibrate properties of individual layers. We refined the grid in the vicinity of the hot-springs district ($\Delta x=\Delta y=50$m; 164 ft). The maximum grid dimension was 250 m (820 ft) in the x and y directions. We did not assign recharge across the water table to the MODFLOW model to be consistent with evapotranspiration calculations discussed in Section 3.

We assigned constant-head boundary conditions to layers one through six along the western edge of the model domain. We assigned a constant head along the Rio Grande to the upper layer and no-flow boundaries to the remaining five lower layers along the southern boundary in and around Truth or Consequences. A no-flow boundary was assigned along the northern boundary to all layers. A constant head boundary was assigned to the eastern boundary along Elephant Butte Reservoir. We included pumping of 17 hot-springs district wells. While this number is arbitrary, the wells are spatially distributed throughout the hot-springs district. We varied the pumping rate in each well between 300, 1000, and 2000 m^3/day (0.24. 0.81, and 1.6 acre-ft/day). The individual pumping rates from the 17 wells represented in our simulations represents the following fraction of natural geothermal discharge estimated by Theis et al. (1941): 60% (300 m^3/day/well) and 200% (1000 m^3/day/well), and 400% (2000 m^3/day/well). The net water withdraws from all of these scenarios does not exceed the estimated Maxey-Eakin recharge when considering the entire watershed (4460 m^3/day/well; 3.6 acre-ft/day).

Our three-dimensional analysis neglects the effects of variable-density flow that could be important in the deepest parts of the hot-springs district (crystalline basement), but we feel that this approach is valid for the shallow alluvial units. The three-dimensional model is intended to evaluate the effects of pumping on drawdown patterns and to evaluate the area of contribution to the hot-springs district wells.

We developed the six-layer model using the hydrologic properties shown in Table 12. The three-dimensional stratigraphy was derived from the cross-sectional profile (Fig. 3A) and surface geologic map of Kelley and Silver (1952) and Lozinsky (1987). The Percha Shale was allowed to pinch out in the hot-springs district to be consistent with our reconnaissance mapping. Permeability and porosity were taken mostly from the cross-sectional model calibration

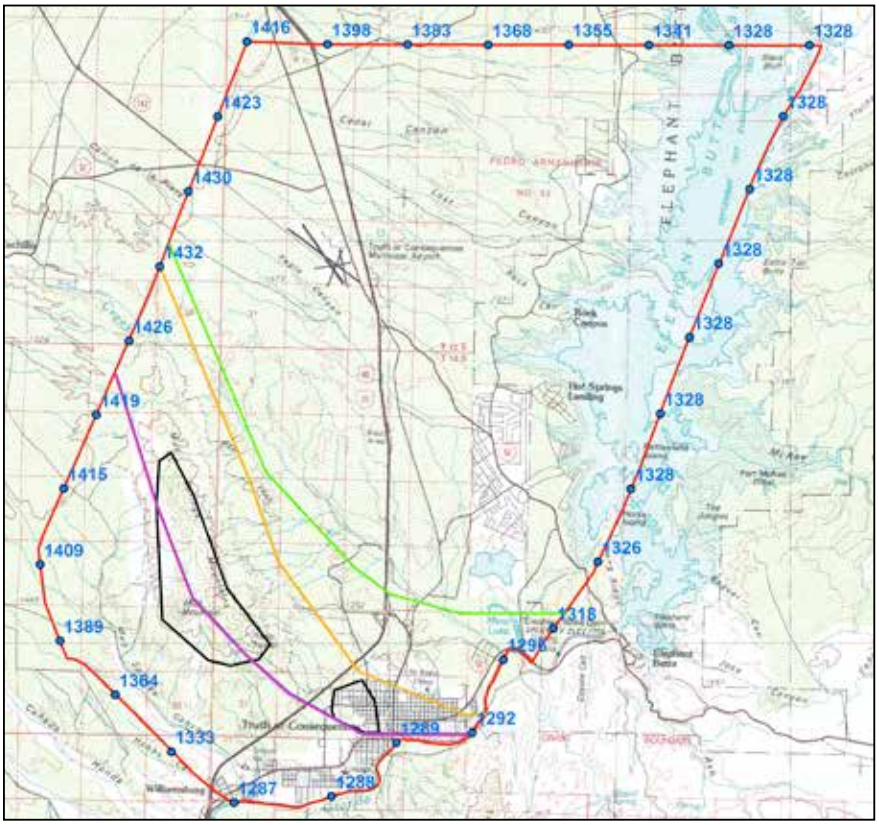

Figure 34–Values of constant head boundary conditions (blue circles) for MODFLOW model domain (red line) and limits of stratigraphic layers (black, orange, green, blue and pink lines) used to depict hydrogeologic conditions within the MODFLOW model. Faint red lines on the map are section lines, representing 1 mile. Colored stratigraphic layer lines represent MODFLOW layers as follows: Black = 1, Green = 2, Orange = 3, Blue (covered by pink) = 4, Pink = 5 (see Table 12).

exercise. We used a horizontal:vertical permeability anisotropy ratio that was varied between 1:1 for the crystalline basement to 10:1 and 100:1 for other units. We assigned a hydraulic conductivity for the alluvial aquifer of 4 m/day. This is approximately the intermediate value between the values of hydraulic conductivity derived from the hydrothermal model and the Rorabaugh analysis, which range from 1 to 7 m/day, respectively. Based on our Rorabaugh-type analysis using an alluvial thickness of 50 meters that was discussed in section 5J the hydraulic conductivity of the alluvial aquifer (4 m/day; 13 ft/day).

Using this hydraulic conductivity resulted in wells closest to the Rio Grande drawing water from the river for a pumping rate of 2000 m^3/day/well (Fig. 36). As pumping increased, more water is drawn from the deeper formations (Fig. 37). The intermediate and lower pumping rates (300 and 1000 m^3/day/well) did not draw water from the Rio Grande into the hot-springs district. It is important to note that our MODFLOW model results are highly sensitive to the hydraulic conductivity assigned to the alluvial aquifer. Simulations run assigning a hydraulic conductivity of 1 m/day to the alluvial aquifer resulted in a cone of depression forming in the hot-springs district at a production rate of 1000 m^3/day/well (not shown). A hydraulic conductivity of 1 m/day (3.3 ft/day) was used in our cross-sectional model for the alluvial

Table 12–Hydrologic parameters assigned to different stratigraphic units in three-dimensional MODFLOW model.

Unit Number	Unit Name	Permeability (m^2)	Permeability Anisotropy (k_x/k_z)	Hydraulic Conductivity m/day)
6	Precambrian Granitic and Metamorphic Rocks & Lower Paleozoic Units	10^{-12}	1	1
5	Percha Shale, Lake Valley Formation	$10^{-18.3}$	100	0.000004
4	Magdalena	10^{-12}	10	1
3	Abo	4×10^{-14}	10	0.04
2	Abo, Yeso, and San Andres Formations, Mancos Shale, Dakota Sandstone, Cretaceous Sediments, Tertiary Volcanics	10^{-14}	100	0.01
1	Tertiary Palomas Formation, and Younger Fluvial Deposits	10^{-10}, 10^{-12}	10	1

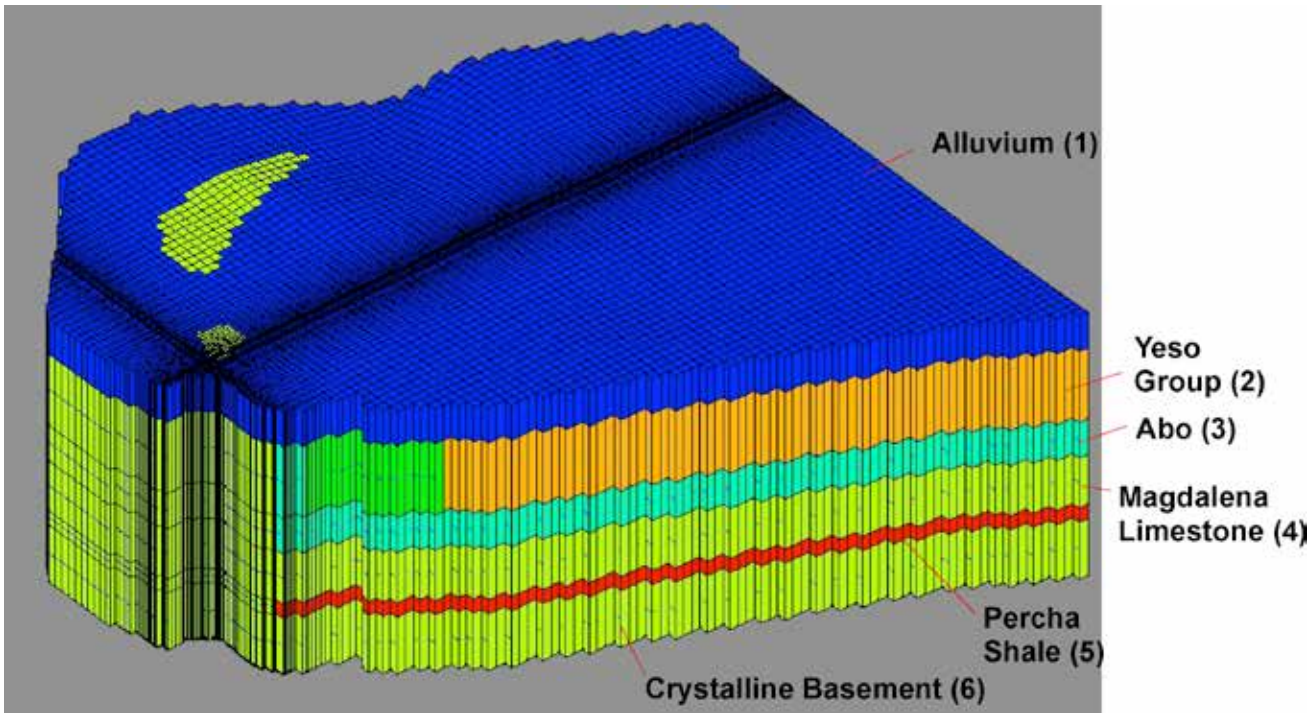

Figure 35–Three-dimensional view of six layer MODFLOW model. Unit 1 is comprised of alluvial material (Palomas and Santa Fe Formations). Permian through Cretaceous aquifers and confining units are lumped into layer 2. The Abo Formation is unit 3. The Magdalena Group limestone is unit 4. The Percha Shale is unit 5. The Proterozoic basement is comprised of unit 6. The hot-springs district is located in the region where the east-west and north-south mesh refinement intersect. Colors denote hydraulic conductivity assigned to 6 hydrostratigraphic units in m/day listed in Table 12.

aquifer. Additional testing of the alluvial aquifer's horizontal and vertical conductivities, primarily by pumping a deep well that fully penetrates the alluvial aquifer into the bedrock below and monitoring the response in the alluvial aquifer, would help further constrain these sensitive parameters.

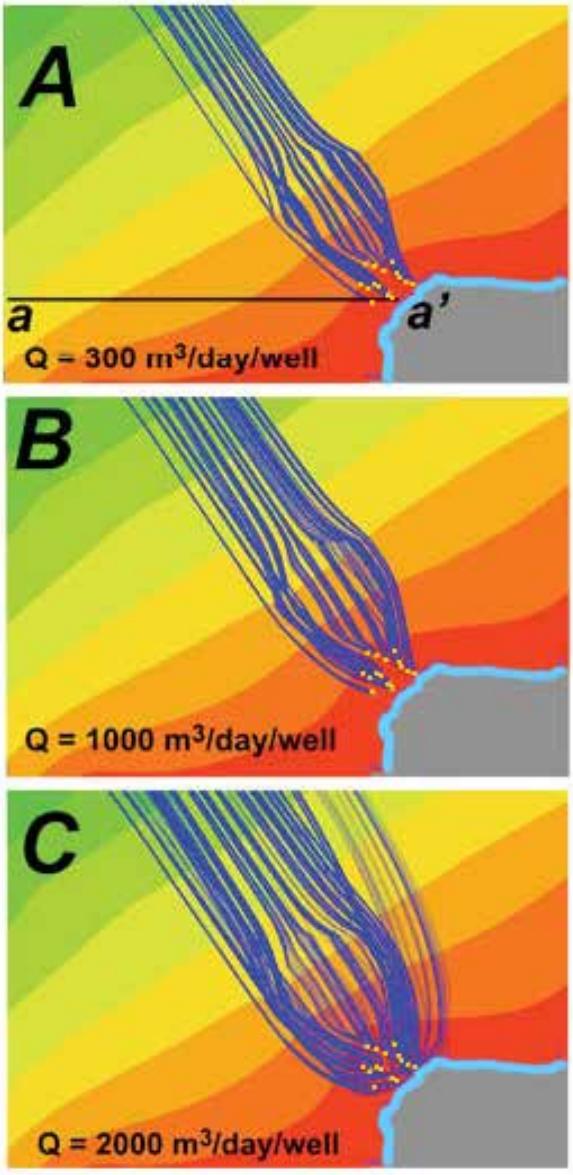

Figure 36–Plan view depiction of steady-state heads and flow directions (blue lines) for hot-springs district using three different pumping rates. The 17 hypothetical wells are indicated by the yellow points, with the Rio Grande as the light blue line boundary on the edge of the modeled area. Colored contours are simulated heads in m. The simulations compare the computed zone of contribution for hot-springs district pumping wells assuming different production rates and hydraulic conductivity for the shallow alluvium. The line labeled a-a' denotes the position of the cross sections shown in Figure 37.

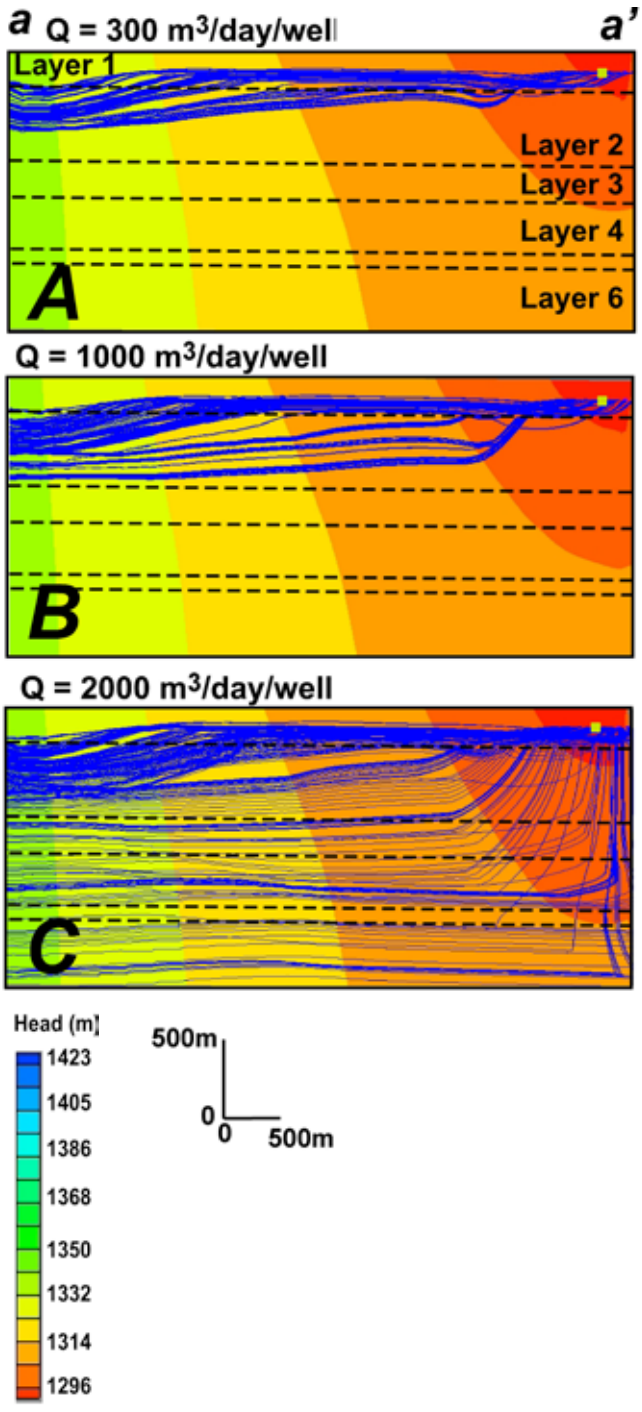

Figure 37–Cross-sectional depictions of steady-state heads (colored contours) and flow directions (blue lines) for hot-springs district for three pumping rates for the 17 production wells. The location of this cross section is indicated on Figure 36, as a-a'. The simulations compare the computed zone of contribution for hot-springs district pumping wells assuming different production rates. The black dashed lines denote the boundary between the six layers of the MODFLOW model. It the hot-springs district area, layer 1 has a hydraulic conductivity of 4 m/day (alluvium) and all other layers have a hydraulic conductivity of 1 m/day.

VI. DISCUSSION & CONCLUSIONS

Comparison of contour plots of water table elevations and temperatures suggests that some change in hydrologic and thermal conditions has occurred since Theis' study. However, because different wells were used in these two studies, it is difficult to establish with certainty that the observed changes are due to increased production. Long-term monitoring of temperatures and water levels in wells would help city managers arrive at results that are more conclusive.

What pumping rate should be used to ensure sustainability of the geothermal resources within the hot-springs district? Mass balance arguments suggest that the total hot-springs district pumping rate should be some fraction of the estimated natural geothermal discharge (2.2 million gallons per day or 490 m^3/day/well (0.4 acre-ft/day) using 17 wells). We estimate that about 70% of this volume is already appropriated by existing users, according to records of the Office of the State Engineer (343 m^3/day/well (0.28 acre-ft/day) using 17 wells). However, many of the existing hot-springs resource owners are probably not currently using their entire water right. Therefore, some limited growth in geothermal development may be permissible. Probably the biggest impediment to the responsible development and management of the geothermal resources within the hot-springs district is the lack of comprehensive production data. Another impediment to managed development of geothermal resources is related to information regarding well locations. There are significant inaccuracies that were discovered for reported well locations in the database maintained by the Office of the State Engineer while conducting our study.

The MODFLOW simulations that used a hydraulic conductivity of 4 m/day (13 ft/day) showed that pumping rate of 2000 /day/well (1.6 acre-ft/day/well; about four times the natural geothermal discharge) would result in drawing water from the Rio Grande into the hot-springs district. While pumping at a rate of 1000 /day/well (0.8 acre-ft/day/well) did not cause Rio Grande water to be drawn into the hot-springs district, it is possible that cool shallow alluvial water would drawn in to the hot-springs district from the northwest and may result in a net cooling to the hot-springs district. Using a lower (and perhaps more conservative) hydraulic conductivity of 1 m/day in our MODFLOW model (not shown) resulted in a cone of depression forming within the hot-springs district at a pumping rate of 1000 /day/well (0.8 acre-ft/day/well). The overturns in temperature profiles with depth found in some wells do suggest some ongoing transient incursion of cooler Rio Grande water. However, this will require further study before anything definitive can be said about this.

One limitation of our study is the lack of high-quality hydrologic and thermal data from deep wells (>100 m; 330 ft). This is important because there is some evidence the fluid pressures have declined in the Paleozoic limestone. The city may want to consider installing such a well for monitoring purposes.

VII. RECOMMENDATIONS

Rational management of the geothermal resource requires comprehensive data on the system. The most critical missing information is the stress put on the system by the collective pumping and artesian discharges. We strongly recommend that the City set up a program to collect data on well discharges. This could be accomplished by meters, records of electrical consumption, voluntary reporting or other means.

In spite of the excellent baseline information provided by the report of Theis et al. (1941), we have had difficulty defining the extent to which water levels in the alluvial aquifer have actually declined, due to lack of continuous records and lack of continuity in the locations of wells. We recommend that the City set up a monitoring program to collect continuous, or at least periodic, data on water levels and temperatures in selected wells at carefully selected locations.

The formerly-artesian carbonate aquifer is the immediate source of supply for all of the geothermal water uses in Truth or Consequences, but at present access to that aquifer has been reduced to one well. We are unable to ascertain whether differences in temperature between 1939 and 2013 are due to shallower well depths or an actual temperature decline. Locating or drilling at least one well near the source of geothermal upflow that can be used to monitor hydraulic head and temperature could provide unambiguous data, early warning of declines in the system, and enable analysis of its sensitivity to pumping of the alluvial aquifer.

With regard to the sustainability of the geothermal discharge, our analysis indicates grounds for concern. Artesian flow has declined to the vanishing point in the remaining artesian well and water-table elevations have pervasively declined by one to two feet. Temperatures are now lower than those measured by Theis in 1939, but whether this is due to a change in the system temperature, or just well depths, cannot be definitively established. These changes are still fairly mild, but they dictate caution regarding overexploiting the system. There is little doubt that unlimited pumping will result in lowered water levels and cooling of the system as Rio Grande water flows in to replace over-pumped geothermal water. As an absolute upper limit for pumping, the estimated system discharge of about two million gallons per day could be used. We would recommend a more conservative limit, ranging from 25% to 50% of the natural discharge (i.e., 0.5 to 1.0 million gallons per day). The degree to which the City wishes to be conservative or expansive in setting limits is one that has to be made by entities with appropriate political accountability, and should obviously be made in consultation with potentially affected businesses, landowners, and other stakeholders.

We feel that a well-drilling moratorium is of limited value in managing the geothermal resource. The critical issue is the amount of geothermal water pumped, not the number of wells. As described above, this is at present poorly quantified, preventing any meaningful management of the resource. Only after the present level of total pumping is quantified can prudent future expansion of exploitation (if any) be estimated. The most reasonable procedure would be to first establish a legal basis for regulation of the resource, taking into account, of course, existing water rights. Then, once data has been obtained on current pumping by each well, the optimal next step would be to establish an equitable and agreed-upon allocation among existing users and a procedure for approving additional future uses, if these were deemed prudent. Future wells will need to be allowed, if for no other reason, due to the short lifetime of wells as a result of the corrosive water. In summary, although the drilling moratorium may be useful in the short run in preventing overdrilling due to a 'hot-water rush', it should be replaced as soon as possible by a true management system.

Lack of knowledge regarding the nature of the geothermal system, its current state, and the possible effects of future changes in exploitation have hindered discussion that might have been helpful to its management. We feel that it would be beneficial for the City to set up a venue, such as a web page, where this information could be readily available and kept up to date. The City might also wish to explore the option of setting up a public forum in which issues related to the management of the geothermal resource could be discussed and that could provide input to the City Council regarding the management. We would be glad to assist in these efforts.

REFERENCES

Anderholm, S. K., 2001, Mountain-front recharge along the east side of the Albuquerque Basin, Central New Mexico, U.S. Geol. Surv. Water-Resour. Invest. Rep. 00-4010, 36 pp.

Bredehoeft, J. D. and Papodoupoulos, I.S.,1965, Rates of vertical groundwater flow estimated from the Earths thermal profile: Water Resources Research 1 325-328.

Carslaw, H. S. and J. C. Jeager, 1959, Heat conduction in solids, Oxford Science Publications, 510 p.

Chiodini, G., Frondini, F. and Marini, L., 1995. Theoretical geothermometers and PCO2 indicators for aqueous solutions coming from hydrothermal systems of medium-low temperature hosted in carbonate-evaporite rocks. Application to the thermal springs of the Etruscan Swell, Italy: Applied Geochemistry 10 337-346.

Cox, E. and Reeder, H., 1962, Ground-water conditions in the Rio Grande Valley between Truth or Consequences and Las Palomas, Sierra County: New Mexico State Engineer Office Technical Report 25, 47 p.

Dingman, S. L., 2002, Physical Hydrology, 2nd Edition, Waveland Press, Long Grove, Illinois, 656 p.

Ellis, A. J. and Mahon, W. A. J., 1964, Natural hydrothermal systems and experimental hot water/rock interactions: Geochimica et Cosmochimica Acta, v. 28, p. 1323-1357.

Ellis, A. J. and Mahon, W. A. J., 1967, Natural hydrothermal systems and experimental hot water/rock interactions (Part II): Geochimica et Cosmochimica Acta, v. 31, p. 519-538.

Ferguson, ,C. A., Osburn, G. R., and McIntosh, W. C., 2012, Oligocene calderas in the San Mateo Mountains, Mogollon-Datil volcanic field, New Mexico: New Mexico Geological Society Guidebook 63, p. 74-77.

Ferguson, G. and S. Grasby, 2011, Thermal springs and heat flow in North America: Geofluids 11 294–301.

Fournier, R. O., 1981, Application of water geochemistry to geothermal exploration and reservoir engineering: chapter 4 in Geothermal Systems: Principles and Case Histories (L. Rybach and L. P. J. Muffler, eds.), Wiley New York, p. 109-143.

Fournier, R. O., and R. W. Potter, II, 1979. "Magnesium correction to the Na-K-Ca chemical geothermometer." Geochim. Cosmochim. Acta 43: 1543-1550.

Fournier, R. O., White, D. E., and Truesdell A. H., 1974, Geochemical indicators of subsurface temperature - Part I. Basic assumptions, J. Res. U.S. Geol. Survey 2, 259-262.

Freeze and Cherry, 1979, Groundwater: Prentice Hall, 292 p.

Gilmer, A., Mauldin, R., and Keller, G. 1986, A gravity study if the Jornado Del Muerto and Palomas Basins: New Mexico Geological Society Guidebook, 37th Field Conference

Goode, D. J., 1996, Direct simulation of groundwater age: Water Resources Research 32, 289–296, doi: 10.1029/95WR03401.

Hantush, M.S., and C.E. Jacob, 1955, Non-steady radial flow in an infinite leaky aquifer, Transactions, American Geophysical Union, 36(1), 95-100.

Harrison, R., Lozinsky, R., Eggleston, T. and McIntosh, W. 1993, Geologic map of the Truth or Consequences 30x60 minute quadrangle: New Mexico Bureau of Mines and Mineral Resources, Open-file Report 390, 1:100,000 scale, 1 sheet, 16 p.

Harrison, R. and Cather, S. 2004, The Hot Springs fault system of south-central New Mexico—evidence for the northward translation of the Colorado Plateau during the Laramide orogeny: New Mexico Bureau of Geology and Mineral Resources, Bulletin 160

Kelley, S. A., and Chapin, C. E., 1997, Cooling histories of mountain ranges in the southern Rio Grande rift based on apatite fission-track analysis – a reconnaissance survey: New Mexico Geology, v. 19, no. 1, p. 1-14.

Kelley, V. C. and Silver, C., 1952, Geology of the Caballo Mountains with special reference to regional stratigraphy and structure and to mineral resources, including oil and gas, New Mexico University, Publication, Geology Series, v. 4, pp. 1-286.

Kühn, M., 2004. Concepts, classification, and chemistry of geothermal systems. In: M. Kühn (Editor), Reactive Flow Modeling of Hydrothermal Systems. Springer, Amsterdam, pp. 11-46.

Lu, N. and S. Ge, 1996, Effect of horizontal heat and fluid flow on the vertical temperature distribution within a confining unit: Water Resources Research 32 1449-1453.

Lozinsky, R. P., 1985, Geology and late Cenozoic history of the Elephant Butte area, Sierra County, New Mexico: New Mexico Bureau of Mines and Mineral Resources, Circular 187, 40 pp.

Lozinsky, R. P., 1987, Cross section across the Jornada del Muerto, Engle, and Northern Palomas Basins, south-central New Mexico: New Mexico Geology 9(3) 55– 57.

Lund, J. W., and Witcher, J., 2002, Truth or Consequences, New Mexico – A Spa City, Oregon Institute of Technology-Geo Heat Center Bulletin 23, No. 4, p. 20-24.

Maxwell, C. H., and Oakman, M. R., 1990, Geologic Map of the Cuchillo Quandrangle, Sierra County, New Mexico: Geologic map of the Cuchillo Quadrangle, Sierra County, New Mexico: U. S. Geological Survey Geologic Quadrangle Map GQ-1686, 1:24,000 scale.

McDonald MG, Harbaugh AW, 1988, A modular three-dimensional finite-difference ground-water flow model: Techniques Water Res Invest US Geol Survey, Book 6, Chapter A1.

Minton, E. G., 1941, Report of investigation Hot Springs Artesian Basin, New Mexico, 14th and 15th Biennial Repots, State Engineers Office, 1938-1942, p. 349-365.

McDonald MG, Harbaugh AW, 1988, A modular three-dimensional finite-difference ground-water flow model: Techniques Water Res Invest US Geol Survey, Book 6, Chapter A1.

Person, M., Banerjee, A., Hofstra, D., Sweetkind, D., and Y. Gao, 2008, Hydrologic Models of Modern and fossil geothermal systems within the Great Basin: Implications for Carlin-Type gold mineralization: Geosphere 4 888-917.

Powell, T., and Cumming, W., 2010, Spreadsheets for geothermal water and gas geochemistry: in Proceedings of the 35th Workshop on Geothermal Reservoir Engineering, SGP-TR-188, Stanford University, Stanford, CA: <http://pangea.stanford.edu/ERE/pdf/IGAstandard /SGW/2010/powell.pdf > (accessed on January 5, 2012).

Reiter, M., Edwards, C. L., Hartman, H., and Weidman, C., 1975, Terrestrial heat flow along the Rio Grande rift, New Mexico and southern Colorado: Geological Society of America Bulletin, v. 86, p. 811-818.

Reiter, M., Mansure, A. J., and Peterson, B. K., 1980, Precision continuous temperature logging and correlation with other types of logs, Geophysics, 45, 1857-1868.

Rorabaugh, M. I., 1964, Estimating changes in bank storage and groundwater contribution to streamflow, International Association of Scientific Hydrology Publication no. 63, 432-441.

Sanford, R. M., Bowers, R. L., and Combs, J., 1979, Rio Grande rift geothermal exploration case history, Elephant Butte prospect, south-central New Mexico: Transactions, Geothermal Resources Council, v. 3, p. 609-612.

Seager, W. R., and Mack, G. H., 2003, Geology of the Caballo Mountains, New Mexico: New Mexico Bureau of Geology and Mineral Resources Memoir 49, 136 p.

Theis, C. V., Taylor, G. C. Jr., and Murray, C. R., 1941, Thermal Waters of the Hot Springs Artesian Basin, Sierra County, NM, Fourteenth and Fifteenth Biennial Reports of the State Engineer of New Mexico, 1938-1942, p. 419-4-2.

Wade, S. C., and Reiter, M., 1994, Hydrothermal estimation of vertical ground water flow, Cañutillo, Texas: Ground Water 32 735–742.

Wells, S. G. and H. Granzow, 1981. Hydrogeology of the Thermal Aquifer near Truth or Consequences, NewMexico in State-Coupled Low-Temperature Geothermal Resource Assessment Program, Fiscal Year 1980, p. 3-5 to 3-51.

Witcher, J. C.,1986, Geothermal resources of southwestern New Mexico and southeastern Arizona: Field Conference Guidebook N.M. Geological Society, v. 39 191-198.

New Mexico Tech Hydrology Program

New Mexico Bureau of Geology and Mineral Resources

A division of New Mexico Institute of Mining and Technology

Socorro, NM 87801
(575) 835-5490
Fax (575) 835-6333
www.geoinfo.nmt.edu

Appendix 1–Well inventory

Point ID	SiteType	Elevation (ft ASL)	UTM NAD83		Field Parameters only	Water Sample	Water Level	Site Visit	Date Inventoried	Data Reliability
			Easting	Northing						
TC-001	GW	4232	287069	3666393			x	x	10/19/12	C
TC-002	GW	4234	287091	3666245			x	x	10/19/12	C
TC-003	GW	4241	287102	3666765			x	x	10/19/12	C
TC-004	GW	4254	286627	3667063				x	10/19/12	C
TC-005	GW	4691	286422	3677031				x	10/19/12	C
TC-006	GW	4287	285743	3666878				x	10/19/12	C
TC-007	GW	4245	286314	3666773				x	10/19/12	C
TC-008	GW	4240	286722	3666672				x	10/19/12	C
TC-009	GW	4260	286013	3666971				x	10/19/12	C
TC-010	GW	4241	289766	3667831	x		x	x	10/19/12	C
TC-011	GW	4241	289828	3667841	x		x	x	10/19/12	C
TC-012	GW	4247	289524	3667924		x	x	x	10/19/12	C
TC-013	GW	4240	289772	3667577		x	x	x	10/19/12	C
TC-014	GW	4240	289772	3667572			x	x	10/19/12	C
TC-015	GW	4240	289775	3667577				x	10/19/12	C
TC-016	GW	4245	289849	3667808	x		x	x	10/19/12	C
TC-017	GW	4247	289653	3667666		x	x	x	10/26/12	C
TC-018	GW	4244	289651	3667673		x	x	x	10/26/12	C
TC-019	GW	4243	289627	3667745	x		x	x	10/26/12	C
TC-020	GW	4243	289609	3667730	x		x	x	10/26/12	C
TC-021	GW	4243	289439	3667679			x	x	10/26/12	C
TC-022	GW	4243	289799	3667695			x	x	10/26/12	C
TC-023	GW	4259	289224	3667786			x	x	10/26/12	C
TC-024	GW	4259	289231	3667787			x	x	10/26/12	C
TC-025	GW	4250	289211	3667761			x	x	10/26/12	C
TC-026	GW	4247	289247	3667770	x		x	x	10/26/12	C
TC-027	GW	4259	289217	3667804			x	x	10/26/12	C
TC-028	GW	4248	289230	3667808				x	10/26/12	C
TC-029	GW	4260	289199	3667816			x	x	10/26/12	C
TC-030	GW	4250	289195	3667810	x		x	x	11/9/12	C
TC-031	GW	4247	289239	3667842				x	10/26/12	C
TC-032	GW	4260	289264	3667825				x	10/26/12	C
TC-033	GW	4260	289272	3667836				x	10/26/12	C
TC-034	GW	4260	289285	3667819			x	x	10/26/12	C
TC-035	GW	4244	289398	3667845		x	x	x	10/26/12	C
TC-036	GW	4233	290076	3667679			x	x	10/26/12	C
TC-037	GW	4243	290053	3667623	x		x	x	10/26/12	C
TC-038	GW	4241	289989	3667658			x	x	10/26/12	C
TC-039	GW	4232	286947	3666273			x	x	10/19/12	C
TC-040	GW	4233	286986	3666394			x	x	10/19/12	C
TC-041	GW	4245	289822	3667773	x		x	x	11/2/12	C
TC-042	GW	4242	289842	3667712			x	x	11/2/12	C
TC-043	GW	4245	289826	3667777			x	x	11/2/12	C
TC-044	GW	4242	289887	3667822	x		x	x	11/9/12	C
TC-046	GW	4241	289889	3667656			x	x	12/5/12	C
TC-047	GW	4240	289912	3667727			x	x	12/5/12	C

Point ID	SiteType	Elevation (ft ASL)	UTM NAD83		Field Parameters only	Water Sample	Water Level	Site Visit	Date Inventoried	Data Reliability
			Easting	Northing						
TC-001	GW	4232	287069	3666393			x	x	10/19/12	C
TC-002	GW	4234	287091	3666245			x	x	10/19/12	C
TC-003	GW	4241	287102	3666765			x	x	10/19/12	C
TC-004	GW	4254	286627	3667063				x	10/19/12	C
TC-005	GW	4691	286422	3677031				x	10/19/12	C
TC-006	GW	4287	285743	3666878				x	10/19/12	C
TC-007	GW	4245	286314	3666773				x	10/19/12	C
TC-008	GW	4240	286722	3666672				x	10/19/12	C
TC-009	GW	4260	286013	3666971				x	10/19/12	C
TC-010	GW	4241	289766	3667831	x		x	x	10/19/12	C
TC-011	GW	4241	289828	3667841	x		x	x	10/19/12	C
TC-012	GW	4247	289524	3667924		x	x	x	10/19/12	C
TC-013	GW	4240	289772	3667577		x	x	x	10/19/12	C
TC-014	GW	4240	289772	3667572			x	x	10/19/12	C
TC-015	GW	4240	289775	3667577				x	10/19/12	C
TC-016	GW	4245	289849	3667808	x		x	x	10/19/12	C
TC-017	GW	4247	289653	3667666		x	x	x	10/26/12	C
TC-018	GW	4244	289651	3667673		x	x	x	10/26/12	C
TC-019	GW	4243	289627	3667745	x		x	x	10/26/12	C
TC-020	GW	4243	289609	3667730	x		x	x	10/26/12	C
TC-021	GW	4243	289439	3667679			x	x	10/26/12	C
TC-022	GW	4243	289799	3667695			x	x	10/26/12	C
TC-023	GW	4259	289224	3667786			x	x	10/26/12	C
TC-024	GW	4259	289231	3667787			x	x	10/26/12	C
TC-025	GW	4250	289211	3667761			x	x	10/26/12	C
TC-026	GW	4247	289247	3667770	x		x	x	10/26/12	C
TC-027	GW	4259	289217	3667804			x	x	10/26/12	C
TC-028	GW	4248	289230	3667808				x	10/26/12	C
TC-029	GW	4260	289199	3667816			x	x	10/26/12	C
TC-030	GW	4250	289195	3667810	x		x	x	11/9/12	C
TC-031	GW	4247	289239	3667842				x	10/26/12	C
TC-032	GW	4260	289264	3667825				x	10/26/12	C
TC-033	GW	4260	289272	3667836				x	10/26/12	C
TC-034	GW	4260	289285	3667819			x	x	10/26/12	C
TC-035	GW	4244	289398	3667845		x	x	x	10/26/12	C
TC-036	GW	4233	290076	3667679			x	x	10/26/12	C
TC-037	GW	4243	290053	3667623	x		x	x	10/26/12	C
TC-038	GW	4241	289989	3667658			x	x	10/26/12	C
TC-039	GW	4232	286947	3666273			x	x	10/19/12	C
TC-040	GW	4233	286986	3666394			x	x	10/19/12	C
TC-041	GW	4245	289822	3667773	x		x	x	11/2/12	C
TC-042	GW	4242	289842	3667712			x	x	11/2/12	C
TC-043	GW	4245	289826	3667777			x	x	11/2/12	C
TC-044	GW	4242	289887	3667822	x		x	x	11/9/12	C
TC-046	GW	4241	289889	3667656			x	x	12/5/12	C
TC-047	GW	4240	289912	3667727			x	x	12/5/12	C

Point ID	SiteType	Elevation (ft ASL)	UTM NAD83		Field Parameters only	Water Sample	Water Level	Site Visit	Date Inventoried	Data Reliability
			Easting	Northing						
TC-048	GW	4242	289951	3667745			x	x	12/5/12	C
TC-049	GW	4236	289965	3667714			x	x	12/5/12	C
TC-050	GW	4237	289918	3667668			x	x	12/5/12	C
TC-051	GW	4242	290048	3667712			x	x	12/5/12	C
TC-052	GW	4248	289699	3667946			x	x	11/29/12	C
TC-053	GW	4237	289774	3667485	x		x	x	11/29/12	C
TC-054	GW	4240	289592	3667442	x		x	x	11/29/12	C
TC-055	GW	4262	289203	3667825				x	10/26/12	C
TC-056	GW	4248	289558	3667652			x	x	12/18/12	C
TC-057	GW	4242	289480	3667722			x	x	12/18/12	C
TC-058	GW	4247	289840	3667962	x		x	x	12/18/12	C
TC-059	GW	4243	289688	3667756		x	x	x	12/18/12	C
TC-060	GW	4245	289623	3667882			x	x	12/18/12	C
TC-061	GW	4242	289996	3667633		x	x	x	11/29/12	C
TC-062	GW	4822	288638	3679885		x		x	1/9/13	C
TC-063	GW	4241	289775	3667472		x	x	x	1/8/13	C
TC-064	GW	4331	290436	3671828		x		x	1/9/13	C
TC-065	GW	4320	290782	3671749		x		x	1/9/13	C
TC-066	GW	4508	286429	3675538			x	x	1/9/13	C
TC-067	GW	4243	289847	3667738			x	x	1/9/13	C
TC-068	GW	4565	285724	3676718				x	1/9/13	C
TC-071	GW	4243	289470	3667668			x	x	1/9/13	C
TC-072	GW	4242	289530	3667647			x	x	2/19/13	C
TC-073	GW	4232	290792	3667664			x	x	2/19/13	C
TC-074	GW	4321	289374	3668447			x	x	2/19/13	C
TC-075	GW	4752	281391	3679529				x	2/19/13	C
TC-076	GW	4251	289253	3667755		x	x	x	3/22/13	C
TC-077	GW	4343	288581	3667721			x	x	3/22/13	C
TC-078	GW	4722	281477	3679132			x	x	3/22/13	C
TC-079	GW	4243	289865	3666801			x	x	3/23/13	C
TC-080	GW	4269	290097	3666867			x	x	3/22/13	C
TC-081	GW	4678	282949	3678686				x	2/19/13	C
TC-082	GW	4240	289528	3667839		x	x			U
TC-083	GW	4241	289786	3667757	x		x			U
TC-084	GW	4241	289600	3667757	x		x			U
TC-085	GW	4241	289678	3667753	x		x			U
TC-086	GW	4241	289447	3667663	x					U
TC-087	GW	4239	289534	3667662	x		x			U
TC-088	GW	4241	289661	3667657	x		x			U
TC-089	GW	4237	289763	3667575	x		x			U
TC-090	GW	4241	289654	3667876	x					U
TC-091	GW	4261	289156	3667758	x					U
TC-092	GW	4261	289662	3667945	x					U
TC-093	GW	4241	289712	3667851	x		x			U
TC-094	GW	4241	289765	3667869		x	x			U
TC-095	GW	4256	289758	3667924	x					U

Appendix 1–Well inventory

Point ID	SiteType	Elevation (ft ASL)	UTM NAD83		Field Parameters only	Water Sample	Water Level	Site Visit	Date Inventoried	Data Reliability
			Easting	Northing						
TC-096	GW	4256	289758	3667914	x					U
TC-097	GW	4246	289977	3667846		x				U
TC-098	GW	4238	289863	3667626		x	x			U
TC-099	GW	4242	289859	3667916	x		x			U
TC-100	GW	4263	290458	3668222		x				U
TC-101	GW	4244	289756	3667667		x				U
TC-102	GW	4244	289760	3667671	x					U
TC-103	GW	4244	289760	3667667	x					U
TC-104	GW	4243	289667	3667562	x					U
TC-105	GW	4272	290577	3668377	x		x			U
TC-106	GW	4292	290150	3668389			x			U
TC-107	GW	4305	290209	3668610			x			U
TC-108	GW	4312	289594	3668555			x			U
TC-109	GW	4319	289366	3668451			x			U
TC-110	GW	4370	289142	3668608			x			U
TC-111	GW	4371	289018	3668743	x		x			U
TC-112	GW	4334	289250	3668485	x		x			U
TC-113	GW	4316	289521	3668507			x			U
TC-501	SP	4242	289794	3667643	x		x	x	11/9/12	C
TC-502	SP	4243	289813	3667671	x			x	1/9/13	C
TC-503	SP	4242	289851	3667684	x			x	1/9/13	C
TC-504	PS	4237	290082	3667645			x	x	2/19/13	C
TC-505	SP	4257	289825	3667969		x		x	1/23/13	C
TC-506	SP	4243	289803	3667671	x			x	1/9/13	C
TC-507	SP	4244	289756	3667671		x				U
TC-508	SP	4262	289602	3667919		x				U
TC-509	SP	4242	289851	3667677	x					U
TC-510	SP	4244	289647	3667562	x					U
TC-511	SP	4241	289739	3667558	x					U
TC-512	SP	4244	289826	3667714	x					U
TC-513	SP	4242	289823	3667682	x					U
TC-514	SP	4232	289959	3667530				x	9/5/13	C
TC-901	M	4231	287099	3666247		x		x	1/23/13	C
TC-902	M	5014	284444	3671426		x		x	1/23/13	C

Site Type	**Meaning**
GW	Groundwater other than spring (well)
SP	Spring
PS	Perennial stream
M	Meteorological (rain, snow)

Data Reliability	**Meaning**
C	Data field checked by reporting agency
U	Data not field checked, but considered reliable

ASL Above sea level

Appendix 2–Well information and water levels

Point ID	Well depth (ft bgs)	Date of most recent water level measurement	Depth to water (ft below MP)	Water Level Elevation (ft)	Measure-ment point (MP) height (ft)	NMOSE well record	Drill date	Driller's static water level (ft bgs)	Screen top (ft bgs)	Screen bottom (ft bgs)
TC-001		19-Oct-12	14.33	4218	0.58	X				
TC-002	24	05-Sep-13	13.96	4222	2.00	X				
TC-003		19-Oct-12	18.41	4225	1.79	X				
TC-004	405					HS-0011-S-2	12/10/89	38.00		
TC-005					0.50	HS-0011		50.15		
TC-006					1.92	HS-0011-S-5				
TC-007	530				1.00	HS-0011-S-4	6/11/76		230	507
TC-008	600				1.75	HS-0011-S-10	8/26/98	77.00	247	595
TC-009	598				1.61	HS-0011-S-9	7/10/98	84.00	252	598
TC-010	30	19-Oct-12	3.91	4238	0.67	HS-668	12/31/26			
TC-011	40	19-Oct-12	1.07	4240	0.00	X	1/1/28			
TC-012	110	23-Mar-13	5.36	4242	0.42	HS-0001	10/1/29			
TC-013	176	19-Oct-12			0.00	HS-0209	1/1/30	0.00		
TC-014	154	19-Oct-12				HS-0209-S	3/24/62			
TC-015						HS-0209-S2				
TC-016		19-Oct-12	5.25	4240	0.00	X				
TC-017	93				0.00	HS-0009	11/28/73			
TC-018	30	22-Mar-13	3.69	4239	-1.67	HS-0939	5/6/06	22.00	20	30
TC-019	42	05-Sep-13	6.49	4239	1.60	HS-1090	8/11/12	9.00	22	42
TC-020	38	05-Sep-13	6.19	4238	1.20	HS-0944	8/4/06	5.00	30	40
TC-021	40	05-Sep-13	6.36	4237	0.42	HS-0924	6/30/06	6.00	30	40
TC-022	12	22-Mar-13	5.09	4237	-0.60	X				
TC-023	15	26-Oct-12	11.90	4246	-0.59	X				
TC-024	20	26-Oct-12	10.84	4247	-0.47	X				
TC-025	17	22-Mar-13	12.17	4238	-0.41	X				
TC-026	18	22-Mar-13	8.45	4238	-0.55	X				
TC-027	19	26-Oct-12	9.74	4249	-0.49	X				
TC-028		22-Mar-13	10.07	4238	0.00	X				
TC-029	18	26-Oct-12	11.53		0.00	X				
TC-030		22-Mar-13	11.01	4239	0.00	X				
TC-031		22-Mar-13	9.49	4238	0.00	X				
TC-032						X				
TC-033						X				
TC-034	20	26-Oct-12	6.71	4251	-1.50	X				
TC-035	208	26-Oct-12	3.31	4242	1.29	HS-55 or 56	1/1/30			
TC-036	43	26-Oct-12	10.11	4223	0.92	HS-0379-S	11/6/89	12.00	31	41
TC-037	60	05-Sep-13	11.89	4232	1.06	HS-1017	8/12/10	8.00	40	60
TC-038	60	05-Sep-13	9.71	4234	2.63	HS-0950	5/29/07	4.00	40	60
TC-039		19-Oct-12	14.91	4215	-1.19	X				
TC-040		19-Oct-12	15.11	4220	2.54	X				
TC-041	14	02-Nov-12	5.41	4239	-0.44	X				
TC-042		02-Nov-12	4.10	4237	-0.35	X				

Appendix 2–Well information and water levels

Point ID	Well depth (ft bgs)	Date of most recent water level measurement	Depth to water (ft below MP)	Water Level Elevation (ft)	Measure-ment point (MP) height (ft)	NMOSE well record	Drill date	Driller's static water level (ft bgs)	Screen top (ft bgs)	Screen bottom (ft bgs)
TC-043	15	02-Nov-12	5.56	4239	-0.91	X				
TC-044	125	09-Nov-12	4.19	4239	0.81	X	1/1/29			
TC-046	45	05-Sep-13	6.28	4235	0.89	HS-0912	4/10/06	7.00	25	42
TC-047	60	05-Dec-12	5.92	4235	1.50	HS-926 POD2	5/12/10	4.00	40	60
TC-048	42	22-Mar-13	6.10	4236	0.66	HS-1076	7/9/12	9.00	22	42
TC-049	43	05-Dec-12	6.33	4230	0.78	HS-450	1/3/78	5.00	30	41
TC-050	57	05-Dec-12	5.88	4233	1.29	HS-0915	3/17/06	6.00	40	53
TC-051	50	22-Mar-13	8.17	4234	0.56	HS-0826	8/20/00	10.00	40	50
TC-052	10	22-Mar-13	4.41	4243	-0.10	X				
TC-053		29-Nov-12	4.61	4230	-2.15	X				
TC-054	40	22-Mar-13	6.93	4234	1.25	HS-0903	10/7/04	8.00	20	40
TC-055						X				
TC-056	150	18-Dec-12	1.26	4247	0.00	HS-0004	1/1/38			
TC-057		22-Mar-13	6.04	4237	0.84	X				
TC-058	13	05-Sep-13	5.82	4241	0.40	HS-0203?				
TC-059	60	22-Mar-13	4.08	4239	0.00	HS-0927?	1/1/08			
TC-060	8	05-Sep-13	3.77	4241	0.00	HS-0024 CLW	12/20/44			
TC-061	71	05-Sep-13	10.61	4233	2.35	HS-1034	2/4/09		49	69
TC-062	600	22-Mar-13	436.68	4387	2.00	X				
TC-063	99	22-Mar-13	7.28	4234	0.05	HS-1035-POD2	1/18/10	6.00	0	99
TC-064	100					X				
TC-065	200					X				
TC-066		22-Mar-13	80.83	4432	4.67	X				
TC-067		22-Mar-13	4.92	4238	0.00	X				
TC-068						X				
TC-071		22-Mar-13	6.30	4237	1.00	X				
TC-072	219	22-Mar-13	2.25	4241	1.00	HS-0076	11/10/49	0.00		
TC-073		19-Feb-13	14.40	4218	0.40	X				
TC-074	50	22-Mar-13	50.32	4274	3.20	X				
TC-075						X				
TC-076		22-Mar-13	0.80	4247	-3.00	HS-0002	1/1/37			
TC-077	263	22-Mar-13	98.52	4245	1.38	X	1/1/93			
TC-078		22-Mar-13	25.29	4699	1.75	X				
TC-079		23-Mar-13	17.70	4226	0.60	X				
TC-080		22-Mar-13	41.17	4230	1.70	X				
TC-081					2.00	X				
TC-082	105	29-Mar-39	-0.38	4241	0.00	X	1/1/24			
TC-083	125	29-Mar-39	0.73	4240	0.00	X	1/1/28			
TC-084	105	06-Apr-39	0.20	4241	0.00	X				
TC-085	125	28-Mar-39	0.11	4240	0.00	X	1/1/23			
TC-086	165				0.00	X	1/1/36			
TC-087	205	29-Mar-39	-1.88	4241	0.00	X	1/1/38			

Point ID	Well depth (ft bgs)	Date of most recent water level measurement	Depth to water (ft below MP)	Water Level Elevation (ft)	Measure-ment point (MP) height (ft)	NMOSE well record	Drill date	Driller's static water level (ft bgs)	Screen top (ft bgs)	Screen bottom (ft bgs)
TC-088	186	29-Mar-39	0.34	4240	0.00	X	1/1/39			
TC-089	176	29-Mar-39	-3.69	4241	0.00	X	1/1/29			
TC-090	125				0.00	HS-0024	1/1/24			
TC-091	225				0.00	X	1/1/37			
TC-092	162				0.00	X	1/1/28			
TC-093	101	28-Mar-39	1.59	4240	0.00	X	1/1/28			
TC-094	27	28-Mar-39	0.96	4240	0.00	X	1/1/26			
TC-095	158				0.00	X	1/1/28			
TC-096	165				0.00	X				
TC-097	100				0.00	X	1/1/26			
TC-098	185	23-Mar-39	-2.03	4240	0.00	X	1/1/21			
TC-099	239	30-Mar-39	0.06	4242	0.00	X	1/1/26			
TC-100	120				0.00	X				
TC-101	14				0.00	X				
TC-102	6				0.00	X				
TC-103	15				0.00	X				
TC-104					0.00	X				
TC-105	182	08-Apr-40	1.01	4271	0.00	X	1/1/29			
TC-106		29-Mar-39	29.25	4262	0.00	X				
TC-107	55	29-Mar-39	48.44	4257	0.00	X				
TC-108		28-Feb-39	51.53	4261	0.00	X				
TC-109		28-Feb-40	54.75	4264	0.00	X				
TC-110		28-Feb-40	95.88	4274	0.00	X				
TC-111		12-Sep-39	89.40	4281	0.00	X				
TC-112		28-Feb-40	62.79	4271	0.00	X				
TC-113		16-Jun-39	45.00	4271	0.00	X				

X = unavailable
bgs = below ground surface
MP = measurement point

In order to characterize the Engle Basin's present day and paleohydrology, we sequentially solved a series of two-dimensional transient, groundwater flow, heat, and solute/isotope transport equations. The heat, solute, and isotope transport equations were solved using a finite element implementation of the Lagrangian-based modified method of characteristics (MMOC). The groundwater flow equation was also solved using standard finite element methods.

Groundwater Flow

We solved for variable-density groundwater flow using the following stream function based groundwater equation:

$$\nabla_x \times \left[\mu_f \frac{k}{|k|} \nabla_x \psi \right] = -g \frac{\partial \rho_r}{\partial x} \quad \text{(A1)}$$

where ∇_x is the gradient operator in the x- and z-directions, k is the permeability tensor, |k| is the magnitude of k, Ψ is the stream function, ρr is the relative density, μ_f is the water viscosity. The right-hand-side of equation (A1) accounts for variable-density fluid flow. Density-gradients in our model are primarily due to lateral and vertical salinity variations.

Relative density (ρr) and relative viscosity (μr) used in equations (A1) and (A3) are given by

$$\rho_r = \frac{\rho_f - \rho_0}{\rho_0} \quad \text{(A2)}$$

$$\mu_r = \frac{\mu_0}{\mu_f} \quad \text{(A3)}$$

where ρ_w is the density of water, ρ_f is the density of groundwater, ρ_0 is the water density at standard conditions (10 °C, 0.0ppt Salinity, and 0.0 MPa), μ_0 is the viscosity of water at standard conditions (10 °C, 0 ppt total dissolved solids concentration, and atmospheric pressure) and μ_f is the viscosity of water.
The Darcy flux is related to stream functions through the Cauchy-Reimann equations:

$$\frac{\partial \psi}{\partial z} = q_x \quad \text{(A4)}$$

$$-\frac{\partial \psi}{\partial x} = q_z \quad \text{(A5)}$$

Solute Transport

Transport of solute through porous media is controlled by advection, Fickian diffusion, and hydrodynamic dispersion (Freeze and Cherry, 1979). For relatively low flow velocities (<10^{-5} m/yr), solute transport is dominated by diffusion; dispersive transport and advective transport are more important when fluid velocities are higher. We used the following equation to represent advective/dispersive solute transport

$$\phi \frac{\partial C}{\partial t} = \nabla_x \left[\phi \mathbf{D} \nabla_x C \right] - \vec{q} \ \nabla_x C \quad \text{(A7)}$$

where **D** is the hydraulic dispersion-diffusion tensor, $\vec{q}$ is the groundwater flux, ϕ is porosity, and *C* is species concentration (total dissolved solids concentration reported as solute mass fraction denoting kilograms of solute per kilograms of solution). Equation A7 neglects the effects of solute diffusion into low permeable blocks and rapid advective transport through fractures. Equation (A7) also neglects fluid-rock geochemical reactions at depth. Computed salinity units were converted parts per thousands (ppt) in this report. The tensor **D** has the four components, $\mathbf{D}_{xx}$, $\mathbf{D}_{zz}$, $\mathbf{D}_{zx}$, *and* $\mathbf{D}_{xz}$, defined by

$$D_{xx} = \alpha_L \frac{v_x^2}{|v|} + \alpha_T \frac{v_z^2}{|v|} + D_d$$
$$D_{zz} = \alpha_T \frac{v_x^2}{|v|} + \alpha_L \frac{v_z^2}{|v|} + D_d \quad \text{(A8)}$$
$$D_{zx} = D_{xz} = (\alpha_L - \alpha_T) \frac{v_x v_z}{|v|}$$

where v_x and v_z are components of seepage velocity in the x- and z-directions ($v_x = q_x/f$ and $v_z = q_z/f$), D_d is the solute diffusion coefficient, and |v| is

$$|v| = \sqrt{v_x^2 + v_x^2} \quad \text{(A9)}$$

Heat Transport

Temperature can affect fluid density and permafrost distribution in our model. FEMOC solves a conductive and convective-dispersive heat-transfer equation:

$$\left[c_f \rho_f \phi + c_s \rho_s (1-\phi)\right] \frac{\partial T}{\partial t} = \nabla_x \left[\lambda \nabla_x T\right] - \vec{q} \rho_f c_f \nabla_x T \quad \text{(A11)}$$

where λ is the thermal dispersion-conduction tensor, ϕ is porosity, T is temperature, c_s and cf are the specific heat capacities of the solid and liquid phases, respectively, and ρ_s is the density of the solid phase. The tensor λ has the form:

$$\lambda_{xx} = \rho_f c_f \alpha_L \frac{q_x^2}{|q|} + \rho_f c_f \alpha_T \frac{q_z^2}{|q|} + \lambda_f \phi + (1-\phi)\lambda_s$$
$$\lambda_{zz} = \rho_f c_f \alpha_T \frac{q_x^2}{|q|} + \rho_f c_f \alpha_L \frac{q_z^2}{|q|} + \lambda_f \phi + (1-\phi)\lambda_s \quad \text{(A12)}$$
$$\lambda_{zx} = \lambda_{xz} = (\alpha_L - \alpha_T) \frac{q_x q_z}{|q|}$$

where λ_{xx}, λ_{zz}, λ_{zx}, and λ_{xz} are the tensor components, α_L and α_T are the transverse and longitudinal thermal dispersivities, q_x and q_z are the Darcy fluxes in the x- and z- directions. λ_f and λ_s are the thermal conductivities of the fluid and solid phases, respectively, which are assumed to be isotropic and scalar quantities. q is the absolute value of the Darcy flux, which is given by

$$|q| = \sqrt{q_x^2 + q_x^2} \quad \text{(A13)}$$

Equations of State

Thermodynamic equations of state are used to compute the density and viscosity of groundwater at elevated temperature, pressure, and salinity conditions. FEMOC uses the polynomial expressions of Batzle and Wange (1992). These polynomial expressions are valid for temperatures between 10 and 150 °C and salinities between 0 and 6*m* NaCl. Fluid density is more sensitive to temperature and salinity than fluid pressure.

Groundwater Residence Time

Goode (1996) was the first to develop an advection-dispersion based groundwater transport equation to quantify groundwater residence times:

$$\frac{\partial A}{\partial t} = \nabla_x \cdot \left[D \nabla_x A\right] - q \nabla_x A + 1 \quad \text{(A14)}$$

where A is groundwater age (in years).